

Aus dem Forschungsinstitut Kinderkrebs-Zentrum Hamburg  
und der Klinik für Pädiatrische Hämatologie und Onkologie  
des Universitätsklinikums Hamburg-Eppendorf

**Functional characterization of non-receptor tyrosine  
kinase dependent signal transduction in acute  
lymphoblastic leukemia of childhood**

**Dissertation**

Zur Erlangung der Würde des Doktors der Naturwissenschaften  
des Fachbereichs Biologie, der Fakultät Mathematik, Informatik und  
Naturwissenschaften der Universität Hamburg

vorgelegt von

MSc Mikrobiologie

**Allan Xavier Pernudy Ubau**

Geboren in Granada, Nicaragua

Hamburg, December 2013

Genehmigt vom Fachbereich Biologie  
der Fakultät für Mathematik, Informatik und Naturwissenschaften  
an der Universität Hamburg  
auf Antrag von Professor Dr. M. HORSTMANN  
Weiterer Gutachter der Dissertation:  
Priv.-Doz. Dr. H. LÜTHEN  
Tag der Disputation: 13. Dezember 2013

Hamburg, den 28. November 2013



Professor Dr. C. Lohr  
Vorsitzender des  
Fach-Promotionsausschusses Biologie

**The trick is to never give up!**

---

<b>1.</b>	<b>Introduction</b>	<b>1</b>
1.1.	<i>Acute lymphoblastic leukemia</i>	1
1.1.1.	Primary genetic abnormalities	2
1.1.2.	Cooperative mutations	3
1.2.	<i>Hematopoiesis</i>	4
1.2.1.	B-cell development	5
1.2.2.	Pre-BCR signaling	5
1.3.	<i>Protein tyrosine kinases</i>	6
1.3.1.	Non-receptor protein tyrosine kinases	7
1.3.2.	Architecture of NRTK	7
1.4.	<i>SRC family kinase</i>	8
1.4.1.	Structure and regulation of SFK	8
1.4.2.	Intramolecular regulation of SFK	10
1.5.	<i>The SRC family kinase member Lyn</i>	12
1.5.1.	Subcellular Lyn localization	12
1.5.2.	Lyn and BCR signaling pathway	13
1.6.	<i>SFK and human cancers</i>	13
1.6.1.	Deregulation of the C-terminal negative regulatory domain	14
1.6.2.	Deregulation of SFK by phosphatases	14
1.6.3.	Deregulation of SFK by receptor tyrosine kinases	14
<b>2.</b>	<b>Working hypothesis</b>	<b>16</b>
<b>3.</b>	<b>Material and methods</b>	<b>17</b>
3.1.	<i>Chemicals</i>	17
3.2.	<i>Biological material</i>	17
3.2.1.	Bacteria	17
3.2.2.	Cell lines	17
3.2.3.	Primary cells	18
3.2.4.	Pediatric acute lymphoblastic leukemia (ALL) patient samples	18
3.2.5.	Enzymes	20
3.2.6.	Antibodies	20
3.2.7.	Vectors	23
3.2.8.	Oligonucleotides	23
3.3.	<i>Molecular biology</i>	23
3.3.1.	Media for bacterial culture	23
3.3.2.	Transformation of competent bacteria	23
3.3.3.	Plasmid-DNA isolation	24
3.3.4.	RNA isolation	24
3.3.5.	Nucleic acids concentration	24
3.3.6.	cDNA synthesis	24

3.3.7.	Agarose gel electrophoresis .....	25
3.3.8.	Restriction digest of plasmid-DNA.....	25
3.3.9.	Gel extraction .....	25
3.3.10.	PCR .....	25
3.3.11.	Real time PCR .....	26
3.3.12.	Sequencing .....	26
3.3.13.	Mutagenesis .....	26
3.3.14.	DNA cloning strategy .....	27
3.4.	<i>Protein biochemistry</i> .....	27
3.4.1.	KLB lysate buffer .....	27
3.4.2.	Cell lysate .....	27
3.4.3.	Determination of whole protein concentration .....	28
3.4.4.	SDS-PAGE.....	28
3.4.5.	Western blot.....	28
3.4.6.	Li-Cor detection .....	28
3.4.7.	Stripping of bound antibodies .....	29
3.5.	<i>Cell culture</i> .....	29
3.5.1.	Culture of adherent and suspension cells .....	29
3.5.2.	Composition of the media for cell culture.....	29
3.5.3.	Determination of cell number and vitality .....	30
3.5.4.	Freezing and thawing cells .....	30
3.5.5.	Transfection of HEK 293 cells .....	30
3.5.6.	Density gradient centrifugation .....	30
3.5.7.	Magnetic labeling .....	31
3.5.8.	Stimulation of the pre-BCR.....	31
3.5.9.	Cell proliferation assay .....	31
3.5.10.	Confocal microscopy .....	31
3.5.11.	Sucrose gradient.....	31
3.5.12.	Virus production .....	32
3.5.13.	Transduction of ALL cell lines .....	32
3.5.14.	SFK-specific tyrosine kinase inhibitor .....	32
<b>4.</b>	<b>Results</b> .....	<b>33</b>
4.1.	<i>Protein tyrosine kinase selection</i> .....	33
4.2.	<i>Cloning, mutagenesis and transfection of the PTK</i> .....	34
4.2.1.	Cloning and mutagenesis .....	34
4.2.2.	Transfection.....	35
4.3.	<i>Selection of PTK specific antibodies</i> .....	36
4.3.1.	Validation of PTK specific antibodies.....	36
4.3.2.	Validation of Src family kinase-specific monoclonal antibodies.....	37
4.4.	<i>Reproducibility of the Li-Cor imaging system</i> .....	39
4.5.	<i>PTK expression</i> .....	41

---

4.5.1.	PTK expression in primary ALLs and ALL cell lines .....	41
4.5.2.	PTK expression in childhood ALL .....	42
4.6.	<i>shRNA mediated Lyn repression</i> .....	45
4.6.1.	Selection of shRNA constructs.....	45
4.6.2.	Expression of Lyn in primary ALL and derivate cell lines .....	47
4.6.3.	Specificity of the shRNA_Lyn construct.....	48
4.7.	<i>Repression of Lyn in ALL cell lines</i> .....	48
4.8.	<i>Pre-BCR cross-linking in Lyn-knockdown leukemic cells</i> .....	50
4.8.1.	Specificity of the F(ab') <sub>2</sub> anti-human IgM.....	50
4.8.2.	Tyrosine protein phosphorylation in Lyn-knockdown cells.....	51
4.8.3.	Downstream signaling in Lyn-knockdown cells .....	53
4.9.	<i>Subcellular localization of Lyn</i> .....	54
4.9.1.	Distribution of Lyn in isolated lipid rafts .....	55
4.9.2.	Subcellular localization of Lyn by confocal microscopy.....	56
4.10.	<i>Quantification of Lyn expression at transcript levels</i> .....	57
4.11.	<i>Analysis of Lyn-dependent proliferation and survival</i> .....	57
4.12.	<i>SFK inhibition by tyrosine kinase inhibitor (TKI) in ALL cell lines</i> .....	58
<b>5.</b>	<b>Discussion</b> .....	<b>60</b>
5.1.	<i>PTK expression in ALL</i> .....	60
5.2.	<i>High Lyn expression in a subgroup of ALL patient samples</i> .....	61
5.3.	<i>Analysis of protein activation in Lyn-knockdown ALL cell lines</i> .....	62
5.4.	<i>Repression of Lyn affects proliferation of ALL cells</i> .....	64
5.5.	<i>Proposed models of the dual functions of Lyn</i> .....	65
5.6.	<i>Outlook</i> .....	67
<b>6.</b>	<b>Summary</b> .....	<b>68</b>
<b>7.</b>	<b>Abbreviations</b> .....	<b>69</b>
7.1.	<i>Prefixes</i> .....	69
7.2.	<i>Units</i> .....	69
7.3.	<i>Non-receptor tyrosine kinases</i> .....	69
7.4.	<i>List of abbreviations</i> .....	70
<b>8.</b>	<b>Oligonucleotides</b> .....	<b>72</b>
<b>9.</b>	<b>Declaration on oath</b> .....	<b>77</b>

---

10. Confirmation of linguistic accuracy by a native speaker .....	78
11. Acknowledgement .....	79
12. Literature .....	80

## List of Figures

Figure 1	Kaplan-Meier survival analysis.....	1
Figure 2	Frequency of genetic alteration in ALL in childhood. ....	2
Figure 3	Hierarchy of hematopoiesis. ....	4
Figure 4	B-cell development. ....	5
Figure 5	Human non-receptor protein tyrosine kinase. ....	7
Figure 6	Structure of SFK proteins. ....	9
Figure 7	Activation of the SFK proteins.....	10
Figure 8	The roles of Cbp/Csk and lipid rafts in regulating the function of SFK. ....	11
Figure 9	The tyrosine kinase kinome. ....	33
Figure 10	Detection of cMyc-tagged recombinant protein expression by western blot.....	35
Figure 11	Quantification of the expression of cMyc-tagged recombinant proteins. ....	36
Figure 12	Validation of the specificity of the monoclonal antibodies. ....	37
Figure 13	Specificity of monoclonal antibodies directed against SFK members. ....	38
Figure 14	Reproducibility of western blot analyses by the Li-Cor imaging system. ....	40
Figure 15	PTK expression in primary ALLs and ALL cell lines. ....	41
Figure 16	PTK expression in ALL patient samples.....	44
Figure 17	Lyn-directed RNA interference. ....	46
Figure 18	Lyn expression and SFK activation status in primary ALL and cell lines.....	47
Figure 19	SFK expression in lentivirally-transduced Nalm6 cells.....	48
Figure 20	Monitoring of Lyn repression in Nalm6 and CALL3 cell lines.....	49

---

Figure 21	Specific cross-linking of the pre-BCR by the F(ab') <sub>2</sub> anti-human IgM. ....	50
Figure 22	Tyrosine phosphorylation in Lyn-knockdown Nalm6 cells upon pre-BCR crosslinking. ....	52
Figure 23	Activation of AKT and ERK 1/2 in Lyn-knockdown leukemic cells. ....	53
Figure 24	Isolation of lipid rafts by linear sucrose gradient ultracentrifugation. ....	55
Figure 25	Subcellular distribution of Lyn. ....	56
Figure 26	Transcriptional expression of Lyn in ALL cells. ....	57
Figure 27	Cell proliferation in Nalm6 and CALL3 Lyn-knockdown leukemic cells ....	58
Figure 28	Cell proliferation of Nalm6 and CALL3 upon SU6656 treatment. ....	59
Figure 29	Proposed model for SFK activation and downregulation by Lyn in CALL3 cells. ....	65
Figure 30	Proposed model for deregulated activity of SFK in Nalm6 cells. ....	66

## List of Tables

Table 1	Cell Lines. ....	17
Table 2	Primary cells. ....	18
Table 3	ALL patient samples. ....	20
Table 4	Primary antibodies for western blot. ....	21
Table 5	Secondary antibodies for western blot and confocal microscopy. ....	22
Table 6	Antibodies for flow cytometry. ....	22
Table 7	PCR amplification of plasmid-DNA. ....	25
Table 8	PCR sequencing of plasmid-DNA. ....	26
Table 9	Mutagenesis of plasmid-DNA. ....	27
Table 10	Composition of cell culture media. ....	30
Table 11	Cloning of PTK into the pcDNA3.1 expression vector. ....	34
Table 12	List of Oligonucleotides ....	76

# 1. Introduction

## 1.1. Acute lymphoblastic leukemia

Cancer is the primary cause of death in children between the ages of 1 and 14 years and acute lymphoblastic leukemia (ALL) is the most frequent type of cancer<sup>1</sup>. ALL occurs with an annual incidence of 3 to 4 per 100,000 children between 0 to 14 years, in contrast to the incidence of 1 per 100,000 in children older than 15 years<sup>2</sup>. ALL represents 75% of all acute leukemias in childhood and it consequently corresponds to 34% of all cancers in children<sup>2</sup>. ALL most frequently occurs at the age of 2-5 years, but it can also develop at adulthood. Conversely, acute myeloid leukemia (AML) and chronic myeloid leukemia (CML) are more frequent in older ages<sup>2,3</sup>. Regarding gender and race, male and white children have shown a modest predominance of ALL<sup>2</sup>.

The appealing idea to include ALL in the list of cancers that have succumbed to treatment is the result of cure rates higher than 80%<sup>3,4</sup>. Nevertheless, the poor clinical outcome in adults with ALL (mortality rate higher than 60%)<sup>5</sup>, and the remaining 20% of ALL patients that do not respond favorably to the treatment, not to mention severe acute and long-term adverse effects of conventional cytotoxic treatment, justify the continued search for prognostic markers and improvements in therapeutic approaches.

Prognostic markers used to predict the outcome in ALL are generally grouped in clinical factors (age, gender, and white blood cell count), biological factors (immunophenotype, genotype), and more recently minimal residual disease (MRD)<sup>1</sup>. Over the years, age at diagnosis has remained a strong predictor of outcome<sup>3</sup>. Patients aged 1 to 9 years had a better outcome than either newborns or adolescents<sup>1,3</sup> (Figure 1). The poorest outcome occurs in infants diagnosed at less than 12 months<sup>6</sup>. However this group represents less than 5% of childhood ALL<sup>7</sup>.

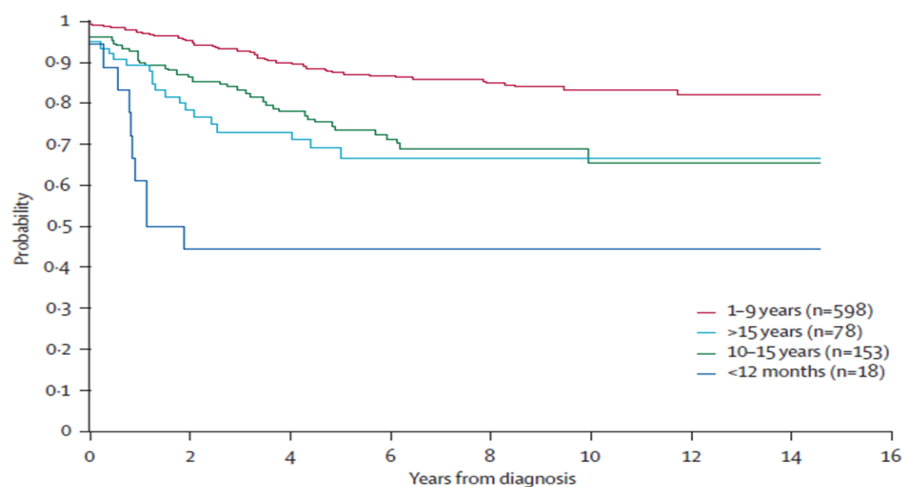


**Figure 1 Kaplan-Meier survival analysis.**

The probability of event-free survival in accordance with years from diagnosis was estimated. Patients between the ages of 1 and 9 exhibit favorable treatment outcomes with 85% of 5 years event-free survival, in contrast to the 44% of 5 years event-free survival in infants younger than 1 year. Graphic adapted from Pui, Lancet. 2008<sup>3</sup>.

### 1.1.1. Primary genetic abnormalities

ALL is a malignant disease that occurs mainly as *de novo* disease, and less commonly as a therapy related or secondary ALL<sup>2</sup>. Although the precise molecular mechanisms that lead to development of ALL remain unknown, it is considered that ALL originates from crucial genetic alterations in hematopoietic precursor cells<sup>8, 9</sup>. Gene deletion, abnormal proto-oncogene expression, chromosomal translocations producing fusion genes that encode active kinases and modified transcription factors, and aneuploidy (hypodiploidy <45 chromosomes or hyperdiploidy >50 chromosomes) are common genetic mutations in ALL<sup>8</sup>.

Chromosomal aberrations constitute the hallmark of ALL. The most frequent chromosomal alterations are aneuploidy, especially hyperdiploidy, and the chromosomal translocation ETV6-RUNX1 t(12:21), which represent 26% and 22% of the B-precursor ALL, respectively (Figure 2)<sup>8, 10</sup>. However, more than 20% of the patients with childhood ALL lack obvious structural and numerical chromosome aberrations and the genetic cause for disease in these individuals remains obscure.

Genetic lesions contribute to the malignant transformation of the hematopoietic progenitor cells that are committed to differentiate into B-cell or T-cell pathways by conferring the ability to overcome regulatory processes that control the capacity of self-renewal, proliferation, differentiation and support resistance to apoptosis<sup>11,12</sup>. Furthermore, these genetic aberrations can be used in risk-adapted treatment stratification<sup>2,5,9</sup>.

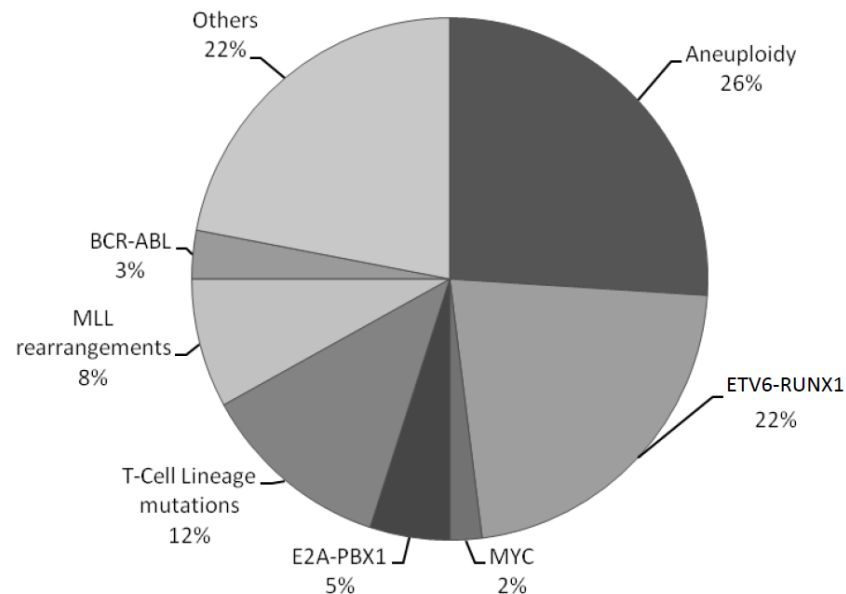


**Figure 2 Frequency of genetic alteration in ALL in childhood.**

Relative frequencies of chromosome alterations found in B-cell and T-cell acute lymphoblastic leukemia. Graphic adapted from Pui, N Eng J Med. 2004<sup>8</sup>.

### 1.1.2. Cooperative mutations

Although chromosomal rearrangements play an essential role in the pathogenesis of ALL by deregulating processes that govern cell fate, these genetic alterations are generally not sufficient to induce overt leukemia<sup>13</sup>. A multi-step model of leukemogenesis<sup>14, 15</sup>, where primary mutations, such as described above, must collaborate with secondary "*cooperative mutations*" to induce leukemia<sup>3, 8, 15</sup>. Some of these secondary mutations that have been extensively studied are listed below.

#### FLT3 receptor

FLT3 (Fms-like tyrosine kinase 3) is a receptor tyrosine kinase expressed in both myeloid and lymphoid stem cells<sup>16</sup>. Typically, the FLT3 receptor is activated by its ligand (FLT3L) and promotes cell growth in hematopoietic stem cells<sup>17</sup>. However, high-level expression of FLT3 receptor, observed in nearly all the cases of AML<sup>18</sup> or in ALL with (mixed-lineage-leukemia) MLL rearrangement<sup>19</sup>, induces self-activation and ligand independency. Furthermore, activation-loop mutations stabilize the receptor in an active conformation and allow free access of the ATP to the kinase domain<sup>20, 21</sup>. These FLT3 mutations induce an aberrant and constitutive downstream signaling of the FLT3 receptor, and promote proliferation and/or survival of the leukemic cells<sup>17</sup>.

#### Retinoblastoma pathways

The tumor suppressor retinoblastoma protein family members (Retinoblastoma protein (RB), p130, p107) have an important role in controlling cell cycle and DNA replication<sup>8, 22</sup>. Binding of RB to E2F transcription factors effectively suppresses the capacity of E2F to transcribe genes essential for entry into S phase by recruitment of histone deacetylases (HDAC)<sup>23</sup>. However, in response to external mitogenic signals, the RB inhibitory functions are abolished due to phosphorylation of RB which is triggered by complex formation between cyclin-D and cyclin-dependent kinase (Cdk)<sup>8, 22</sup>. The INK4 proteins (p16<sup>INK4a</sup>, p15<sup>INK4b</sup>, p18<sup>INK4c</sup>, p19<sup>INK4d</sup>) inhibit the cyclin D-Cdk complexes, thereby restoring the inhibitory properties of RB<sup>24</sup>. Although mutations that affect RB family members are extremely rare, p16<sup>INK4a</sup> and p15<sup>INK4b</sup> loss-of-function mutations and cyclin-D or Cdk overexpression, have been observed at high frequency in ALL<sup>24-27</sup>.

#### p53 pathways

Different stress-signals like DNA damage, hypoxia, and abnormal cell proliferations are well known to activate p53 tumor suppressor transcription factor. The activated p53 in turn induces responses that induce either cell-cycle arrest or apoptosis, depending on the cellular circumstances<sup>28, 29</sup>, therefore preventing malignant transformation. Regulation of the p53 activity is carried out by human double minutes-2 (HDM2) proteins, which have a crucial function in the degradation of p53 by inducing ubiquitylation and subsequent degradation by the proteasomes. HDM2 proteins in turn are regulated by p14<sup>ARF</sup>, consequently preventing p53 degradation<sup>8, 30</sup>. As for RB proteins, mutations affecting p53 itself, are an uncommon event in ALL. However, mutations that either lead to HDM2-overexpression or downregulation of the expression of p14<sup>ARF</sup> or p21<sup>CIP1</sup> (transcriptional target of p53), occur in more than 50% of ALL cases<sup>30, 31</sup>.

## 1.2. Hematopoiesis

Hematopoiesis is the process by which all blood components are made, and after birth and under physiological conditions it is restricted exclusively to the bone marrow. Hematopoiesis is a hierarchical process where hematopoietic stem cells (HSC), that have the potential of self-renewal, develop into multipotent progenitors (MPPs), which lose self-renewal capacity but can differentiate into all hematopoietic lineages<sup>32</sup>. MPPs further give rise to lineage-committed common lymphoid and common myeloid progenitors (CLPs and CPMs, respectively), which in turn differentiate, after many cell divisions, into mature cells (Figure 3)<sup>33, 34</sup>. During the hematopoietic process, several cytokines and growth factors are required at all stages of maturation for cell survival and proliferation (Figure 3)<sup>33</sup>.

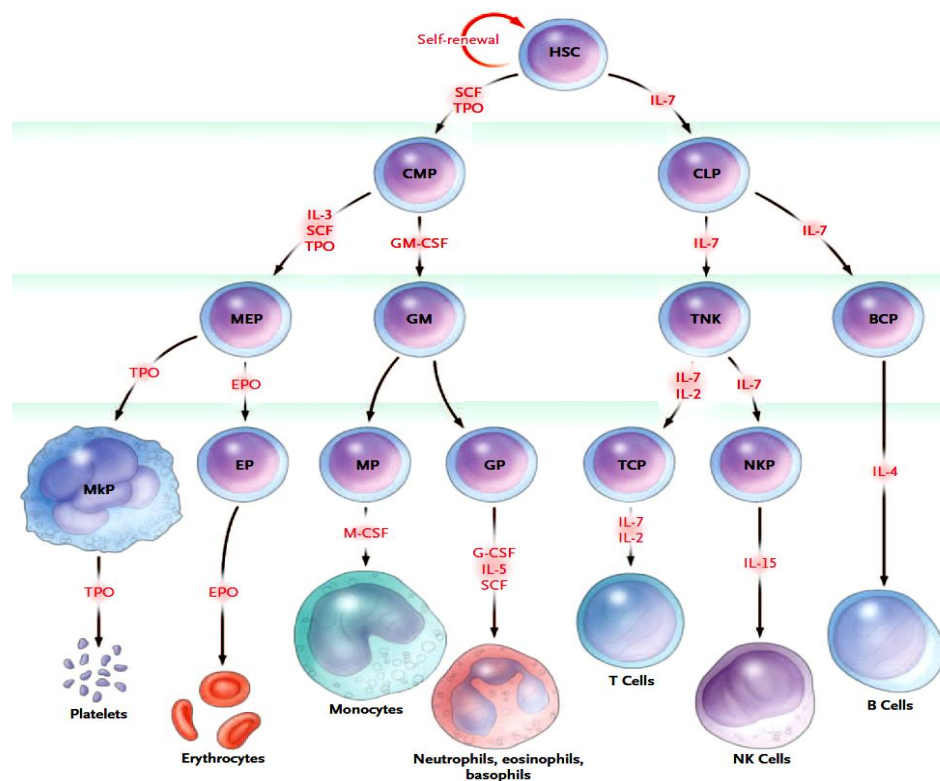


**Figure 3 Hierarchy of hematopoiesis.**

The HSCs can either go through self-renewal or progress to MPPs (without detectable self-renewal potential; for simplicity not shown). The latter gives rise to committed progenitor cells, CLPs and CMPs. Subsequently, CLP and CMP cells give rise to more differentiated progenitors committed to two lineages (TNKs, GMs, MEPs). Finally, these cells give rise to unilineage committed progenitors (BCPs, NKPs, TCPs, GPs, MPs, EPs and MkPs), that in turn differentiate into mature cells. Cytokines and growth factors that support the survival, proliferation, or differentiation of each type of cell are shown in red. TNK= T-cells and natural killer cells (NK) progenitor, GM= granulocyte and macrophage progenitor, MEP= megakaryocyte and erythroid progenitor, BCP= B-cells progenitor, NKP= NKs progenitor, TCP= T-cells progenitor, GP= granulocytes progenitor, MP= megakaryocyte progenitor, EP= erythrocyte progenitor, IL= interleukin, TPO=

thrombopoietin, M-CSF= macrophage colony-stimulating factor, GM-CSF= granulocyte-macrophage colony-stimulating factor, EPO= erythropoietin. Graphic adapted from Kaushansky, N Engl J Med. 2006<sup>33</sup>.

### 1.2.1. B-cell development

The first event in B lymphopoiesis takes place in the bone marrow (*primary B-cell development*), where HSCs undergo differentiation and proliferation through a highly controlled process that leads to surface Ig-expressing B-cells<sup>35</sup>. These cells together with natural killer (NK) cells and T-cells represent the lymphocyte population. Before the release of B lymphocytes into the bloodstream, the immature B-cells migrate to the spleen (*secondary B-cell development*), where they differentiate into mature, naive B-cells<sup>35</sup>. The B lymphocytes constitute an important element of the immune system owing to their crucial functions in humoral immunity and T-cell immune response. Furthermore, B-cells play an essential role in tumor immunity, organ transplant rejection and wound healing<sup>36</sup>.

During the B-cell development, at the early stage of CPLs, rearrangements of  $D_H-J_H$  on the immunoglobulin heavy chain (IgH) locus are initiated by RAGs (recombination activating genes)<sup>37</sup>, whereas, rearrangements of  $V_H-DJ_H$  occur at later pro-B stages<sup>38</sup>. Successful VDJ recombination leads to  $Ig\mu$  chain expression in pre-B-cells<sup>39, 40</sup>. The surrogate light chain (SLC) is a heterodimer made of CD179a and CD179b invariant proteins<sup>37</sup>. Assembly of two  $Ig\mu$  chains, together with two SLCs and two signaling subunits ( $Ig\alpha$  and  $Ig\beta$ ) results in the expression of pre-B-cell receptor (pre-BCR) (Figure 4)<sup>37</sup>.

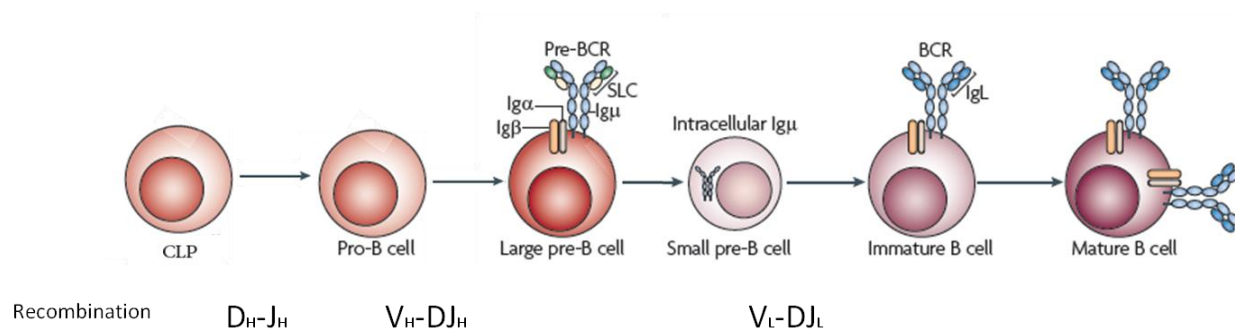


**Figure 4 B-cell development.**

Rearrangements of the IgH locus are initiated at early B-cell development stages, and if successful, lead to expression of  $Ig\mu$  as part of the pre-BCR in large pre-B-cells. Following rearrangements of the IgL locus in small pre-B-cells give rise to BCR expression (consisting of  $Ig\mu$  heavy and  $Ig\lambda$  or  $Ig\kappa$  light chains) in immature B-cells.  $IgL$ = immunoglobulin light chain,  $Ig\mu$ = immunoglobulin heavy chain, D= diversity, J= joining, V= variable. Graph adapted from Herzog, N Eng J Med, 2009<sup>37</sup>.

### 1.2.2. Pre-BCR signaling

The expression of the pre-BCR, albeit only transitory, is a crucial step in the B-lineage development<sup>37</sup>. However, pre-BCR signaling has not been studied as intensely as the BCR signaling<sup>41</sup>. The importance of the pre-BCR has clearly been demonstrated in different mouse model experiments<sup>42</sup>, where induced deletions of exons that encode the transmembrane region of  $Ig\mu$  or the Ig-associated signal transduction chains  $Ig\alpha$  and  $Ig\beta$ , resulted in an increase of pro-B-cells and a complete block of the B-cell development

at this stage. In the same fashion, mutations in the human CD179b gene resulted in a profound blockage of the B-cell development together with agammaglobulinaemia<sup>43</sup>.

Contrary to the BCR, where signaling is initiated by antigen recognition, the dependency of the pre-BCR signaling on ligand-induced activation remains obscure. Several studies have shown that the pre-BCR signaling is activated in a ligand-independent fashion<sup>44, 45</sup>. Consistent with these data, Guo *et al.* suggested that without any extracellular ligand, pre-BCR signaling can be initiated in a lipid-raft-dependent manner owing to the high concentration of Src kinases (described in section 1.4) and/or low presences of inhibitors<sup>41</sup>.

On the other hand, further studies have revealed the crucial role of the non-immunoglobulin like region of CD179b during the initiation of the pre-BCR signaling<sup>46</sup>. In agreement with these findings, the positively charged CD179b chain may interact with multiple molecules including DNA, insulin, lipopolysaccharide, galectin and heparan sulphate, and induce aggregation and signaling<sup>47, 48</sup>.

It has been proposed that the BCR or pre-BCR induce the same signal transduction pathways owing to the fact that the same signaling molecules are recruited and similar signaling interactions are initiated<sup>41, 49</sup>. These interactions include several important signaling proteins, such as protein tyrosine kinases (PTK) and B-cell adaptor proteins (e.g. BLNK). These factors are indispensable for initiation of pre-BCR signaling and activation of downstream targets, which in turn, have a critical role modulating B-cell fate decisions<sup>49</sup>.

### 1.3. Protein tyrosine kinases

Cellular communication and development in metazoans is frequently achieved by tyrosine phosphorylation<sup>50</sup>. This is a reversible and highly regulated post-translational modification, which involves the transfer of phosphate groups from ATP to tyrosine residues on target proteins. Tyrosine phosphorylation is catalyzed by protein tyrosine kinases. PTK are important components of cell signaling networks and have essential functions in normal physiological processes during development and adult homeostasis<sup>50</sup>.

The Human Genome Project has revealed that approximately 0.3% of the 32,000 human coding genes encode for PTK<sup>51</sup>. According to this data, the human genome encloses 90 tyrosine kinase genes and 5 presumably tyrosine kinase pseudogenes<sup>52</sup>. 58 of the 90 tyrosine kinase genes are categorized as receptor tyrosine kinases (RTKs), because they encode a protein with a predicted transmembrane domain. In turn, these 58 RTKs can be further divided into 20 subfamilies based on similarities in the kinase domain sequence<sup>52</sup>. The remaining 32 tyrosine kinase genes encode for non-receptor tyrosine kinases (without predictable transmembrane domain) and are grouped in 10 subfamilies based on their structure similarities (Figure 5)<sup>51, 52</sup>. The five pseudogenes are characterized by the absence of protein expression, due to the lack of intronic sequences, truncation of the coding region and presence of in-frame stop codons<sup>52</sup>.

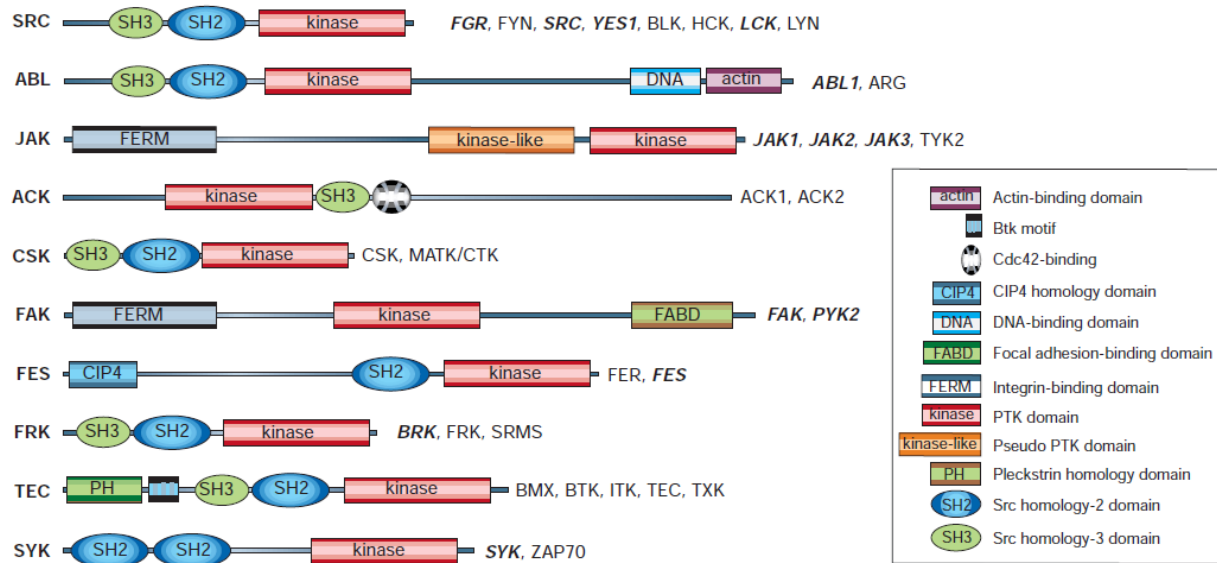


**Figure 5 Human non-receptor protein tyrosine kinase.**

The name of the family is shown to the left and the family members are indicated to the right. The tyrosine kinase members in bold and italic have been implicated in human cancers. Descriptions of the protein structures are noted. SRC= v-src (Schmidt-Ruppin A-2) viral oncogene homolog (avian), ABL= Abelson murine leukemia viral oncogen homolog, JAK= janus kinases, ACK= acetate kinase, CSK= c-src tyrosine kinase, FAK= focal adhesion kinase, FES= Feline sarcoma oncogen, FRK= fyn-related kinase, TEC= tec protein tyrosine kinase, SYK= sleep tyrosine kinase. Graph adapted from Blumen-Jensen, Nature, 2001<sup>51</sup>.

### 1.3.1. Non-receptor protein tyrosine kinases

The non-receptor tyrosine kinases (NRTK) are fundamental elements of the signaling networks triggered by several receptors present on the cell surface, such as tyrosine kinase receptors, G-protein-coupled receptors and receptors that are involved in the immune response (e.g. B-cell receptor)<sup>53</sup>. The NRTK families are implicated in different signaling processes that generally include cell proliferation, cell motility, and metabolism as well as survival<sup>54</sup>. The NRTK exhibit a domain structure that executes the catalytic function of the protein (kinase domain) as well as domains involved in protein-protein interaction and protein-DNA interaction (Figure 5)<sup>51</sup>. Although Src homology 2 (SH2) and 3 (SH3) domains are the most frequent protein-protein association domains, there are NRTK families that possess additional family specific domains for protein-protein interactions (e.g. the PH domain in the TEC family. See below.)<sup>55</sup>.

### 1.3.2. Architecture of NRTK

#### Kinase domain

The kinase domain of the NRTK conserves the bilobal protein kinase domain (kinase N-lobe and kinase C-lobe) present in all tyrosine and serine/threonine kinases<sup>56</sup>. Overall, the function ascribed to the kinase domain involves binding of ATP (usually as a complex with divalent cations such as  $Mg^{2+}$ ) and transfer of phosphate to tyrosine, serine or threonine residues of the protein substrate. Transfer of phosphate

groups as well as nucleotide binding occurs in the fissure between the two lobes<sup>56</sup>. The crucial role of the kinase domain in the NRTK context is discussed in further detail in section 1.4.1.

### Src homology domain (SH-domain)

As mentioned above, protein-protein interaction is achieved mainly through SH2 and SH3 domains. The SH2 domain can be found in many signaling proteins<sup>57</sup>. These domains are made of around 100 amino acids localized exclusively N-terminal to the kinase domain<sup>58</sup>. Furthermore, SH2 domains have ligand-preferences for phosphotyrosine-containing sequences, which make them important tools in the protein tyrosine kinase pathway analysis<sup>59</sup>. Although the kinase activity of the catalytic domain does not require SH2 domains *per se*, the SH2 domains play an important role in regulating the kinase domain and its interaction with other proteins in the cellular context<sup>58</sup>.

The SH3 domain is a small motif (approximately 60 amino acids) and unlike the SH2 domain, the SH3 domain commonly recognizes proline-containing sequences independent from further posttranslational modifications<sup>58</sup>. The most common structure formed by proline-rich sequences is the proline-type II helix (a left-handed helix with three residues per turn), which has a dominant role in the recognition of cellular binding proteins<sup>60</sup>.

## 1.4. SRC family kinase

NRTK are critical elements in the regulation of many signaling networks. However, due to the high number and complexity of these processes, only the role of SFK regulating signal transduction as well as regulatory mechanisms are discussed in detail in the next section.

The SFK are the largest subfamily of the NRTK, which include Blk (B lymphoid tyrosine kinase), Fgr (Gardner-Rasheed feline sarcoma viral oncogene homolog), Fyn (FYN oncogene related to SRC, FGR, YES), Hck (hematopoietic cell kinase), Lck (lymphocyte-specific protein tyrosine kinase), Lyn (v-yes-1 Yamaguchi sarcoma viral related oncogene homolog), c-Src (v-src sarcoma (Schmidt-Ruppin A-2 viral oncogene homolog), Yes1 (v-yes-1 Yamaguchi sarcoma viral oncogene homolog 1). Among the SFK members, c-Src was the first oncogene identified and is the best characterized SFK member<sup>61</sup>. All SFK members exhibit a highly conserved domain structure along with similar mechanism of activation and regulation. In the following sections SFK structure and activation as well as their roles in signaling pathways are discussed in further detail.

### 1.4.1. Structure and regulation of SFK

Basically, all the SFK members possess the same domain structure which consists of four SRC-homology domains and a C-terminal tail (Figure 6). The SH4 domain, also termed the unique domain, is located in the N-terminal tail of the protein. The SH4 domain is the most divergent domain among the SFK members. Although the precise functions of the SH4 domain are not well defined, this domain contains a myristoylation site (present in all SFK) and a palmitoylation site (for all SFK except Src and BIK) which play an important role in the association of SFK to the plasma membrane<sup>61, 62</sup>. Palmitoylation sites are further necessary for association of the SFK with cholesterol-enriched membrane micro-domains called "lipid-rafts"<sup>63</sup>.

The SH1 domain or kinase domain is composed of kinase-N and kinase-C lobes. The kinase-N lobe contains the C-helix, which in turn bears a glutamic acid residue 310 (Glu-310) involved in regulatory mechanisms displayed for SFK members<sup>56</sup>. The kinase-C lobe contains the autophosphorylation site tyrosine 416 (Tyr-416) in chickens or tyrosine 419 (Tyr-419) in humans, and is required for full activation of all SFK members<sup>56</sup>. The SH2 and SH3 domains together with the C-terminal tail are implicated in the activity and interaction of the SFK.

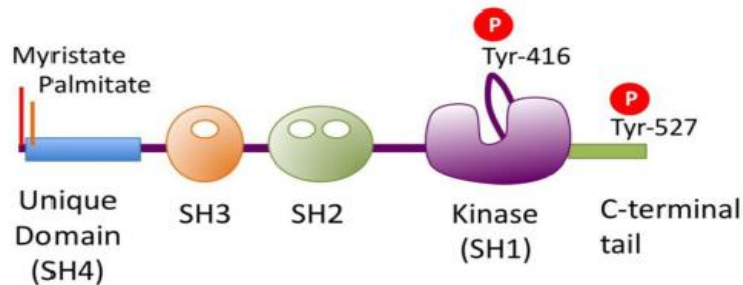


**Figure 6 Structure of SFK proteins.**

Molecular structure of SFK. Despite the fact that c-SRC of the SFK was the first oncogene described and is one of the most studied, here it is used as an example to represent the entire SFK family. The four SH-domains as well as the N-terminal and C-terminal tails are shown. The C-terminal tail contains the negative regulatory tyrosine residue 527 (Tyr-527), which downregulates the c-SRC activity. The kinase domain contains the tyrosine residue 416 (Tyr-416), which is necessary for full activation of the protein. Graph adapted from Okada, *Int J Biol Sci.* 2012<sup>62</sup>.

In resting cells inactivation of the SFK takes place when the C-terminal tail is phosphorylated at the tyrosine residue 527 (Tyr-527). This phosphorylated residue stabilizes the inactive conformation through two mechanisms: 1) binding of the SH2-domain to the phosphorylated C-terminal Tyr-527, and 2) binding of the SH3-domain to the SH2-kinase domain linker (a segment that connects the SH2 and kinase domains). As a result of these intramolecular interactions, the protein assumes a closed molecular structure<sup>56, 61, 64</sup> (Figure 7A). In addition, the inactive conformation also disrupts the hydrogen-bond between Glu-310 and Lys-295 residues of the C-helix, crucial for Mg-ATP binding in the catalytic pocket of the kinase domain and sequesters the Tyr-416 residue making it inaccessible for phosphorylation<sup>62</sup>.

Activation of the SFK members occurs when the C-terminal Tyr-530 is dephosphorylated. This leads to the release of all inhibitory intramolecular interactions and results in dramatic conformational changes that uncover the kinase domain<sup>64</sup>. The active SFK members catalyze the autophosphorylation at the Tyr-419, necessary for full protein activation and increase its potential for substrate interactions (Figure 7B)<sup>61</sup>.

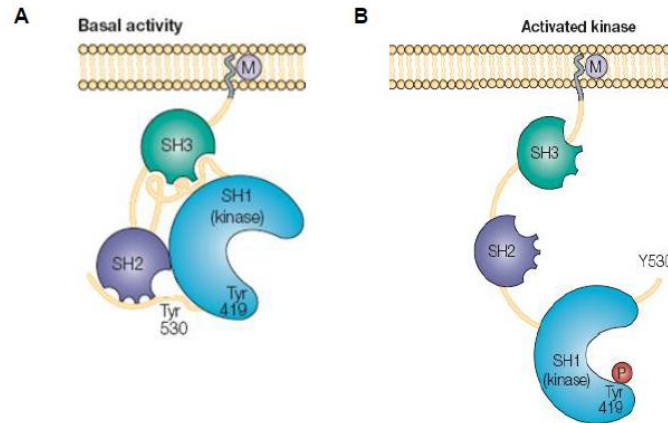


**Figure 7 Activation of the SFK proteins.**

A) The inactive state of the SFK results from the phosphorylation of the C-terminal tyrosine negative residue 530 (Tyr-530), and it binds back to the SH2 domain. This interaction between the kinase domain and the SH3 domain, maintains SFK in a closed molecular structure. B) Conversely, the removal of the phosphate group at the Tyr-530 results in displacement of inhibitory intramolecular interactions and opening of the molecular structure. Full activation of the SFK requires phosphorylation at Tyr-419. The human c-Src is used to exemplify the activation of SFK members. Graph adapted from Yeatman, Nat Rev Cancer. 2004<sup>61</sup>.

### 1.4.2. Intramolecular regulation of SFK

SFK members are able to activate downstream target proteins either because of high levels of SFK proteins or because they are activated<sup>61</sup>. Indeed, both highly active and high levels of SFK proteins have been described in human cancer<sup>65</sup>. Therefore, it is not surprising that SFK members can be regulated in terms of both activity and quantity via C-Src tyrosine kinase (Csk) and ubiquitin ligase proteins, respectively. Recently, the observation that the catalytic activities of the SFK can be regulated by their subcellular localization has emerged as a new regulatory mechanism<sup>66</sup>. On the other hand, interactions of the SH2 and SH3 domains of SFK with proteins, such as focal adhesion kinase (FAK)<sup>67</sup> or growth factor receptors<sup>68</sup>, contribute to SFK activation<sup>69</sup>.

#### Regulation of SFK by Csk

Csk is structurally related to SFK, but Csk lacks the N-terminal acylation sites, the autophosphorylation site, and the C-terminal regulatory sites<sup>62</sup>. Csk performs the inactivation of all SFK members by phosphorylation of the C-terminal negative regulatory tyrosine residue<sup>61</sup>, and induces the closed molecular structure described above.

The vital role of Csk as a negative regulator of SFK members was revealed by *in vivo* experiments in mice lacking Csk<sup>70</sup>. In this study, the loss of Csk leads to constitutive activation of SFK and aberrant mice development, and increased activity of all SFK in Csk-deficient cell lines. Furthermore, activation of SFK upon downregulation of Csk has been found in human cancer<sup>71</sup>. These results led to the conclusion that Csk is indispensable for the regulation of all SFK. Conversely, phosphatases, such as protein tyrosine phosphatase- $\alpha$  (PTP $\alpha$ ), are able to dephosphorylate the C-terminal tyrosine regulatory residue *in vitro*

and *in vivo*<sup>72</sup> and therefore, promote SFK activation. Csk however, is predominantly present in the cytosol, whereas its substrates are anchored to the plasma membrane, therefore an additional mechanism for its recruitment to the plasma membrane is thought to be a critical step in Csk regulation<sup>62, 66</sup>. The discovery of palmitoylated-transmembrane Csk binding protein/phosphoprotein associated with glycosphingolipid-1 (Cbp/PAG1), which is ubiquitously expressed and co-localized with SFK in membrane lipid rafts, unveiled how Csk is recruited to lipid rafts<sup>73</sup>. A single molecule of PAG/Cbp phosphorylated by SFK binds Csk through the Csk-SH2 domain. Thus, Csk is brought into close proximity to SFK and efficiently inactivates all the Src family members by phosphorylation of the negative regulatory tyrosine residue<sup>62, 63</sup> (Figure 8).

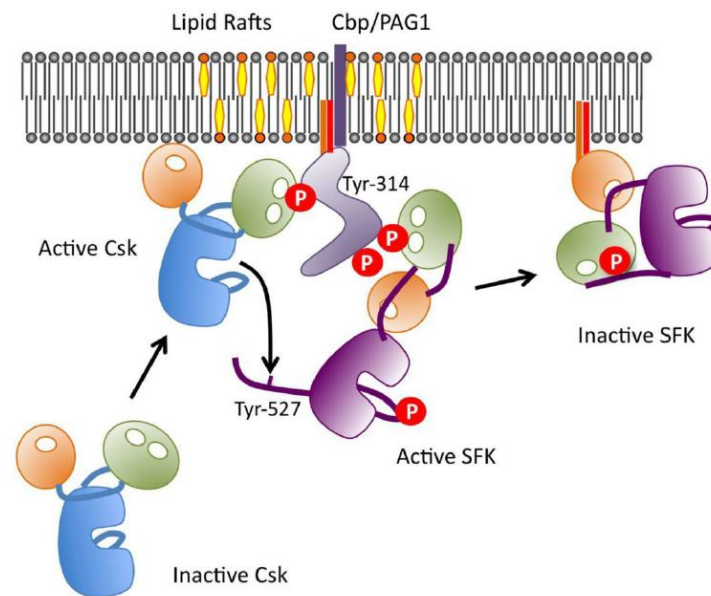


**Figure 8 The roles of Cbp/Csk and lipid rafts in regulating the function of SFK.**

When Cbp is phosphorylated by active SFK, Csk is recruited to lipid rafts via binding to Cbp at phosphorylated tyrosine 314 (pTyr-314) and phosphorylates Tyr-527 to inactivate the catalytic activity of SFK. The inactivated SFK then relocate to non-raft compartments. Graph adapted from Okada, *Int. J. Biol. Sci.* 2012<sup>62</sup>.

### Regulation of SFK by ubiquitylation

Regulation of SFK in a quantitative manner is mediated by ubiquitin ligase proteins, such as E3-ubiquitin ligase CBL, which promotes SFK ubiquitylation and subsequent degradation by the proteasome<sup>61</sup>. The relevant function of CBL was shown by Kim and collaborators, where the transforming potential of c-Src was suppressed by Cbl-c through ubiquitin-dependent protein degradation<sup>74</sup>. In addition, it has been shown that cancer cells exhibit a deregulated proteasome pathway, which might result in Src activation<sup>75</sup>.

### Regulation of SFK by subcellular localization

Beyond the direct inhibition of kinase activity by protein kinases and phosphatases, catalytic activity of SFK can be regulated by its subcellular localization within sphingolipid- and cholesterol-rich membrane microdomains called lipid-raft. Since all SFK are myristoylated and seven out of nine are palmitoylated at the N-terminal domain, it has been thought that they are either permanently localized within lipid rafts or move to lipid rafts after receptor cross-linking<sup>76</sup>. The localization of the SFK inside of this cholesterol-rich microdomains, represent a spatial as well as temporal sequestration of SFK either because they are concentrated in close proximity to regulatory mechanisms or because they are kept away from downstream targets<sup>66</sup>.

### Receptor-mediated activation of SFK

The SFK can also be activated by a wide range of receptor tyrosine kinases, including platelet-derived growth factor receptor (PDGFR), epidermal growth factor receptor (EGFR), fibroblast growth factor receptor (FGFR), insulin-like growth factor receptor (IGFR), stem cell factor receptor (SCFR) and others<sup>61</sup>. The SFK interact with these receptors through association between their SH2 domain and phosphorylated tyrosine residue of the activated receptor<sup>77</sup>. This interaction promotes SFK activation probably by releasing the intramolecular interaction between the SH2 and the C-terminal tail that hold SFK in a closed molecular configuration, thus allowing SFK to adopt an open conformation<sup>77</sup>.

## 1.5. The SRC family kinase member Lyn

The SFK Lyn is widely expressed in hematopoietic cells and is the predominant SFK in B-cells<sup>78, 79</sup>. The *lyn* gene is localized on 8q13 of the human chromosome 8 and it can be found in two isoforms, p53 and p56, as a product of alternative splicing of the exon 2<sup>80</sup>. The larger p56 isoform is designated LynA and has additional 20 amino acids in the SH4 domain compared to the smaller isoform p53, designated as LynB<sup>81</sup>. Although there is less evidence of a potential isoform-specific function between LynA and B, further research involving Lyn in an isoform-specific manner is required<sup>81</sup>. Lyn, like other SFK members, can be regulated and activated by mechanisms described above. Interestingly, whereas Lyn is not expressed in T-cells, it has been found to play an important role in several hematopoietic cells including stem progenitor cells, B-cells, macrophages, red blood cells, mast cells and platelets<sup>82</sup>.

In addition, Lyn is expressed in non-hematopoietic cells, for example prostate, colon and breast cells, but the specific role of Lyn in these cells remains largely unknown<sup>81</sup>. Finally, Lyn has a significant impact on signal initiation upon BCR cross-linking, reflected by a rapid augmentation of Lyn phosphorylation and kinase activity after BCR engagement<sup>83</sup>. The critical role of Lyn in the initial BCR signaling events is discussed in further detail in the following sections.

### 1.5.1. Subcellular Lyn localization

The N-terminal domain of Lyn possesses a myristoylation and palmitoylation site at Gly-2 and Cys-3, respectively<sup>62</sup>. These lipid modifications are required for attachment of Lyn to the inner layer of the plasma membrane<sup>84</sup>. There is evidence suggesting that the subcellular distribution of Lyn is important for its function, for example, caspase 3 cleaves Lyn in the 18 aspartic residue at unique N-terminal

domains, resulting in complete removal of the myristoylation and palmitoylation sites<sup>84</sup>. Whereas the full length Lyn is located in the plasma membrane, caspase-cleaved Lyn remains exclusively in the cytosol and acts as a negative regulator of apoptosis<sup>85</sup>. In agreement with this concept, Contri et al. found that B-cell chronic lymphocytic leukemia (B-CLL) cells harbored higher levels of Lyn aberrantly distributed throughout membrane and cytosolic compartment and not confined to lipid raft structures as compared with normal B-cells<sup>86</sup>. Moreover, inhibition of Lyn by ATP-competitive inhibitors in these leukemic cells resulted in increased apoptosis, highlighting the anti-apoptotic role of Lyn and underlining the relevance of Lyn subcellular distribution in leukemogenesis<sup>86</sup>.

### 1.5.2. Lyn and BCR signaling pathway

As mentioned above, the recruitment of similar signaling molecules after pre-BCR or BCR cross-linking indicates that both receptors utilize identical signal transduction pathways<sup>37</sup>. The ligand-binding complex of the pre-BCR is made of a transmembrane immunoglobulin heavy chain (IgH) covalently associated with a light chain (IgL) together with a non-covalently associated Ig $\alpha$ /Ig $\beta$  heterodimer. During the earliest biochemical events after receptor-engagement, a single tyrosine residue in immunoreceptor tyrosine-based activation motif (ITAM) at the cytoplasmic tail of Ig $\alpha$  becomes phosphorylated, and in turn, promotes the recruitment and activation of Lyn<sup>87</sup>. Although Lyn is dispensable for BCR signaling initiation, it seems to be a major player recruited to this process, emphasizing the crucial role of Lyn activating downstream targets<sup>37</sup>.

Additionally, activation of Lyn results in double-phosphorylation of the ITAM (db-ITAM) in the Ig $\beta$  and subsequent recruitment of SYK. Binding of SYK to the dp-ITAM releases the inhibitory interaction that holds SYK inactive, thereby, facilitating activation of its kinase domain. Ultimately, activated SYK plays an essential role in phosphorylating downstream targets that trigger signaling pathways involved in B-cell proliferation<sup>87</sup>. The relevance of SYK as a key molecule that promotes B-cell proliferation was demonstrated by Tuner et al<sup>88</sup>. In this study, SYK-depleted B-cells showed a complete arrest of the B-cell maturation at pre-B stage<sup>88</sup>. Moreover, one of the SYK targets is the lipid-modifying kinase phosphoinositide 3 kinase (PI3K), which was described to be involved in manifold biological responses, including cell growth, proliferation, and survival<sup>89</sup>.

## 1.6. SFK and human cancers

Aberrant kinase activation and/or high protein levels of SFK members are a common feature in several human cancers, although mutations that lead to activation or amplification of these proteins are rare events. Therefore, many efforts have been made to study kinases and phosphatases that have a role in activation or repression of SFK. There are several ways to regulate SFK activity, and the failure of any of these could potentially contribute to the SFK activation observed in human cancers. The most common regulatory dysfunctions observed in cancer cells are briefly discussed below.

### 1.6.1. Deregulation of the C-terminal negative regulatory domain

The phosphorylation of the C-terminal negative regulatory tyrosine residue (Tyr-530 in Src, and the respective homologous site in the other SFK members) represents one of the mechanisms for downregulating SFK activity and is thus well balanced by the action of protein kinases and phosphatases. As described before, the C-terminal Src kinase (Csk) represents a critical mediator for SFK activity and it might act as a tumor suppressor in human cancer<sup>90</sup>. Therefore, reduction of the Csk expression leads to reduction of phosphorylation at the inhibitory tyrosine residue, which promotes SFK activation. Indeed, reduction of Csk levels has been observed in hepatocellular carcinoma and it correlates with augmentation of Src kinase activity<sup>71</sup>.

Furthermore, other mechanisms of regulating Csk play a role in human malignancies; for example, the transmembrane adaptor protein Cbp/PAG1, a lipid raft associated binding partner of Csk. Several studies have highlighted the role of Cbp/PAG1 suppressing the oncogenic potential of SFK either by downregulating the kinase activity or by sequestering SFK within lipid raft structures<sup>91</sup>. Concurring with this hypothesis, Cbp/PAG1 expression was found to be downregulated in colorectal cancer (CRC)<sup>90</sup>. Moreover, complete loss of PAG1 expression was observed in 10% of near-haploid ALL<sup>92</sup>. Furthermore, re-introduction of Cbp/PAG1 in CRC cells increased Csk membrane localization and reduced cell invasion, whereas in Cbp/PAG1 depleted cells an increase of SFK activity and invasive potential was observed<sup>93</sup>.

### 1.6.2. Deregulation of SFK by phosphatases

While only Csk has so far been described to phosphorylate SFK members at the C-terminal negative regulatory residue, several protein tyrosine phosphatases (PTPs) are responsible for the removal of the C-terminal phosphate and thus function as activators of SFK, such as PTP $\alpha$ , PTP $\gamma$ , SH2-containing phosphatase 1 (SHP-1), SHP-2 and PTP1B<sup>61, 94</sup>. It has been shown that high levels of PTPs correlate with diminished phosphorylation on the C-terminal tyrosine residue and high SFK activity<sup>94</sup>. Although the exact role of PTPs in tumor development and progression is largely unknown, in some cancers like breast cancer PTP1B was found to be overexpressed and promoted activation of SFK<sup>95</sup>.

Moreover, SFK can be activated through indirect mechanisms, for example, SHP-2 can dephosphorylate the pTyr-317 of Cbp/PAG, which is responsible for the recruitment of CSK to the plasma membrane, and therefore disrupt the CSK-Cbp/PAG1 association crucial for inactivation of SFK<sup>96</sup>. Finally, downregulation of PTPs could also benefit aberrant activation of SFK. Indeed, full activation of SFK members involves autophosphorylation of the conserved Tyr-416 in the kinase domain and it is dephosphorylated by PTPN13E. In accordance with this theory, PTPN13 inactivation was described in CRC cells and contributed to SFK deregulated activity<sup>90</sup>.

### 1.6.3. Deregulation of SFK by receptor tyrosine kinases

SFK are overexpressed and/or activated in several tumors which overexpress many different receptor tyrosine kinases, indicates a possible cooperation of those proteins in tumorigenesis. Indeed, SFK and

RTKs interact directly in a SH2-pTyr-dependent manner, and this interaction disrupts the SH2-pTyr C-terminal intramolecular interactions that hold SFK in a closed configuration and therefore promote its activation<sup>61, 90</sup>. Additionally, SFK can eventually phosphorylate RTKs, including EGFR, PDGFR, IGFR and fully activate these receptors in a ligand-independent manner<sup>90</sup>. In CRC, deregulated SFK activity was found to activate RTKs, e.g. the hepatic growth factor receptor (HGFR), and these activated receptors were required to uphold SFK activity<sup>97</sup>. These data unveiled a chain of events, in which SFK promote RTK activation, and those receptors further induce a positive feedback on SFK. How this cycle is activated remains unknown<sup>90</sup>.

## 2. Working hypothesis

A fundamental feature of all human cancers, including childhood acute lymphoblastic leukemia (ALL), is the overcoming of cellular regulatory mechanisms, for example by aberrant activation of signaling pathways and networks.

As starting hypothesis, alterations in critical components of the signal transduction pathways and/or networks in ALL contribute to sustaining its leukemic phenotype. The primary aim of this study is the quantitative analysis of the protein tyrosine kinase (PTK) expression and activation state in ALL patients and the functional assessment of their role in leukemogenesis.

The selected PTK will be cloned into appropriate expression vectors to establish and validate immunological assays. Mammalian cell lines will be used for recombinant expression of selected PTK. Recombinant proteins will be employed to select specific antibodies for quantitative detection of the expression and activation of PTK in ALL patient samples, cell lines, and xeno-transplanted primary lymphoblasts from ALL patients by western blot analysis.

The extensive analysis of ALL samples will provide an overview of the expression profiles of PTK in ALL at the protein level. Moreover, to determine the functional role of these PTK in leukemogenesis, shRNA knockdown experiments will be used and cell proliferation and apoptosis will be monitored by appropriate assays. Additional functional studies, including the analysis of ligand-induced activation and subcellular localization of key PTK, will be performed to improve our understanding of the functional role of PTK in leukemogenesis.

### 3. Material and methods

#### 3.1. Chemicals

Chemicals for standard laboratory procedures were used from Applied Biosystems, Becton Dickinson, GE Healthcare, Invitrogen, J.T. Baker, Merck, Qiagen, Roche and Sigma Aldrich. All the solutions and media were prepared with double deionised water (ddH<sub>2</sub>O) or with water for injection purposes.

#### 3.2. Biological material

##### 3.2.1. Bacteria

The chemically competent *Escherichia coli* (*E. coli*) strain One Shot® TOP10 (Invitrogen), JM109 (Sigma-Aldrich) and the XL10-Gold Ultracompetent cells (Agilent Technologies) were used for high-efficient cloning and plasmid propagation.

##### 3.2.2. Cell lines

Cell line	Description
<b>697</b>	B-cell precursor leukemia. Expresses the translocation t(1;19) which leads to E2A-PBX fusion gene. DSMZ no. ACC 42.
<b>293T</b>	Human embryonic kidney cell line. Human flat-mode near-triploid karyotype. Highly transfectable derivative of the human primary embryonic kidney cell line 293 (ACC 305) carrying a plasmid containing the temperature sensitive mutant of SV-40 large T-antigen. DSMZ no. ACC 635.
<b>CCRF-CEM</b>	Human T-cell leukemia cell line. Human near-tetraploid karyotype with extensive subclonal variation. DSMZ no. ACC 240.
<b>MHH-CALL-2</b>	Human B-cell precursor leukemia cell line. Human hyperdiploid karyotype with 13% polyploidy. Hyperdiploidy with tetrasomy 21 associated with pre B-ALL in children. DSMZ no. ACC 341.
<b>MHH-CALL-3</b>	Human B-cell precursor leukemia cell line. (1;19)(q23;p13) primary and 6q-secondary rearrangements associated with pre B-ALL - resembles published karyotype. Expresses the E2A-PBX fusion gene. DSMZ no. ACC 339
<b>Nalm6</b>	Human B-cell precursor leukemia cell line. Carries t(5;12)(q33.2;p13.2). Expresses TEL-PDGFRb fusion gene. DSMZ no. ACC 128.
<b>REH</b>	Human B-cell precursor leukemia cell line. Carries t(12;21) and del(12) producing respectively ETV6-RUNX1 fusion and deletion of residual TEL. DSMZ no. ACC 22.
<b>SEM</b>	Human B-cell precursor leukemia cell line. Carries t(4;11) with breakpoints at AF4 and MLL. Carries MLL-AF4 fusion gene. DSMZ no. ACC 546.
<b>SUP-B15</b>	Human B-cell precursor leukemia cell line. Carries t(9;22)(q34;q11). Expresses BCR-ABL (e1-a2) fusion gene. DSMZ no. ACC 389.

**Table 1 Cell Lines.**

Above are listed the human suspension cell lines that were used. The most remarkable characteristics are specified.

### 3.2.3. Primary cells

Primary material	Description
CD3 <sup>+</sup>	CD3 <sup>+</sup> cells were isolated from buffy coat
CD19 <sup>+</sup>	CD19 <sup>+</sup> cells were isolated from buffy coat.

**Table 2** Primary cells.

Isolation of Human primary cells was performed as described below. The material was kindly provided by the institute of Transfusion Medicine, University Medical Center Hamburg-Eppendorf.

### 3.2.4. Pediatric acute lymphoblastic leukemia (ALL) patient samples

ALL subtype	Id number	Sex	Age	Blast in %	Material
c-ALL	5	M	2	93	BM
c-ALL	19	M	12	95	BM
c-ALL	22	F	14	90	PB
c-ALL	28	M	8	97	BM
c-ALL	31	F	8	70	BM
c-ALL	38	M	1	95	BM
c-ALL	42	F	4	99	BM
c-ALL	44	M	5	99	BM
c-ALL	45	F	3	99	BM
c-ALL	46	M	6	92	BM
c-ALL	47	M	7	89	PB
c-ALL	56	M	14	97	PB
c-ALL	66	F	6	70	PB
c-ALL	67	F	2	88	PB
c-ALL	73	M	10	91	BM
c-ALL	76	M	4	100	BM
c-ALL	82	F	2	99	BM
c-ALL	99	F	8	98	BM
c-ALL	103	M	13	87	PB
c-ALL	105	F	2	93	BM
Pre-B-ALL	9	F	7	99	BM
Pre-B-ALL	10	F	3	63	PB
Pre-B-ALL	14	M	13	100	BM
Pre-B-ALL	16	M	10	59	PB
Pre-B-ALL	25	M	2	72	PB
Pre-B-ALL	26	F	3	97	BM
Pre-B-ALL	32	M	3	96	PB
Pre-B-ALL	48	F	6	96	BM
Pre-B-ALL	58	F	7	96	BM
Pre-B-ALL	60	F	12	80	BM

Pre-B-ALL	63	F	16	89	PB
ETV6-RUNX1 c-ALL	3	F	1	93	PB
ETV6-RUNX1 c-ALL	4	F	12	98	BM
ETV6-RUNX1 c-ALL	17	M	6	97	BM
ETV6-RUNX1 c-ALL	21	F	4	92	BM
ETV6-RUNX1 c-ALL	29	M	2	96	PB
ETV6-RUNX1 c-ALL	30	M	3	95	BM
ETV6-RUNX1 c-ALL	41	F	11	92	BM
ETV6-RUNX1 c-ALL	43	M	2	99	PB
ETV6-RUNX1 c-ALL	59	M	3	90	BM
ETV6-RUNX1 c-ALL	75	M	3	95	BM
ETV6-RUNX1 c-ALL	81	M	1	94	BM
ETV6-RUNX1 c-ALL	92	M	9	96	BM
ETV6-RUNX1 c-ALL	100	M	4	97	BM
ETV6-RUNX1 Pre-B-ALL	7	M	4	96	BM
ETV6-RUNX1 Pre-B-ALL	39	F	3	97	PB
ETV6-RUNX1 Pre-B-ALL	52	F	2	98	BM
T-ALL	6	M	12	87	PB
T-ALL	15	M	4	96	BM
T-ALL	20	M	12	80	PB
T-ALL	23	M	7	86	BM
T-ALL	33	M	12	98	PB
T-ALL	36	M	2	54	PB
T-ALL	37	F	9	94	BM
T-ALL	50	M	10	93	BM
T-ALL	51	M	12	99	BM
T-ALL	53	M	11	97	PB
T-ALL	54	M	10	78	PB
T-ALL	64	M	10	99	BM
T-ALL	65	M	10	99	PB
T-ALL	68	M	11	50	PB
T-ALL	74	M	7	100	BM
T-ALL	79	M	9	61	BM
T-ALL	80	M	8	99	BM
T-ALL	85	F	12	98	PB
T-ALL	88	M	11	96	BM
T-ALL	89	F	1	96	BM
T-ALL	90	F	1	96	PB
T-ALL	93	M	11	79	BM
T-ALL	94	M	8	91	PB

<b>T-ALL</b>	97	F	8	93	PB
<b>T-ALL</b>	98	M	8	94	PB
<b>T-ALL</b>	101	M	5	96	BM
<b>Pro-B-ALL</b>	11	F	1	87	PB
<b>Pro-B-ALL</b>	55	F	1	?	BM
<b>Pro-B-ALL</b>	62	M	11	89	BM
<b>Pro-B-ALL</b>	84	F	1	80	BM
<b>MLL-AF4 Pro-B-ALL</b>	57	F	1	96	PB
<b>MLL-AF4 Pro-B-ALL</b>	69	F	16	82	PB

**Table 3 ALL patient samples.**

Above are listed the ALL patient samples (n=79) that were analyzed. Immunophenotype, internal Id number, sex, age, percentage of blasts and analyzed material are indicated. c-ALL = common ALL; ETV6-RUNX1 = ALL with ETV6-RUNX1 rearrangement; MLL-AF4 = ALL with MLL-AF4 rearrangement; ALL = acute lymphoblastic leukemia; M=male; F=female; PB = peripheral blood; BM = bone marrow. Adapted from Prall, 2010.

### 3.2.5. Enzymes

Enzymes were purchased from Fermentas, Invitrogen and New England Biolabs.

### 3.2.6. Antibodies

Target	Distributor	Clone	Species	Clonality	Incubation time	Temperature
<b>Akt</b>	Cell-Signaling	11E7	Rabbit	Monoclonal	ON	4°C
<b>Anti-human IgM</b>	HyTest	1F4	Mouse	Monoclonal	TP	37°C
<b>Anti-Cholera toxin</b>	Abcam	2/63	Mouse	Monoclonal	35 min	RT
<b>Anti-Phosphotyrosine</b>	Millipore	4G10	Mouse	Monoclonal	ON	4°C
<b>beta-actin</b>	Sigma-Aldrich	AC-74	Mouse	Monoclonal	1 h	RT
<b>Bmx</b>	Santa-Cruz		Rabbit	Polyclonal	ON	4°C
<b>Bmx</b>	Santa-Cruz	E-2	Mouse	Monoclonal	ON	4°C
<b>Blk</b>	Cell-Signaling		Rabbit	Polyclonal	ON	4°C
<b>Btk</b>	Cell-Signaling	C82B8	Rabbit	Monoclonal	ON	4°C
<b>BLNK</b>	Cell-Signaling		Rabbit	Polyclonal	ON	4°C
<b>cMyc</b>	Santa-Cruz	9E10	Mouse	Monoclonal	ON	4°C
<b>Csk</b>	Cell-Signaling	C74C1	Rabbit	Monoclonal	ON	4°C
<b>Erk1/2</b>	Cell-Signaling	137f5	Rabbit	Monoclonal	ON	4°C
<b>Fak</b>	Cell-Signaling		Rabbit	Polyclonal	ON	4°C
<b>F(ab')<sub>2</sub> Anti-human IgM</b>	Jackson-ImnuResearch		Rabbit	Fragment specific	TP	37°C
<b>Fes</b>	Cell-Signaling		Rabbit	Polyclonal	ON	4°C
<b>Fyn</b>	Cell-Signaling		Rabbit	Polyclonal	ON	4°C

<b>Fgr</b>	Cell-Signaling		Rabbit	Polyclonal	ON	4°C
<b>Hck</b>	Cell-Signaling		Rabbit	Polyclonal	ON	4°C
<b>Itk</b>	Cell-Signaling	2F12	Mouse	Monoclonal	ON	4°C
<b>JAK3</b>	Cell-Signaling		Rabbit	Polyclonal	ON	4°C
<b>JAK2</b>	Santa-Cruz		Rabbit	Polyclonal	ON	4°C
<b>Lck</b>	Cell-Signaling	73A5	Rabbit	Monoclonal	ON	4°C
<b>Lck</b>	Cell-Signaling	L22B1	Mouse	Monoclonal	ON	4°C
<b>Lsk</b>	Santa-Cruz	H-2	Mouse	Monoclonal	ON	4°C
<b>Lyn</b>	Santa-Cruz	H-6	Mouse	Monoclonal	ON	4°C
<b>Lyn</b>	Cell-Signaling	C13F9	Rabbit	Monoclonal	ON	4°C
<b>PAG1</b>	Novus-Biological		Rabbit	Polyclonal	ON	4°C
<b>Pyk2</b>	Cell-Signaling	5E2	Rabbit	Monoclonal	ON	4°C
<b>Src</b>	Cell-Signaling	AL41	Mouse	Monoclonal	ON	4°C
<b>Src</b>	Cell-Signaling	32G6	Rabbit	Monoclonal	ON	4°C
<b>Syk</b>	Cell-Signaling		Rabbit	Polyclonal	ON	4°C
<b>TfR</b>	Invitrogen	H68.4	Mouse	Monoclonal	1 hr	RT
<b>Tyk2</b>	Cell-Signaling		Rabbit	Polyclonal	ON	4°C
<b>Zap-70</b>	Cell-Signaling	99F2	Rabbit	Monoclonal	ON	4°C
<b>Phospho-Akt (Ser473)</b>	Cell-Signaling	D9E	Rabbit	Monoclonal	ON	4°C
<b>Phospho-Btk (Tyr223)</b>	Cell-Signaling		Rabbit	Polyclonal	ON	4°C
<b>Phospho-Erk1/2 (Thr202/204)</b>	Cell-Signaling	D13.14.4e	Rabbit	Monoclonal	ON	4°C
<b>Phospho-Lyn (Tyr507)</b>	Cell-Signaling		Rabbit	Polyclonal	ON	4°C
<b>Phospho-Src Family (Tyr416)</b>	Cell-Signaling	D49G4	Rabbit	Monoclonal	ON	4°C
<b>Phospho-Syk (Tyr525/526)</b>	Cell-Signaling	C87C1	Rabbit	Monoclonal	ON	4°C
<b>Phospho-Syk (Tyr323)</b>	Cell-Signaling		Rabbit	Polyclonal	ON	4°C

**Table 4 Primary antibodies for western blot.**

List of the primary antibodies. Clones are specified in the case that monoclonal antibodies were used. Species and clonality for the antibodies are provided. Rabbit antibodies were diluted in 5% w/v BSA, 1X TBS 0.1% Tween-20 with gentle shaking. Mouse antibodies were incubated in freshly prepared PBS containing 3% non fat dry-milk. ON= overnight, RT= room temperature, TP= time points.

Target	Distributor	Fluorochrome conjugated	Incubation time	Temperature
Mouse IgG (H+L)	Li-Cor	IRDye 680	1 h	RT
Rabbit IgG (H+L)	Li-Cor	IRDye 680LT	1 h	RT
Rabbit IgG (H+L)	Cell-Signaling	DyLight 800 conjugate	1 h	RT
Mouse IgG (H+L)	Invitrogen	Alexa Flour®488	30 min	RT
Rabbit IgG (H+L)	Invitrogen	Alexa Flour®488	30 min	RT
Rabbit IgG (H+L)	Invitrogen	Alexa Flour®555	30 min	RT
Rabbit IgG (H+L)	Jackson-ImmunoResearch	Cy <sup>TM</sup> 3 conjugated	30 min	RT
DRAQ5®	Cell signaling	Far-red fluorescent DNA dye	5 min	RT

**Table 5 Secondary antibodies for western blot and confocal microscopy.**

List of the secondary antibodies. The conjugated fluorescent dye is indicated for all the antibodies. Secondary antibodies for western blot were diluted in 1X TBS 0.1% Tween-20 with gentle shaking. Secondary antibodies for confocal microscopy were diluted in PBS 3% FCS.

Target	Distributor	Clone	Fluorochrome conjugated
CD10	Beckman Coulter	ALB1	PE
CD10	Beckman Coulter	ALB1	APC
CD19	Beckman Coulter	J3-119	APC
CD34	Beckman Coulter	581	FITC
CD179b (Igλ5)	Biolegend	HSL11	PE
Human IgM	Biolegend	MHM-88	APC
Human Ig light chain κ	Biolegend	MHK-49	APC
Human Ig light chain λ	Biolegend	HSL-11	APC
Human Ig light chain λ	Biolegend	MLH-38	PE
IgG1, κ Isotype control (FC)	Biolegend	MOPC-21	PE
IgG1, κ Isotype control (FC)	Biolegend	MOPC-21	APC
IgG2a, κ Isotype control (FC)	Biolegend	MOPC-173	PE

**Table 6 Antibodies for flow cytometry.**

List of the flow cytometry antibodies. The clone and conjugated fluorochrome for all the antibodies are indicated. APC= allophycocyanin; PE= R-phycoerythrin; FITC= fluorescein isothiocyanate.

### 3.2.7. Vectors

pcDNA3.1(+/-)	A 5.4 kb vector designed for high-level stable and transient expression in mammalian hosts. The vector contains the human cytomegalovirus promoter and carries the ampicillin/neomycin resistance genes. Several cloning sites in the forward (+) and reverse (-) orientation aid subcloning. (Invitrogen)
pCR2.1-TOPO	A plasmid vector which provides a highly efficient cloning strategy for direct insertion of PCR products and further subcloning into an expression vector. Carrying ampicillin or kanamycin for positive clone selection. (Invitrogen)
pCR4-TOPO	A plasmid vector which provides a highly efficient cloning strategy for direct insertion of PCR products and further subcloning into an expression vector. Carrying ampicillin or kanamycin for positive clone selection. (Invitrogen)
pCRXL-TOPO	A plasmid vector which provides a highly efficient cloning strategy for long PCR products (3 to 10 kb) and further subcloning into an expression vector. Carrying ampicillin or kanamycin for positive clone selection. (Invitrogen)

### 3.2.8. Oligonucleotides

For amplification and sequencing of the DNA from tyrosine kinases oligonucleotide primers were commercially synthesized. Mutagenesis primers were designed only for those TKs which present variation in the amino acid sequence. The complete primer list is shown at the end of this document (see section 8).

## 3.3. Molecular biology

### 3.3.1. Media for bacterial culture

Luria-Bertani (LB)-media or agar (Lysogeny broth; 10 g tryptone, 5 g yeast extract, 10 g NaCl ad 1 L, pH 7.0) were utilized in the cultivation of bacteria. Prior to the addition of antibiotics, dissolved media were autoclaved for 20 minutes at 121°C and 2.1 bar in a Systec V-100 autoclave. Antibiotics carbenicillin (100 ng/ml) or kanamycin (50 ng/ml) was added after LB-agar had been cooled to 55°C or immediately before the use of LB-media.

### 3.3.2. Transformation of competent bacteria

The heat-shock method was used to transform competent bacteria after thawing the cells on ice. Before an incubation period of 30 minutes on ice, 2 µl of the plasmid-DNA were added. The cells were

heated for 30 seconds at 42°C, followed by 2 minutes on ice. 250 µl prewarmed SOC media (super optimal broth with catabolite repression; 2% tryptone, 0.5% yeast extract, 10 mM NaCl, 2.5 mM KCl, 10 mM MgCl<sub>2</sub>, 10 mM MgSO<sub>4</sub>, 20 mM glucose) was added before the cells were incubated at 37°C on a shaker for 1 hour. 100 µl cells were plated out onto a LB-agar plate with appropriate antibiotic and incubated at 37°C overnight.

### **3.3.3. Plasmid-DNA isolation**

Mini- and maxi- preparations were used to isolate plasmid-DNA from bacteria. For mini-preparations the manufacturer's instructions of the Illustra™ plasmidPrep Mini Spin Kit (GE Healthcare) were followed. For maxi-preparations the Qiagen Plasmid Maxi Kit (Qiagen) was used. 2-3 ml of bacterial overnight culture were used for mini-preparations and 200 ml (high copy plasmids) to 500 ml (low copy plasmids) for maxi-preparations. Isolated plasmid-DNA was dissolved in TE buffer (Tris-EDTA; 10 mM Tris-HCl, 1 mM EDTA, pH 8.0) and stored at -20°C.

### **3.3.4. RNA isolation**

Fresh or cryopreserved material (cell lines or primary cells) was used to isolate RNA. 5-10x10<sup>6</sup> cells were pelleted, suspended in 1 ml TRIzol® Reagent and incubated at room temperature for 5 to 10 minutes. 0.2 ml chloroform were added after lysis, shaken vigorously and incubated for 5-10 minutes at room temperature. After the incubation the samples were spun at maximum speed in the centrifuge (13,000 rpm) at 4°C for 15 min. Following the addition of chloroform and centrifugation, the solution separated into two phases, an aqueous (RNA phase) and an organic phase (containing DNA). The aqueous (upper phase) was placed into a new 1.5 ml tube and 1 volume of isopropanol was added and incubated for 15 min while the remaining organic phase was discarded. The RNA precipitated within the aqueous phase was centrifuged at 13,000 rpm for 10 min at 4°C. The supernatant was removed and the RNA pellet was mixed with 1 ml of 75% ethanol followed by centrifugation (4°C, 5 min at 7,500 rpm). The wash was discarded and the RNA pellet was air-dried for 10 minutes. The pellet was subsequently resuspended in 50 µl of RNase-free water, incubated in a water bath at 60°C and stored at -80°C.

### **3.3.5. Nucleic acids concentration**

The concentration of nucleic acids (RNA and DNA) was determined by using a NanoDrop 2000 spectrophotometer (Peqlab / Thermo Scientific). TE buffer (Tris-EDTA; 10 mM Tris-HCl, 1 mM EDTA, pH 8.0) or sterile water was used as blank solution.

### **3.3.6. cDNA synthesis**

To transcribe RNA into cDNA, 3 µl of dissolved RNA were added to 35 µl water. 1 µl Random Primers (Promega) and 5 µl peqGOLD dNTP Mix (Peqlab) were added. The mixture was heated for 5 minutes at 70°C and cooled for five minutes at 4°C. 5x M-MLV Reverse Transcriptase Puffer, M-MLV Reverse Transcriptase, and RNasin Plus RNase Inhibitor (Promega) were subsequently added. Synthesis took place for 60 minutes at 37°C followed by heating at 95°C for 5 minutes. The cDNA was stored at 4°C.

### 3.3.7. Agarose gel electrophoresis

DNA fragments were separated through the use of 1% agarose gels. TAE buffer (Tris-acetate-EDTA; 40 mM Tris acetate, 1 mM EDTA with 0.005% ethidium bromide) was used to dissolve the agarose which was boiled in a microwave. A 6x loading buffer (10 mM Tris-HCl (pH 7.6), 0.03% bromophenol blue, 0.03% xylene cyanol FF, 60% glycerol, 60 mM EDTA, Fermentas) was used to dilute samples. Gels were run at 80 to 120 volts and DNA was visualized under UV-light.

### 3.3.8. Restriction digest of plasmid-DNA

Restriction digest of the plasmid-DNA was performed with FastDigest enzymes (Fermentas) in order to screen for positive clones and to sub clone inserts from TOPO-TA cloning vectors into the pcDNA3.1 vectors. 1  $\mu$ l of given restriction endonucleases were used to digest 1  $\mu$ g plasmid-DNA for 5-15 min at 37°C. The volume of restriction endonucleases did not exceed 1/10 of the total reaction volume in order to avoid star activity effects.

### 3.3.9. Gel extraction

PCR products and DNA were extracted and purified from standard agarose gels. Conventional gel electrophoresis was used to separate the DNA fragments of interest, followed by excision from the gel with the use of a scalpel. Excised fragments were purified through the use of the QIAquick Gel Extraction Kit following the manufacturer's instructions. DNA was finally eluted either in 30  $\mu$ l EB (elution buffer; 10 mM Tris-HCl, pH 8.5) or water (pH7.0-8.5).

### 3.3.10. PCR

Plasmid-DNA was amplified by PCR utilizing the Expand High FidelityPLUS (Roche) following the manufacturer's recommendations. In general, 6 ng of plasmidDNA were used as a template in a 50- $\mu$ l PCR reaction. Annealing temperatures were modified according to primer specific conditions.

Step	Description	Temperature in °C	Time in sec	Cycles
1	Initial Denaturation	95	60	1x
2	Denaturation	94	30	
3	Annealing	60	30	
4	Extension	72	180	Step 2/ 45x
5	Final Extension	72	240	
6	Pause	10		1x

**Table 7 PCR amplification of plasmid-DNA.**

Amplification of DNA was performed following the manufacturer's protocol (Roche). All PCR reactions were performed in 96-well TProfessional Thermocyclers (Biometra). Description, temperature and time for each step are indicated.

### 3.3.11. Real time PCR

Quantitative real time PCR was utilized to quantify the amount of cDNA with the use of the LightCycler FastStart DNA Master<sup>PLUS</sup> HybProbe Kit (Roche) according to the manufacturer's protocols. All samples were measured in triplicate using LightCycler 480 system (Roche). The HybProbe probes (#34, #42, and #60) were supplied by Roche Universal Probe Library, while the specific primers were purchased by Metabion. Relative quantification of the target genes were made through the use of the Livak method using the Roche Light Cycler 480 software. The target gene was normalized to the reference gene  $\beta$ 2-microglobulin (NM\_0040408).

### 3.3.12. Sequencing

Following amplification, the plasmid-DNAs were sequenced by using the BigDye<sup>®</sup> Terminator v1.1 Cycle Sequencing Kit (AB, Applied Biosystems) according with the manufacturer's recommendations. In general, 1  $\mu$ l Ready Reaction Premix (BigDye), 3  $\mu$ l HT buffer, 2  $\mu$ l primer and proximally 300 ng plasmid-DNA were used. All sequencing primers were used at annealing temperatures of 60°C.

Step	Description	Temperature in °C	Time in sec	Cycles
1	Initial Denaturation	95	60	1x
2	Denaturation	94	30	
3	Annealing	60	30	
4	Extension	60	180	Step 2/ 49x
6	Pause	10		1x

**Table 8 PCR sequencing of plasmid-DNA.**

Plasmid-DNA was sequenced according the dideoxy-chain-termination method. Description, temperature and time for each step are indicated.

After the thermocycling, the sequencing reactions were analyzed by the Clinic for Pediatric Hematology and Oncology, University Medical Center Hamburg-Eppendorf (Hamburg, Germany). The sequences were analyzed by using the Lasergene Suite program and compared with the wild type sequence, seeking for mutations.

### 3.3.13. Mutagenesis

Non conservative mutations, which had occurred during the PCR cloning procedure, were switched to the wild type by using QuikChange<sup>®</sup> Site-Directed Mutagenesis Kit (Agilent Technologies). Generally, per 50  $\mu$ l mutant strand synthesis reaction 5-50 ng of dsDNA template, 5  $\mu$ l of 10x reaction buffer, 1  $\mu$ l of the Dpn I restriction enzyme and 125 ng primers, were used. Standard cycling parameters for the QuikChange Site-Directed Mutagenesis Method are shown in Table 11.

Step	Description	Temperature in °C	Time in sec	Cycles
1	Initial Denaturation	95	30	1x
2	Denaturation	95	30	
3	Annealing	55	60	
4	Extension	68	60	Step 2/ 10-18x
6	Pause	10		1x

**Table 9 Mutagenesis of plasmid-DNA.**

Mutagenesis was performed following the instructions recommended by the manufacturer (Agilent Technologies). For extension at 68 °C, 1 min per kb of plasmid was used. Adjustment of the cycling parameters in accordance with the type of mutation was performed.

### 3.3.14. DNA cloning strategy

PCR products were separated by agarose gel electrophoresis, extracted from the gel, and cloned into the TA Cloning Vectors (see section 3.2.5) following the manufacturer's procedures. For subcloning the same restriction enzymes were used to digest the pcDNA3.1-vector and the insert DNA proceeding with separation by agarose gel electrophoresis and gel extraction.

Ligation between pcDNA3.1 vector and insert-DNA was performed by using T4 DNA Ligase (Invitrogen) according to the manufacturer's instructions. The molar ratio vector:insert was 1:3. In order to reduce self-ligation of the vector backbone, the rAPid Alkaline Phosphatase (Roche) was used to dephosphorylate the vector.

Transformation of competent bacteria (see section 3.3.2) was performed using 3 µl of the ligation reaction. Plasmid preparations were performed from bacteria clones grown on LB-agar plates and restriction digest enzymes were used to select positive clones which integrated insert DNA. To verify accurate orientation, the pcDNA3.1-vector and the insert-DNA were partly sequenced by using BGH and T7 primers.

## 3.4. Protein biochemistry

### 3.4.1. KLB lysate buffer

KLB base buffer was prepared by using 25 mM Tris, 150 mM NaCl, 5 mM EDTA, 10% glycerol, 1% triton X-100, 10 mM Na-pyrophosphate, 1 mM Na-orthovanadate, 10 mM glycerolphosphate and stored at 4°C. KLB' lysate buffer was freshly produced by adding 1 µl/ml 1 M PMSF, 10 µl/ml aprotinin, 20 µl/ml 0.5 M NaF and 2 µl/ml 40 mM Na-pervanadate (40 mM Na-pervanadate was always freshly prepared by adding 16 µl 30% H<sub>2</sub>O<sub>2</sub> to 100 µl of 50 mM orthovanadate following incubation for 30 min at room temperature) to the KLB base buffer and incubated for 30 min on ice.

### 3.4.2. Cell lysate

PBS (phosphate buffered saline, 155.17 mM NaCl, 2.97 mM Na<sub>2</sub>HPO<sub>4</sub>-7H<sub>2</sub>O, 1.06 KH<sub>2</sub>PO<sub>4</sub>, pH 7.4, Gibco/Invitrogen) was ice cooled and used twice to wash primary cells and cell lines, respectively. Cell pellets were resuspended in 200 µl pre-chilled KLB' buffer, incubated for 30 minutes on ice and

centrifuged at maximum speed for 15 min at 4°C. The cell lysate supernatant was transferred to a new tube and the cellular debris was discarded. Cell lysates were kept at -20°C or at -80°C for long-term storage.

### 3.4.3. Determination of whole protein concentration

The DC Protein Assay (Bio-Rad) was used to determine protein concentrations. Standard curves were used each time the assay was performed. The standard was prepared in the same buffer (KLB') as the sample and contained Albumin Fraction V (Roth) diluted to 8 different concentrations (0 to 6 µg/µl). Cell lysates from cell lines and primary cells were diluted 1:6 and 1:4, respectively. Absorbance was detected at 750 nm in an ELISA reader (Infinite 200M, TECAN).

### 3.4.4. SDS-PAGE

For sodium dodecyl sulfate polyacrylamide gel electrophoresis (SDS-PAGE) the Novex-NuPAGE® Bis-Tris pre-cast Midi-Gels (Invitrogen) were used and run in the XCell4 Surelock™ Midi-Cell according to the manufacturer's instructions. The system allows running of up to 4 gels at one time. Each Midi-Gel can run up to 26 samples, so that over 100 samples can be run simultaneously, therefore minimizing possible variations due to differences in gel-running. Prior to SDS-PAGE, 4x NuPAGE® LDS Sample Buffer and 10x NuPAGE® Sample Reducing Agent were used to dilute cell lysates, followed by incubation at 95°C for 5 minutes.

### 3.4.5. Western blot

Immediately after protein separation by SDS-PAGE, proteins within the polyacrylamide gel were transferred to nitrocellulose or PVDF membrane (Immobilion-P, Millipore). Prior to blotting, nitrocellulose membranes were soaked in freshly prepared 1x CAPS buffer (20 ml CAPS (0.5 M, pH 11.0 (Sigma-Aldrich), 200 ml methanol in 1L with double-distilled water (ddH<sub>2</sub>O) for at least 10 min, whereas the PVDF membranes were incubated for 30 sec in methanol, 2 min in water and at least 10 min in 1x CAPS buffer. Western blots were performed in a tank blot chamber filled with 1x CAPS buffer at a constant current of 400 mA for 2 hours at 4°C. After blotting, the membranes were blocked with 5% low-fat powder milk diluted in TBST (1x TBST, 0.1 % Tween-20) either for 1 hour at room temperature or overnight at 4°C.

After blocking, the membranes were washed twice with TBST and then incubated with the first antibody diluted in TBST 5% BSA. Subsequently, the membranes were washed 3 times with TBST and the appropriate fluorescent secondary antibody, diluted in TBST, was applied. The membranes were protected from light by using aluminum foil and shaken at a low setting of revolutions. Dilutions and conditions of the first and secondary antibodies are provided in the tables 4 and 5, respectively.

### 3.4.6. Li-Cor detection

After several washings with PBS, the membranes were imaged by the use of the Li-Cor Odyssey Infrared Imaging System, according to the manufacturer's protocols. Overall, two different wave lengths were

detected simultaneously on the same blot by using secondary antibodies conjugated to the infrared dyes IRDye 800CW and IRDye 680LT, respectively. Due to the fact that fluorescent signals are directly proportional to the amount of target protein, changes in the protein expression or phosphorylation were monitored and quantified by using fluorescent Integrated Intensity values (the sum of the intensity values (I.I.) for all pixels enclosed by a feature, multiplied by the area of the feature)(Odyssey®). Normalization of quantified proteins was performed by utilizing their respective  $\beta$ -actin I.I. values. Blots from ALL patient samples were further normalized by calculating a normalization factor (NF), employing the I.I. from serial dilutions of recombinant protein standards (20 to 2.5  $\mu\text{g}/\mu\text{l}$ ).

The NF was calculated individually for every blot and is defined as follows:

$$\text{NF} = \sum (S_N) / n$$

$S_N$  represent standard normalization and was calculated by  $S_N = \text{I.I. of } X / \text{highest (I.I.) } X$ ; where "X" represents standards with the same concentration but in different blots.

### 3.4.7. Stripping of bound antibodies

Nitrocellulose and PVDF blots probed with IRDye 800CW and IRDye 680LT conjugates were stripped using NewBlot Nitrocellulose and PVDF 5x Stripping Buffer, respectively, according to the manufacturer's protocols. The membranes were completely covered with 1X stripping buffer and incubated for 10 min at room temperature on a shaker. Membranes were washed twice with 1x PBS.

To ensure complete removal of sample fluorescence the membranes were imaged using the same instrument settings as that of the original image. If fluorescence remained, 3x stripping buffer was used and the membranes were incubated for 10 min at room temperature. In the case of PVDF membranes 0.5% of (v/v) SDS (Sodium Dodecyl Sulfate) was added to the stripping buffer. After the stripping process, membranes were re-imaged. When no remaining of fluorescence had been detected, the membranes were reused with new primary and secondary antibodies.

## 3.5. Cell culture

### 3.5.1. Culture of adherent and suspension cells

Cells were incubated at 37°C in a 5% CO<sub>2</sub>-atmosphere with 95% of humidity and cultivated in conventional cell culture flasks or plates. Depending on the cellular density, cells were usually split every two to four days. Adherent cells were detached from the surface by using trypsin (0.05% Trypsin-EDTA 1x, Gibco/Invitrogen) for 5 min at 37°C and appropriate media with 10-20% FCS was used to neutralize trypsinization and resuspend the cells. Adherent cells were reseeded at a dilution of 1:10, while suspension cells were reseeded at a dilution 1:3, yield cell densities of 1-2x10<sup>6</sup> per ml.

### 3.5.2. Composition of the media for cell culture

The media and supplements used to support cell growth are listed in Table 10. Cell lines and ALL primary cells were cultivated under the conditions described above. For long-term storage of the cells, freezing media was utilized.

Media	Components
HEK-293T media	DMEM with 10% FCS, 1% L-glutamine, 1% pyruvate, 2% HEPES
697/CALL2/CALL3 media	RPMI 1640 with 20% FCS, 1% L-glutamine, 1% penicillin-streptomycin
CEM/REH/SEM/Nalm6 media	RPMI 1640 with 10% FCS, 1% L-glutamine, 1% penicillin-streptomycin
Sup-B15 media	McCoy's 5A with 20% FCS, 1% L-glutamine, 1% penicillin-streptomycin
Primary ALL media	SFEM with 20% FCS, 1% penicillin-streptomycin
Starving media	RPMI 1640 with 0.1% FCS, 1% penicillin-streptomycin
Freezing media	90% FCS and 10% DMSO

**Table 10 Composition of cell culture media.**

The media utilized and its supplements are indicated. All the media were stored at 4°C and protected from light exposure.

### 3.5.3. Determination of cell number and vitality

An improved Neubauer hemocytometer (Marienfeld) was utilized for counting cells. The number of cells counted in the hemocytometer grid was multiplied by 10,000 and the dilution factor to calculate the total number of cells per ml. A dye exclusion method was performed using Trypan Blue Stain (Biochrom AG) to selectively stain dead cells.

### 3.5.4. Freezing and thawing cells

For storage, approximately  $1 \times 10^7$  cells were washed twice with PBS, resuspended in 1 ml of freezing media (described above), and transferred to 1.5 ml cryotubes. To achieve the optimum rate of cooling (1°C/min), cells were placed into a freezing container (Thermo Scientific) and frozen at -80°C for short-term storage. For long-term storage, cells were kept in liquid nitrogen.

In order to thaw cells, frozen cell suspension were directly placed into a water bath at 37°C. Once the cell suspension was completely thawed, cells were diluted in pre-warmed PBS and centrifuged for 5 min at 2,000 rpm, in order to withdraw residual DMSO. Cells were resuspended in the appropriate pre-warmed media and transferred to culture container.

### 3.5.5. Transfection of HEK 293 cells

For high transfection efficiency of plasmid-DNA into HEK 293T cells, Lipofectamine 2000 (Invitrogen) was used according to the manufacturer's instructions. Prior to the transfection,  $5 \times 10^6$  cells per ml were seeded out in 10 cm plates with 10 ml media. The following day, transfection was performed using 40 µl Lipofectamine 2000 and 24 µg of plasmid-DNA. Lipofectamine 2000 Reagent as well as plasmid-DNA was diluted in antibiotic-free Opti-MEM® Media. The media was replaced 24 hours post transfection and the cells were harvested 48 hours post transfection.

### 3.5.6. Density gradient centrifugation

Isolation of mononuclear cells from buffy coat was performed by density gradient centrifugation using Biocoll separating solution (density 1.077 g/ml, isotonic, Biochrom). 35 ml of buffy coat were layered over 15 ml of Biocoll separating solution and centrifuged at 960 rpm, 30 min without brake in a Heraeus Multifuge 3S-R centrifuge. The mononuclear cells, which were present in the interphase, were

transferred to a new tube and PBS was used to wash the cells twice. Pelleted cells were resuspended in an appropriate amount of buffer (PBS pH7.2, 2 mM EDTA) and used for magnetic labeling.

### 3.5.7. Magnetic labeling

Mononuclear cells isolated by density gradient centrifugation (described above) were utilized for magnetic labeling of CD19<sup>+</sup> cells and CD3<sup>+</sup> cells by using CD19 and CD3 microbeads (Miltenyi Biotec), respectively. For magnetic separation VarioMACS separator and LS MACS column were used, following the instructions recommended by the manufacturer. The eluted magnetically labeled cells were washed twice with pre-chilled PBS and then lysed in ice-cooled KLB' buffer.

### 3.5.8. Stimulation of the pre-BCR

The F(ab')<sub>2</sub> anti-human IgM purified antibody (Jackson-Laboratories) was used to specifically crosslink pre-BCR in ALL cell lines and primary leukemia cells. Overall, 1x10<sup>7</sup> cells were washed twice with PBS, resuspended in 2 ml starving media and incubated for two hours. 20 ng/ml of F(ab')<sub>2</sub> anti-human IgM purified antibody were added to the cells. Cells were then incubated for different time points (0, 1, 5, 10, 20, 40, 60 min) and cell lysates were generated by using freshly prepared ice-cooled KLB' buffer.

### 3.5.9. Cell proliferation assay

The CellTiter 96<sup>®</sup> Non-Radioactive cell proliferation assay (Promega) was used in accordance with the manufacturer's instructions, to measure cell proliferation in ALL cell lines or primary leukemia cells. In generally, 1x10<sup>6</sup> cells in 100 µl were placed into a sterile 96-well plate (Greiner). 15 µl of dye solution were added and cells were then incubated for 2-4 hours. Following incubation, 100 µl of Solubilization Solution/StopMix were added to the culture wells and the plates were incubated overnight at 37°C. An ELISA reader (Infinite 200M, TECAN) was utilized to measure the absorbance of the formazan product at 570 nm with a reference wavelength of 650 nm. The cell proliferation was monitored for five days and measured in triplicates.

### 3.5.10. Confocal microscopy

Confocal microscopy analysis was used to determine the cellular distribution of protein kinases in ALL cell lines. 80 µl of 1x10<sup>5</sup> cells per ml were added to a cytospin slide chamber and centrifuged at 900 rpm for 5 min. Cells were fixed with PBS-4% paraformaldehyde for 10 min, washed three times with PBS-2% BSA and permeabilized with 0.1% Triton X-100 for 4 min at room temperature. Before staining, cells were incubated for 30 min with PBS-2% BSA in order to prevent nonspecific protein binding. After several washings, cells were stained with 1/100 diluted specific antibody for 30 min in the dark. Appropriate fluorescent-conjugated secondary antibody was used to detect the first antibody. Fluorescence was detected using a Zeiss confocal microscope at 63x magnification.

### 3.5.11. Sucrose gradient

Sucrose gradient analyses were used to separate detergent-resistant microdomains, also known as "lipid rafts" and the protocol was kindly provided by Dr. Kentaro Kajiwara, University of Tokyo, Japan. In brief,

$3 \times 10^7$  cells were washed twice with cold PBS to remove remaining media completely. The cells were resuspended in 800  $\mu$ l of homogenization buffer (0.05 M Tris-HCL- pH 7.4, 0.015 M NaCl, 1mM EDTA- pH 7.4, 0.25% Triton X-100, 1 mM  $\text{Na}_3\text{VO}_4$ , 50 nM NaF, 1mM PMSF, 1 tablet of protease inhibitor cocktail) and transferred to a 2 ml tube. After 60 min of incubation at 4°C with rotating, the cell lysate was mixed with 800  $\mu$ l of 85% sucrose buffer (0.05 M Tris-HCL- pH 7.4, 0.015 M NaCl, 1mM EDTA- pH 7.4, sucrose). Next, the cellular mix was layered with 2.8 and 1.1 ml of 35% and 5% of sucrose buffer, respectively. The sucrose gradient was centrifuged at 200,000 g for 12 hours at 4°C (w/o brake). Finally, the sucrose gradient was fractionated from top to bottom and 10 fractions were collected and stored at -20°C until further use.

### **3.5.12. Virus production**

The production of lentiviral particles was carried out in 293T cells. Prior to transfection,  $3 \times 10^6$  cells were seeded in 10 ml of media in 10 cm plates. The next day, the media was replaced with new media containing chloroquine (1:1000). The transfection with the appropriate GFP-tagged plasmids was performed through the use of the ProFection® Mammalian Transfection system-Calcium Phosphate (Promega). In brief, 10 $\mu$ g of DNA plasmids were mixed with 10 $\mu$ g of pMDLg-pRRE (HIV-1 GAG/POL), 5 $\mu$ g of pRSV (REV) and 2 $\mu$ g pHCMV-10A1 (envelope). After vigorous vortexing the solution was incubated 15 min and given dropwise to the cells. 48 hours post transfection, the virus-containing media was strained through a 0.45 mm filter and ultra-centrifuged at 9,000 rpm for 8 hours at 4°C. The pelleted viral particles were resuspended in 2 ml of media from target cells.

### **3.5.13. Transduction of ALL cell lines**

For genomic integration and stable expression of the shRNA-plasmid, lentiviral particles were used to transduce ALL cell lines. Overall,  $5 \times 10^6$  cells were seeded with 3 ml media in 6-well plates and infected with 1 ml virus-containing media (see above) and 10  $\mu$ l/ml polybrene, respectively. The plates were centrifuged at 2,000 rpm for 1 hour at room temperature and incubated overnight at 37°C. The cells were then transferred to a culture flask and the virus infection rate was monitored by flow cytometry (BD Canto).

### **3.5.14. SFK-specific tyrosine kinase inhibitor**

The Src-family kinase inhibitor SU6656 was purchased from Calbiochem®. Overall with 10  $\mu$ l of SU6656 (5 $\mu$ M) were layered with 90  $\mu$ l of  $1 \times 10^6$  leukemic cell lines per well on a 96-well plate (CELLSTAR®). The plates were cultivated for three days at 37°C, and subsequently cells were subjected to an MTT assay (cell proliferation assay, see section 3.5.9.). Results are presented as the mean of the absorbance of the three-well set normalized to 1 for untreated cells.

## 4. Results

### 4.1. Protein tyrosine kinase selection

The selection of candidate PTK was based on the results of *in silico* transcriptome/proteome analyses (GEO/Uniprot) in childhood ALL patients (selection criteria: expression in at least 7.5% of the patients analyzed and a signal intensity value of more than or equal to 200) and the availability of suitable antibodies for immunodetection. Taken together, 18 (BLK, BMX, BTK, CSK, FES, FGR, FYN, HCK, JAK3, ITK, LCK, LYN, MATK, FAK, SRC, SYK, TYK2, ZAP70) out of 32 PTK were chosen as candidates for further analyses at the protein level (Figure 9).

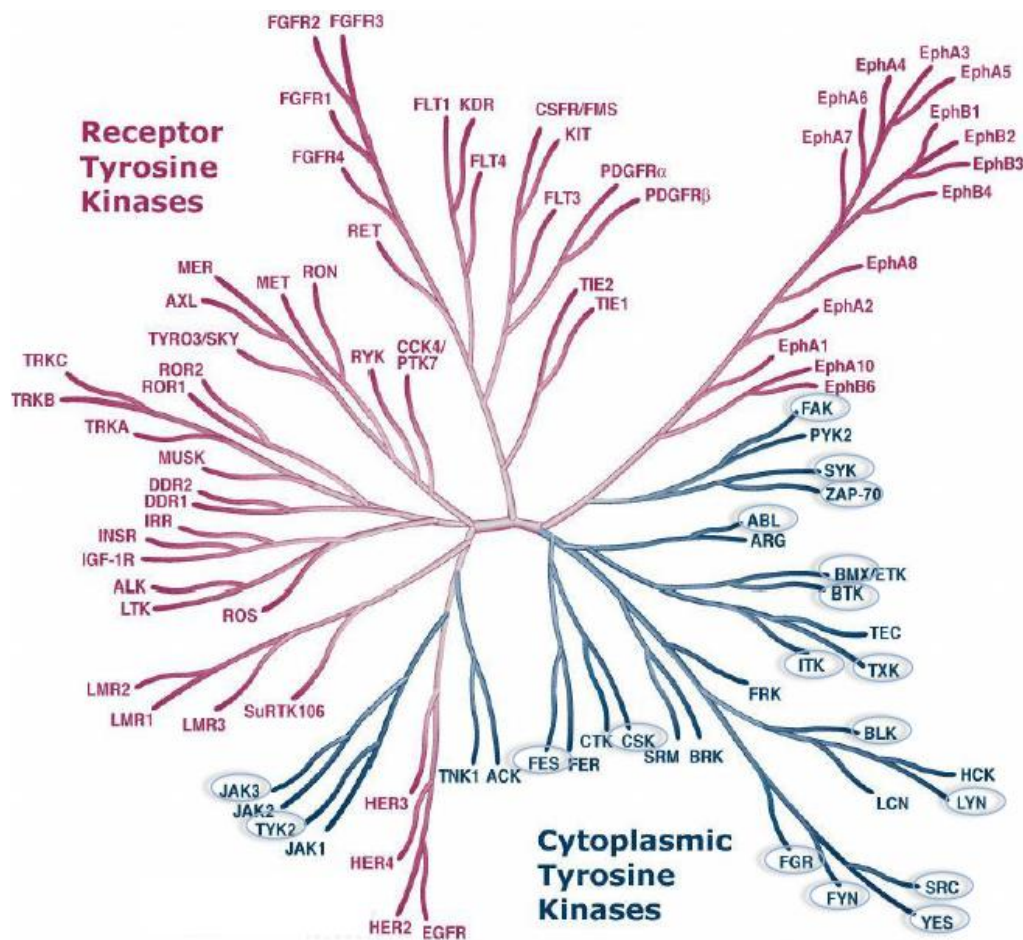


**Figure 9** The tyrosine kinase kinome.

The tyrosine kinome is composed of RTKs and PTK (also known as non-RTKs tyrosine kinases), depicted in red and blue, respectively. The 18 selected PTK are highlighted with blue circles. At least one non-RTK was selected from every major branch of the phylogenetic tyrosine kinome tree except for the ACK family branch. Figure adapted from Cell Signaling ([www.cellsignaling.com/reference/kinase/tyrosine](http://www.cellsignaling.com/reference/kinase/tyrosine)).

## 4.2. Cloning, mutagenesis and transfection of the PTK

### 4.2.1. Cloning and mutagenesis

The pcDNA3.1(+/-) plasmid was used for high-yield and transient expression of the 18 PTK selected as candidates in mammalian hosts. Detailed information is given in Table 13.

GenBank NCBI ID	Insert name	Insert size (bp)	Cloning sites	Vector	Clone ID	Mutation
NM_001715	HsBLK(wt)cMyc	1604	SpeI/NotI	pcDNA3.1(-)	HsCD00035932	Q226R
BC016652	HsBMX(wt)cMyc	2152	KpnI/NotI	pcDNA3.1(+)	HsCD00035969	none
NM_000061	HsBTX(wt)cMyc	2110	KpnI/NotI	pcDNA3.1(-)	HsCD00035915	none
NM_004383	HsCSK(wt)cMyc	1486	HindIII/NotI	pcDNA3.1(-)	HsCD00035752	F433S
BC035357	HsFES(wt)cMyc	2602	HindIII/NotI	pcDNA3.1(-)	HsCD00005615	none
BC002836	HsFGR(wt)cMyc	1721	HindIII/NotI	pcDNA3.1(-)	HsCD00035857	none
NM_002037	HsFYN(wt)cMyc	1747	HindIII/NotI	pcDNA3.1(-)	HsCD00038596	Y39H
NM_002110	HsHCK(wt)cMyc	1649	KpnI/NotI	pcDNA3.1(-)	HsCD00035930	none
NM_000215	HsJAK3(wt)cMyc	3507	HindIII/NotI	pcDNA3.1(-)	HsCD00021445	R895L
NM_005546	HsITK(wt)cMyc	1689	KpnI/NotI	pcDNA3.1(+)	HsCD00035916	none
BC013200	HsLCK(wt)cMyc	1753	HindIII/NotI	pcDNA3.1(-)	HsCD00035772	none
NM_002350	HsLYN(wt)cMyc	1670	KpnI/NotI	pcDNA3.1(-)	HsCD00035900	none
BC003109	HsMATK(wt)cMyc	1647	BamHI/NotI	pcDNA3.1(+)	HsCD00035849	none
BC035404	HsFAK(wt)cMyc	3144	KpnI/NotI	pcDNA3.1(+)	HsCD00021642	F418L
NM_004103	HsFAK2(wt)cMyc	3144	KpnI/NotI	pcDNA3.1(+)	HsCD00022350	none
BC002962	HsSYK(wt)cMyc	2041	HindIII/NotI	pcDNA3.1(-)	HsCD00021523	none
BC014243	HsTYK2(wt)cMyc	3695	HindIII/NotI	pcDNA3.1(-)	HsCD00041694	none
NM_001079	HsZAP70(wt)cMyc	1993	HindIII/NotI	pcDNA3.1(+)	HsCD00022393	none

**Table 11 Cloning of PTK into the pcDNA3.1 expression vector.**

After PCR amplification, cloning into a TA-cloning vector, and sequencing of the listed PTK, they were successfully subcloned into the pcDNA3.1(-) or pcDNA3.1(+) plasmids, depending on the vector orientation, by using specified restriction enzymes (cloning sites). The cloned ID and the GenBank ID of the cDNA clones used as a template are shown and published at <http://www.origene.com> and <http://plasmid.med.harvard.edu/PLASMID/>. The PTK names are indicated

in capital bold letters. The insert sizes and spontaneous point mutations which occurred during the PCR amplification process are listed. The PTK', BLK, CSK, FYN, JAK3 and PTK2 that displayed point mutations were switched to the wild type by using QuikChange® Site-Directed Mutagenesis Kit (see section 3.3.13). Hs= homo sapiens, wt= wild type, c-Myc= C-terminal c-Myc-Tag.

To facilitate the expression of the PTK in eukaryotic cells, the *Kozak* sequence was generated by the insertion of a 5' 9-base-pairs-overhang (bp) (5'-ACCACCGCC-3') and inserted in front of the ATG start codon. Furthermore, all PTK-constructs were c-Myc tagged by the insertion of 30 bp (5'-GAGCAGAAGCTGATCAGCGAGGAGGACCTG-3') before the TGA stop codon. The resulting C-terminal c-Myc tagged proteins (EQKLISEEDL) were used for detection by a monoclonal antibody directed against c-Myc to confirm the PTK protein expression (see section 4.2.3)

#### 4.2.2. Transfection

After the subcloning and mutagenesis process, all the PTK subcloned into the mammalian expression vector (pcDNA3.1) were transfected into human embryonic kidney (HEK) 293T cells. Direct infrared fluorescence on the Odyssey Infrared Imaging System (Li-Cor) was used to detect and quantify the expression of the recombinant PTK proteins. To confirm that all constructs were successfully transfected, cellular lysates of the selected PTK were blotted and tested with anti c-Myc monoclonal antibody (Figure 10).

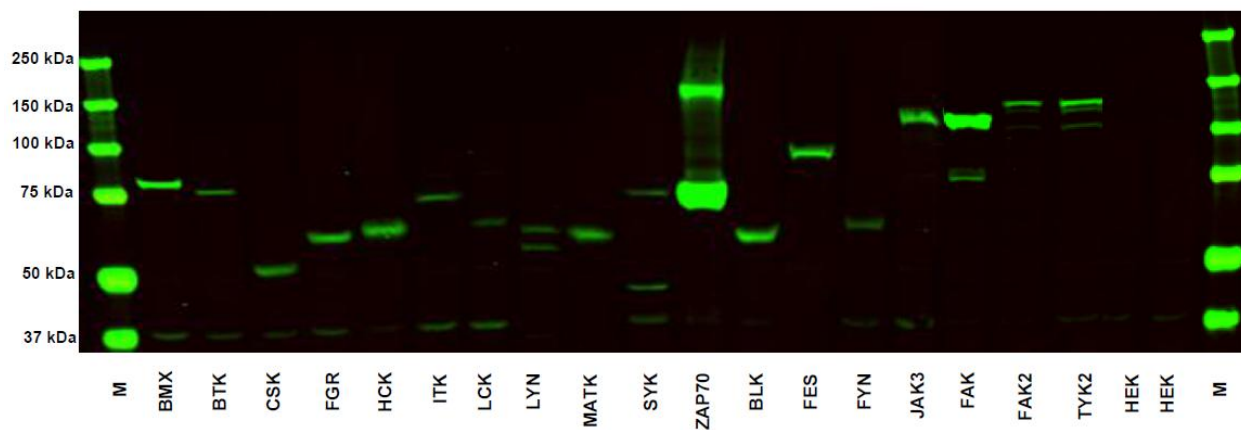


**Figure 10** Detection of cMyc-tagged recombinant protein expression by western blot.

20 µg of whole protein lysates of the recombinant PTK were separated by SDS-PAGE and transferred to nitrocellulose membranes. Detection of the c-Myc-tag was performed using anti-c-Myc antibody (Santa Cruz's sc-40, dilution 1:1,000); followed by secondary antibody (Cell Signaling #5151, dilution 1:15,000). The name of each PTK is indicated. Untransfected HEK 293T cells (HEK) were used as a negative control. M= Protein marker (PageRuler Plus Prestained, Thermo-Scientific). Detection of c-Myc-tagged fusion protein was performed by using infrared fluorescence detection (emission wavelength 700 nm) on the Odyssey Infrared Imaging system. The molecular weight of each marker band is depicted.

The detection of the C-terminal cMyc-tag, together with the detection of a specific band compatible with the expected molecular weight of the corresponding PTK, provided evidence of the full-length protein integrity of all the selected PTK expression constructs. Finally, quantification of the cMyc-tagged fusion protein was performed (Figure 11).

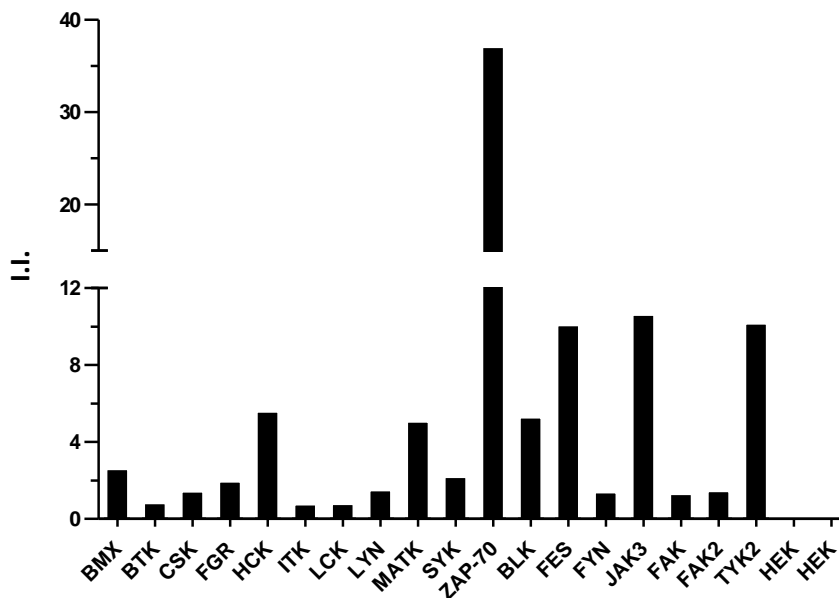


**Figure 11** Quantification of the expression of cMyc-tagged recombinant proteins.

A secondary antibody labeled with IRDye infrared dyes (1:15,000, Cell Signaling) was used to determine the relative expression of c-Myc in recombinant proteins. The integral intensity (I.I.) is defined as the sum of the intensity values for all pixels enclosed by a feature under infrared detection and it was calculated for each PTK. The I.I. is directly proportional to the protein concentration. Arbitrary values of I.I. and the selected PTK are depicted in the y- and x-axis respectively.

### 4.3. Selection of PTK specific antibodies

Commercial antibodies were purchased in order to detect PTK expression in ALL patient materials. Validation of the specificity of the purchased antibodies was performed prior to the analysis of ALL patient samples.

#### 4.3.1. Validation of PTK specific antibodies

After the detection and quantification of the cMyc-tagged fusion proteins, western blot analyses were performed using TK specific monoclonal antibodies (mAbs), in order to select suitable and specific monoclonal antibodies, which in turn, could be used for further analysis of ALL patient samples (Figure 12).

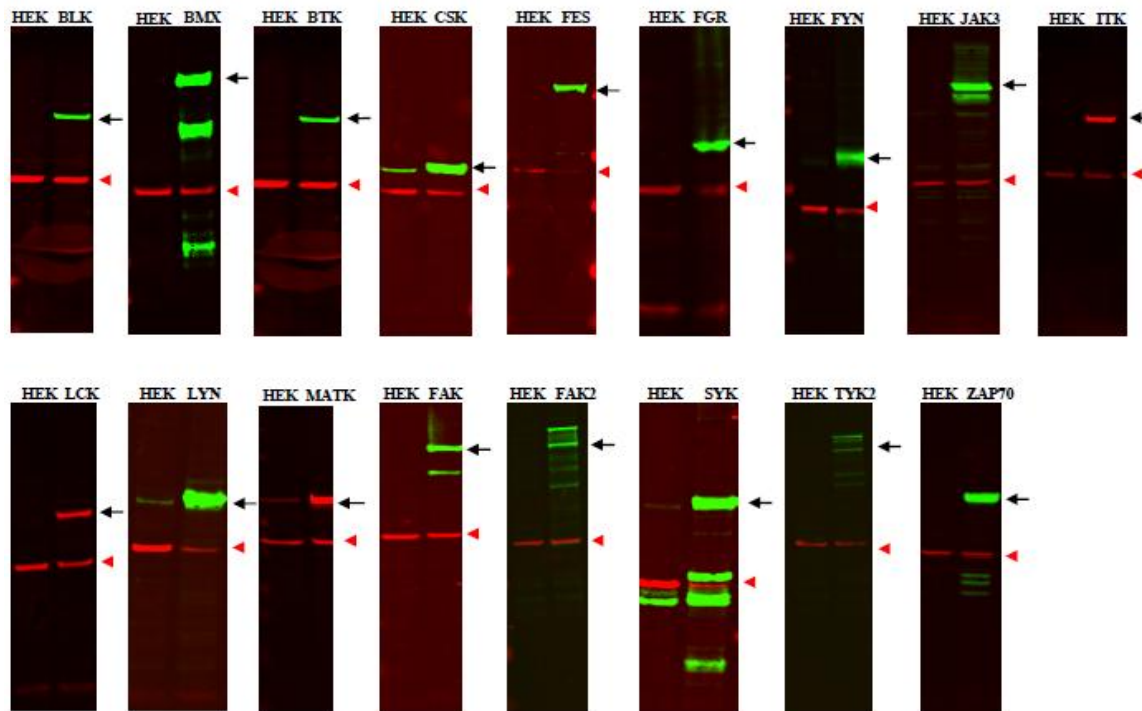


**Figure 12** Validation of the specificity of the monoclonal antibodies.

20  $\mu$ g of whole protein lysates of the recombinant PTK were separated by SDS-PAGE and transferred to nitrocellulose membranes. Detection of the protein of interest was carried out by using specific mAbs (see section 3.2.6). Black arrows indicate the specific recombinant protein and  $\beta$ -actin was used as a loading control (red head arrows). Untransfected human embryonic kidney (HEK) 293T cells were used as a negative control in each assay. Anti-rabbit mAb (DyLight 800 conjugated) and anti-mouse mAb (IRDye 680 conjugated) generated green and red bands, respectively.

High expression of the PTK in all transfected HEK 293T lysates, as compared with the negative control, was observed. Nevertheless, some of the transfected PTK showed a weaker signal intensity (e.g. TYK2 and FAK2) compared to the expression signal intensity of the other transfected PTK, potentially due to variances in transfection efficiency. Additionally, endogenous expression of a subset of PTK was detected in some untransfected HEK 293T cells (CSK, LYN, SYK, FYN and MATK). Thus, it was concluded that these PTK are endogenously expressed in HEK 293T cells. Finally, in some transfectants, bands with lower molecular weight than the target protein were detected, suggesting the presence of degradation products or incomplete protein synthesis.

#### 4.3.2. Validation of Src family kinase-specific monoclonal antibodies

Members of the Src family kinase (SFK) exhibit highly conserved domain structures and a very similar molecular weight at the protein level. Due to these characteristics, distinguishing among SFK members can be difficult. Therefore, evaluation of the capacity of the selected monoclonal antibodies to specifically recognize the target protein without any cross-reaction with other SFK members was required. Furthermore, the specificity of the phospho-SFK antibody was also tested. For this purpose, western blots comprising all selected SFK recombinant proteins were performed (Figure 13).

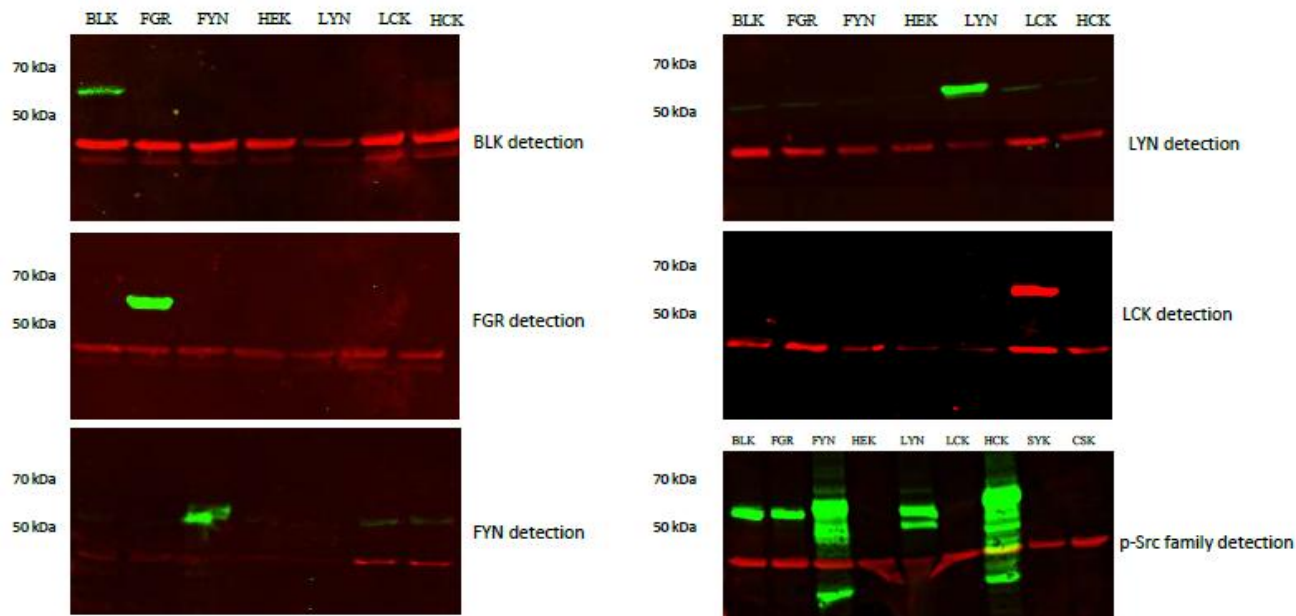


**Figure 13** Specificity of monoclonal antibodies directed against SFK members.

To test the specificity of the SFK directed mAbs, 20  $\mu$ g of whole protein lysates of the recombinant PTK were separated by SDS-PAGE and transferred to nitrocellulose membranes. On top, the loaded recombinant proteins are indicated. Untransfected HEK 293T cells were used as a negative control in each assay. The tested mAb is specified to the right of each membrane. Overall, proteins of interest are depicted in green except for LCK (shown in red).  $\beta$ -actin was used as a loading control (44 kDa; red bands). In the p-SRC family detection two additional recombinant PTK were used (SYK, CSK).

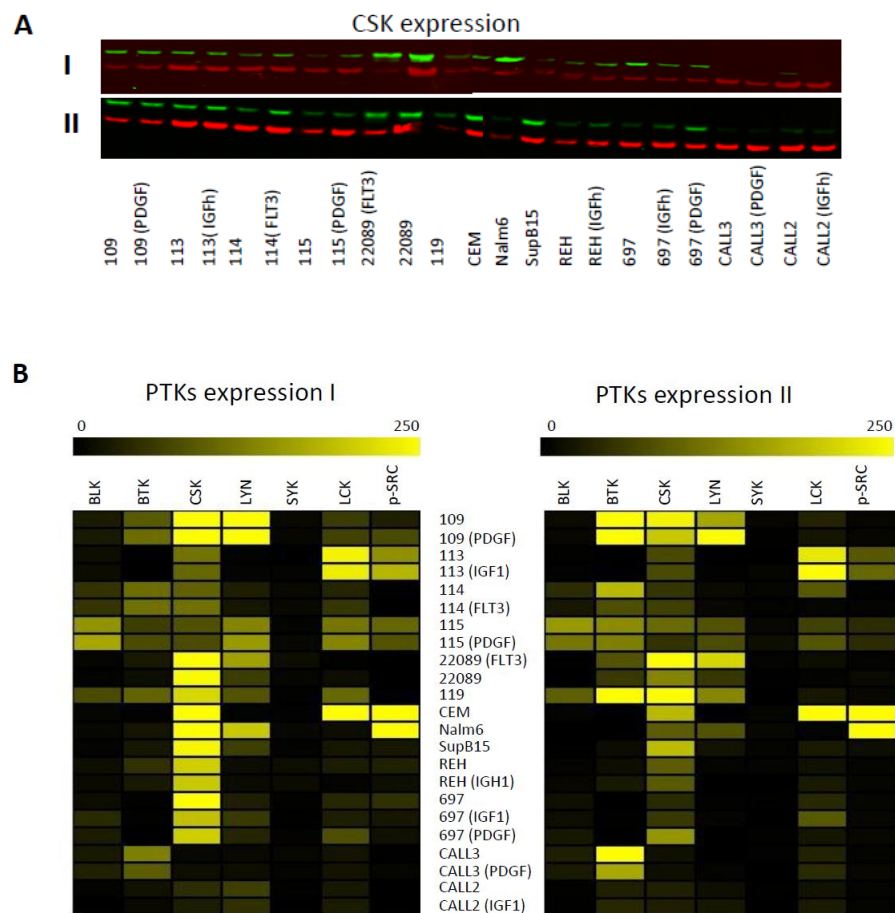
The protein separation by SDS-PAGE is not suited to distinguish SFK members due to the high homology and comparable molecular weight (approximately 60 kDa). However, distinction between the SFK members was confirmed by a very strong signal detected for each specific SFK member when its corresponding mAb was used, indicating that all the mAbs tested recognized their targets with high specificity. Furthermore, low intensity bands were detected on the LYN and FYN western blots and these bands were considered to represent endogenous protein instead of cross-reactivity against SFK members.

Finally, in the p-Src family mAb test, two additional recombinant proteins were included, CSK; because of the high structure homology with the SFK and SYK because it is known that SYK is the immediate target after activation of some SFK members. The specific detection of phospho-signal only for SFK, confirmed that phosphorylated SFK are specifically recognized by the p-Src family mAb without displaying any cross-reactivity with PTK with similar domain structure.

#### 4.4. Reproducibility of the Li-Cor imaging system

Once the specificity of the mAbs was evaluated, quantitative western blot analyses were performed by using direct infrared fluorescence detection on the Odyssey Infrared Imaging System (Li-Cor). Whole protein lysates from xeno-transplanted primary ALLs and ALL cell lines were used to determine whether the results of these quantitative western blot (WB) analyses could be accurately reproduced (Figure 14A). 7 out of the 18 selected PTK were randomly chosen and two independent quantitative WBs were carried out (Figure 14B).

Additionally, cluster analysis of the quantified PTK expression data by using the Spearman's rank correlation coefficient was performed. Due to the high number of data points generated with this analysis, the results are shown as a comprehensive heat map (Figure 14C).



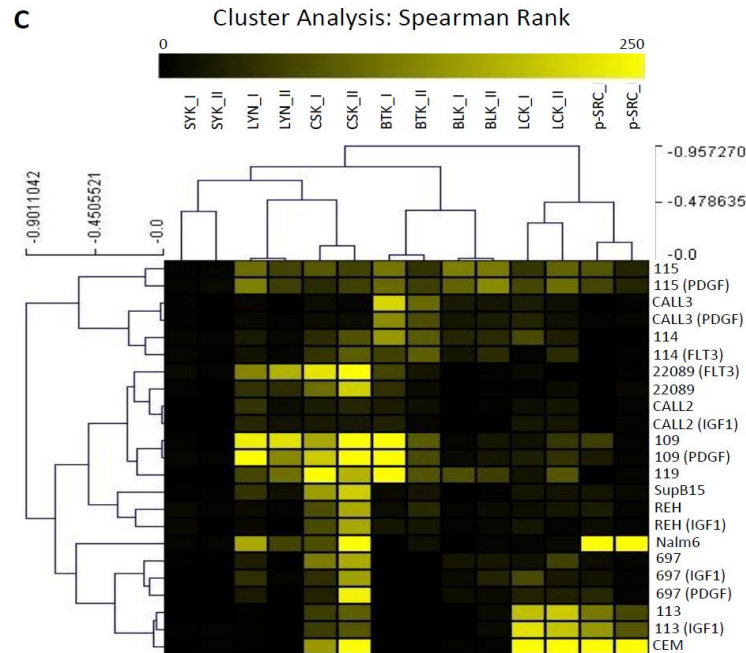


**Figure 14**      **Reproducibility of western blot analyses by the Li-Cor imaging system.**

Primary ALL blasts and cell lines either stimulated with the indicated ligands (shown in brackets) or unstimulated were analysed by quantitative WB. Following cell lysis, 20 µg of whole protein lysate were separated by SDS-PAGE and transferred to nitrocellulose membranes. A) The PTK candidate, CSK, was selected as a representative WB for the 7 PTK randomly chosen and two independent experiments are shown as I and II, respectively. The green fluorescent bands represent the target protein. β-actin was used as a loading control (red fluorescent bands). The remaining PTK were blotted accordingly. B) The arbitrary protein target signal of the selected PTK was quantified by using Li-Cor imaging and heat maps were designed with the software Multi Experiment Viewer (MeV 4.8). Heat maps from two independent experiments are shown as PTK expression-I and -II, respectively. C) Ultimately, the Spearman rank was used to cluster the generated heat maps of two independent experiments shown as I and II, respectively. PTK are displayed in columns and primary ALL blasts and cell lines are displayed in rows. Highly expressed TK are shown in shades of yellow, and non expressed TK are shown in black, according to the color scale. Description of the primary ALL blasts (109, 113, 114, 115, 119, 22089) and ALL cell lines (CEM, Nalm6, SupB15, REH, 697, CALL3, CALL2) are listed in sections 3.2.2 and 3.2.3, respectively. PDGF= platelet-derived growth factor ligand, IGF1= Insulin-like growth factor 1, FLT3= fms-related tyrosine kinase 3 ligand.

Even though relatively small variances were observed in the quantitative western blot analyses of two independent experiments, a high degree of similarity in the PTK expression of seven ALL cell lines was observed. The resemblance of the PTK expression in two independent experiments can be easily discerned by comparison of western or heat map analysis (Figure 14A and B). Furthermore, unsupervised cluster analyses using the Spearman rank confirmed reproducibility of data. In this statistical test, the ranked data points of the evaluated PTK, as well as the analysed primary ALL blasts and ALL cell lines in the first independent experiment, were grouped together with their corresponding partner in the second independent experiment (Figure 14C). It is also noteworthy that the xenotransplanted primary ALL 113 and the CEM cell line, which share the same immunophenotype (T-ALL), were clustered together.

## 4.5. PTK expression

Once the reproducibility of the Li-Cor imaging system was confirmed, this approach was extended to determine the expression at the protein level of 18 PTK candidates in a large cohort of ALL samples. For this purpose 20 µg of whole protein cell lysates from ALL patient samples, xeno-transplanted primary ALL cells, ALL cell lines and from mature B-and T-cells were analyzed by quantitative immunoblots analysis.

### 4.5.1. PTK expression in primary ALLs and ALL cell lines

The expression of 18 PTK was analyzed in xeno-transplanted primary ALLs and ALL cell lines. Additionally, CD3- and CD19-positive cells, extracted from buffy coats by immuno-magnetic separation, were included to investigate the PTK expression status in mature, non-leukemic T- and B-lymphocytes, respectively.

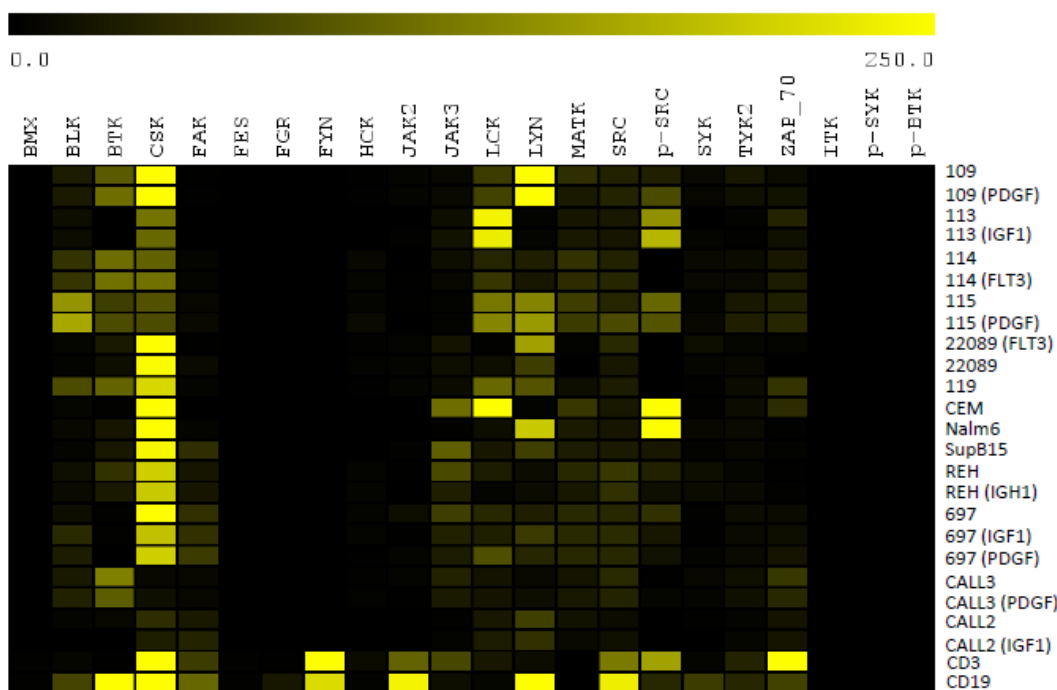


**Figure 15** PTK expression in primary ALLs and ALL cell lines.

Primary ALL blasts and cell lines either stimulated with the indicated ligands (shown in brackets) or unstimulated were analysed by quantitative WB. Following cell lysis, 20 µg of whole protein lysate were separated by SDS-PAGE and transferred to nitrocellulose membranes. The arbitrary protein target signal of the selected PTK was quantified as described in Figure 14. The PTK are displayed in columns and primary ALL blasts, cell lines, and mature lymphocytes are displayed in rows. Highly expressed TK are shown in shades of yellow, and non expressed TKs are shown in black, according to the color scale. Description of the primary ALL blasts (109, 113, 114, 115, 119, 22089), ALL cell lines (CEM, Nalm6, SupB15, REH, 697, CALL3, CALL2), and mature lymphocytes (CD3, CD19) are listed in the sections 3.2.2 and 3.2.3. PDGF= platelet-derived growth factor ligand, IGF1= Insulin-like growth factor 1, FLT3= fms-related tyrosine kinase 3 ligand.

PTK expression at the protein level was detected in 12 of the 18 candidates tested in leukemic cells. Similar results were observed in mature, non-leukemic lymphocytes where PTK expression at the protein level was detected in 13 out of 18 PTK. In both, leukemic and non-leukemic lymphocytes, no signal was detected for BMX, HCK, FES, ITK, and the phosphorylated form of BTK and SYK.

Whereas a relatively high expression of FYN was detected in CD3 and CD19 cells, no expression was found in ALL cells. In the same way, FGR was detected in non-leukemic cells (although at low integrate-intensity values), but FGR was not found to be expressed in leukemic cells. On the other hand, while MATK was expressed in nearly all the ALL cells, it was absent in buffy coat derived cells. A high expression of CSK was observed in almost all tested cells. Indeed, CSK expression in 10 out of 15 analyzed cells reached the highest arbitrary value (250).

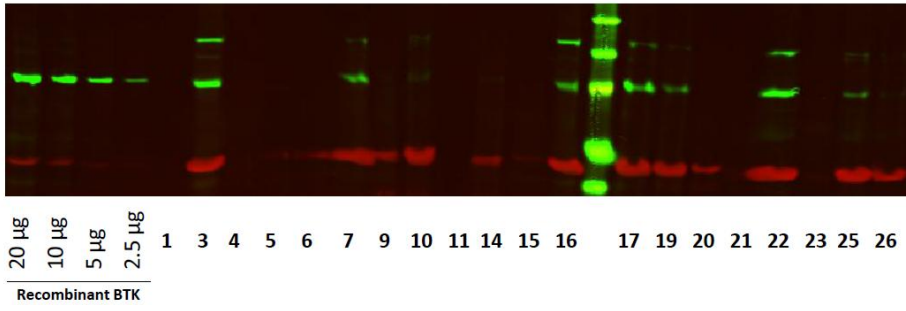
#### **4.5.2. PTK expression in childhood ALL**

To assess the expression as well as phosphorylation state of the PTK in pediatric ALL patients, whole cell lysates from bone marrow (BM) or peripheral blood (PB) from a cohort of 81 ALL patient samples from different ALL subtypes were analyzed by infrared fluorescent quantitative WBs. Cell lysates were kindly provided by Dr. K. Dierck (Research Institute Children's Cancer Center Hamburg), and generated by lysis of the mononuclear cells previously separated by density gradient separation.

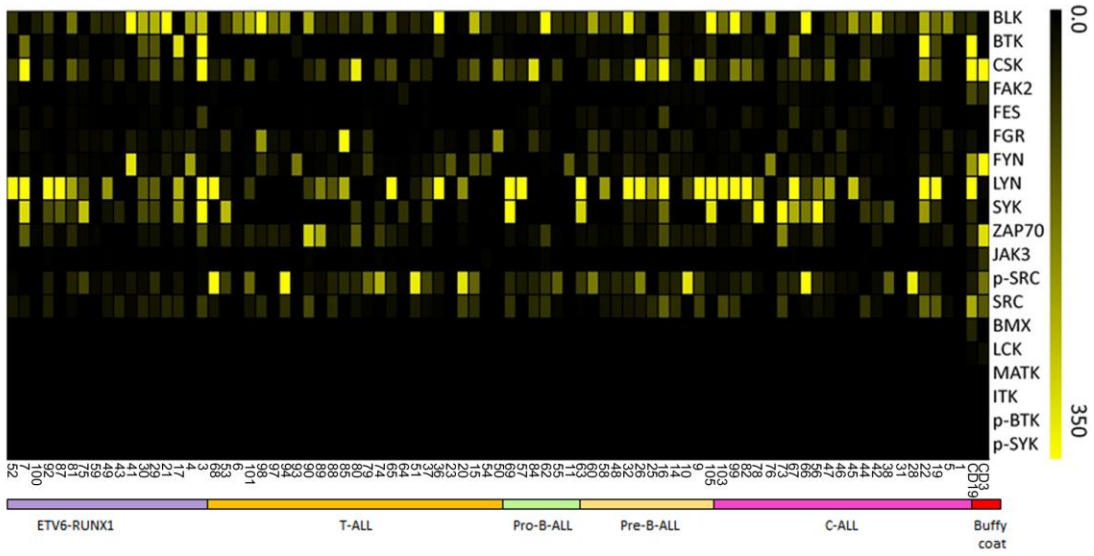
The studied cohort consisted of 22 c-ALL (common ALL), 11 pre-B-ALL without rearrangement, 7 pro-B-ALL (with or without MLL-AF4 rearrangement), 24 T-ALL and 17 pre-B-ALL with ETV6-RUNX1 rearrangement. Whole protein lysate (20 µg) from the indicated cohort of ALL patient samples was used to perform quantitative immunoblot analyses. Serially diluted recombinant protein (20 to 2.5 µg/µl) served as a positive control for antibody detection, as a reference for selection of the target proteins and calculation of the normalization factor, as described in section 3.4.5. Analysis of the 18 PTK with their respective recombinant protein control in 81 ALL patient samples generated roughly 2000 data points. The quantified PTK expression data were displayed as a heat map. Furthermore, unsupervised cluster analyses of PTK expressions was performed and shown as a heat map (Figure 16A, B and C).

A

BTK expression



B



C

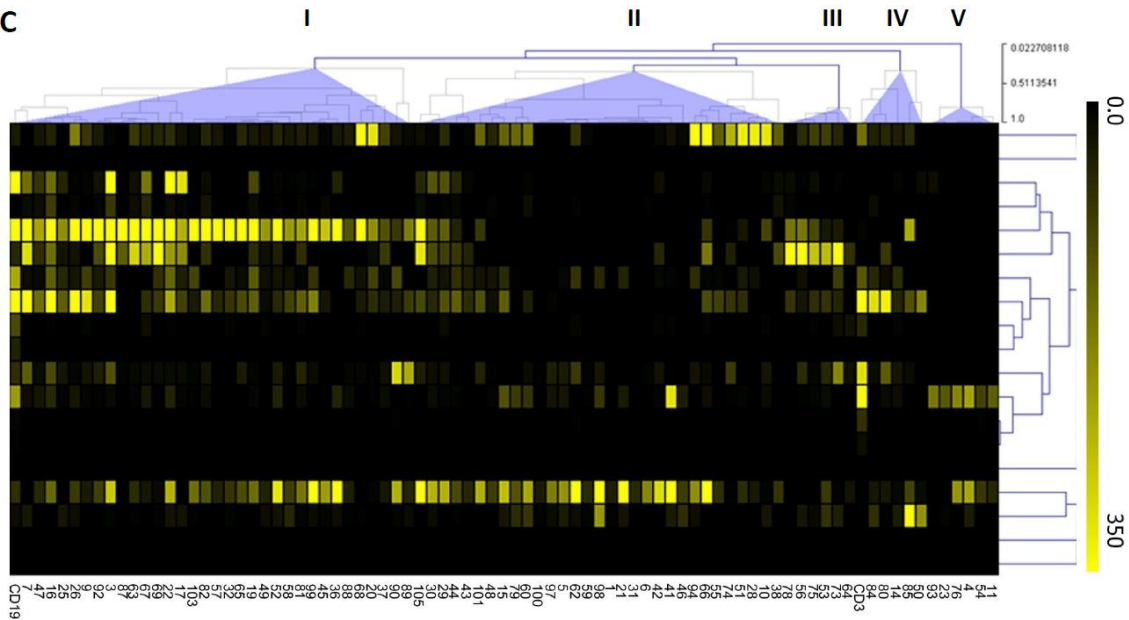


**Figure 16 PTK expression in ALL patient samples.**

20 µg of whole protein lysate from ALL patient samples were used to perform quantitative western blot analysis as described in Figure 14. A) The PTK candidate, BTK, was selected as a representative WB for the selected 18 PTK. The serially diluted recombinant protein was loaded in the first four lanes and the total amount (in µg) is specified. Only green bands that coincided with the molecular weight of the recombinant protein were considered as the target protein. β-actin was used as a loading control (red bands). B) A heat map of the indicated PTK was generated. The analyzed PTK and the ALL patient ID are indicated in the y- and x-axis, respectively. The ALL immunophenotype of the samples is depicted. Highly expressed PTK are shown in shades of yellow, and non-expressed PTK are shown in black, according to the color scale. C) Unsupervised cluster analysis (Pearson correlation) groups patients with related expression profiles. Mature CD3 and CD19 cells isolated from buffy coats were included in the analysis. c-ALL= common ALL; ETV6-RUNX1= ALL with ETV6-RUNX1 rearrangement; ALL= acute lymphoblastic leukemia.

Overall, signals from the serially diluted recombinant proteins were detected by immunoblot analysis at the predicted molecular weight, validating the antibody specificity and the successful antibody-target recognition. Although additional binding of the monoclonal antibodies was observed only in the ALL patient samples, these bands did not coincide with the molecular weight of the recombinant protein and therefore they were considered as unspecific antibody-binding events and excluded from the quantification analysis (Figure 16A). In the same way, ALL patient samples which exhibited protein bands lacked any detectable loading-control band (β-actin) were not included in the quantification analysis.

In general, PTK expression at the protein level was detected in 13 of the 18 candidates tested. No signal could be detected for BMX, ITK, LCK, MATK and the phosphorylated form of BTK and SYK. Additionally, expression of FAK2, FES, and JAK3 was barely detectable in all cases (Figure 16B). The expression of PTK was characterized by a high degree of heterogeneity. The PTK expression in the CD3 and CD19 mature cells was similar to the PTK expression observed in the ALL patient cohort (Figure 16B). A clear association between PTK expression profile and specific ALL immunophenotype could not be determined, cluster analysis by using Pearson correlation (as well as other statistic tests; data not shown) led to the identification of two main clusters, which together represent almost 80% of the analyzed cohort (Figure 16C).

The cluster I is composed of 34 ALL patient samples, which represents approximately 43% of the ALL-cohort, and which are characterized by high expression of the PTK Lyn. This cluster enclosed both, the greatest number of ALL patient samples, and the major number of ALL patient samples with the highest arbitrary intensity values (350). Similarly, cluster II consisted of 29 ALL patient samples and represented 35% of the analyzed cohort (Figure 16C). This cluster is characterized by a high expression of BLK. However, only few ALL patient samples in this subgroup reached the maximum arbitrary intensity value as compared with cluster I. Three small subgroups (III, IV and V) were also clustered, all three of these subgroups represented the remaining 22% of the ALL patient samples and a rather predominant expression of SYK, CSK and Fyn was observed in each subgroup, respectively (Figure 16C). It is noteworthy to mention that phosphorylation could only be detected using the pan-phospho-SRC family mAb showing a broad spectrum of expression in all ALL subgroups. SYK was highly expressed within a

small subgroup of ALL patient samples, whereas its phosphorylated form could not be detected using p-SYK mAb.

## **4.6. shRNA mediated Lyn repression**

Because Lyn was found to be highly expressed within the largest subgroup of ALL patient samples analyzed, we hypothesized that this high Lyn expression could play a relevant role in leukemogenesis. To test this hypothesis, RNA interference was chosen as a method for stable repression of Lyn expression. Short hairpin RNA expression (shRNA) constructs were transfected together with lentiviral-packaging vectors to produce high-titer lentivirus in HEK 293T cells (see section 3.5.11). After selection of the most efficient shRNA lentivirus, leukemic cells were virally transduced to induce RNA interference.

### **4.6.1. Selection of shRNA constructs**

Lyn knockdown efficacy of the generated lentiviral particles was tested in leukemic cells. For this purpose HEK 293T-Lyn transfected cells were transduced with 4 different shRNAs directed against Lyn and one shRNA-scrambled (SCR) as a control (see section 3.5.12). After transduction quantification of Lyn expression at the protein level was performed by quantitative western blot (Figure 17A and B). RNA was extracted and reversely transcribed into cDNA (see section 3.3.4 and 3.3.6), which was used for real time PCR analysis (Figure 17C).

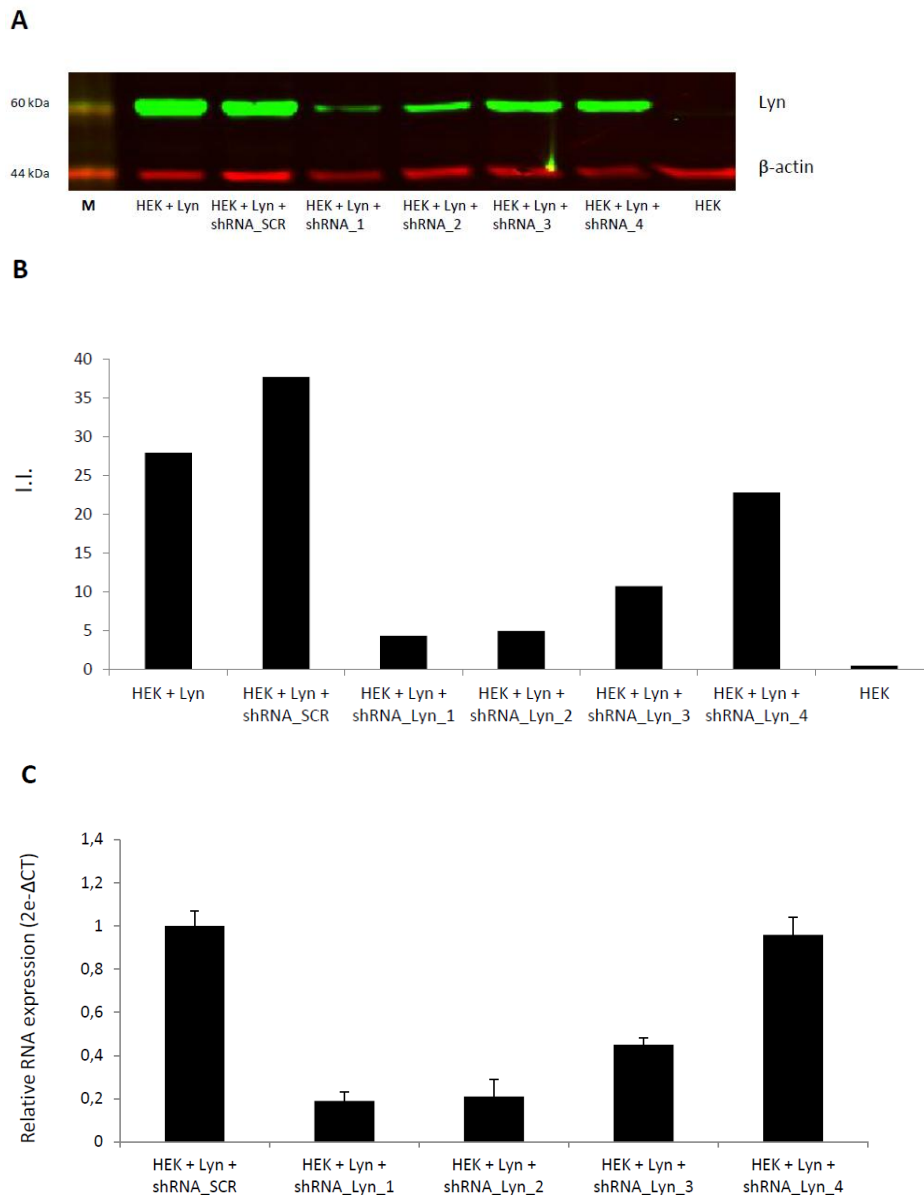


**Figure 17 Lyn-directed RNA interference.**

The efficacy of 4 different shRNA constructs was tested in HEK 293T cells. These cells were transduced with as described in section 3.5.13. A) Following cell lysis, 20  $\mu$ g of whole protein lysate were separated by SDS-PAGE and transferred to nitrocellulose membranes for immunoblot analysis using antibodies specific for Lyn (green bands).  $\beta$ -actin was used as a loading control (red bands). B) Lyn expression was quantified by using the Li-Cor imaging system. Arbitrary values of I.I. and the shRNA constructs are depicted in the y- and x-axis respectively. C) Quantification of the Lyn gene expression was performed by real time PCR (RT-PCR). Lyn gene expression relative to  $\beta$ 2M was normalized to 1 for the shRNA\_SCR construct. HEK= HEK 293T cell line, HEK + Lyn= HEK 293T transfected with a Lyn plasmid, HEK + Lyn + shRNA\_(SCR,1,2,3,4)= HEK 293T transfected with the Lyn plasmid and transduced with lentiviral particles containing the indicated shRNA construct.

The testing of four different Lyn-shRNA constructs in HEK 293T cells revealed that the shRNA\_Lyn\_1 construct was highly effective in repressing Lyn expression. The shRNA\_Lyn\_1 construct markedly reduced Lyn expression at the protein level by more than 30 fold (based on arbitrary I.I. values) (Figure 17A and B). Similarly, at the transcript level, shRNA\_Lyn\_1 showed a Lyn expression reduced by more than 80% in comparison to the scrambled shRNA construct (Figure 17C). In the following, the term shRNA\_Lyn will exclusively refer to shRNA\_Lyn\_1.

#### 4.6.2. Expression of Lyn in primary ALL and derivate cell lines

To investigate the impact of Lyn repression, ALL leukemic blasts and ALL cell lines were used in order to find a model which recapitulated the Lyn expression observed in a subgroup of pediatric ALL samples. Lyn expression and SFK activation status at the protein level were determined by quantitative western blot analysis (Figure 18A and B).

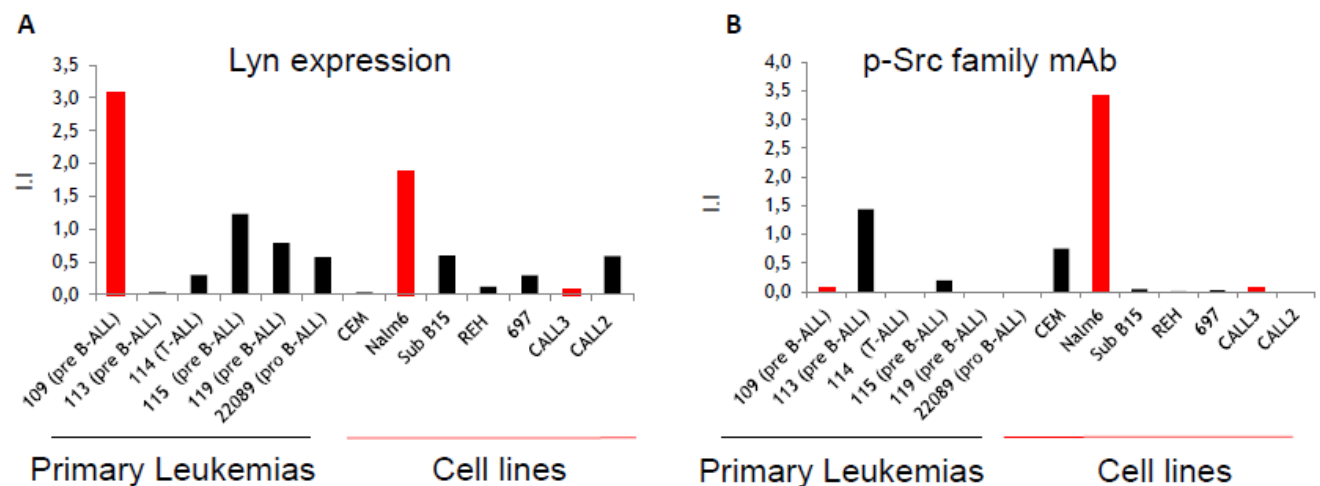


**Figure 18** Lyn expression and SFK activation status in primary ALL and cell lines.

20  $\mu$ g of whole protein lysates of the indicated ALL primary leukemias or ALL cell lines were used for immunoblot analysis. A) I.I. of the Lyn expression was calculated. The ALL primary leukemia (109) and ALL cell line (Nalm6) displayed the highest Lyn expression and are shown in red bars. Additionally, a cell line with low Lyn expression (CALL3) was also selected and is also shown in red bars. B) The p-SRC family activation status was determined. Results are depicted as in A. For ALL primary leukemias the immunophenotype is shown.

In accordance with data displayed above (Figure 15), the primary ALL 109 and ALL cell line Nalm6 showed the highest Lyn expression at the protein level. However, significant phosphorylation of the SFK could only be detected in Nalm6 cells (Figure 18A, B). Hence, the analysis of Lyn expression in leukemic cells led to the selection of Nalm6 as a model that mirrors Lyn expression in primary ALL. CALL3 cells were selected in order to study the effect of Lyn repression in cells that do not exhibit high Lyn expression. Lyn expression in ALL 109 cells was very high; however the availability of primary material was limited. Therefore, it was not used for the following assays.

### 4.6.3. Specificity of the shRNA\_Lyn construct

One remarkable characteristic of the eight members of the SFK (Src, Lck, Fyn, Hck, Blk, Lyn, Fgr, and Yes) is that they share highly conserved domain structures, therefore distinguishing between SFK members represents a challenging task. To evaluate whether the shRNA\_Lyn construct specifically targets Lyn, excluding possible off-target effects on other SFK members, the previously selected Nalm6 cells were lentivirally-transduced either with shRNA\_Lyn or shRNA\_SRC constructs and the expression of the SFK members was evaluated by quantitative immunoblots (Figure 19).

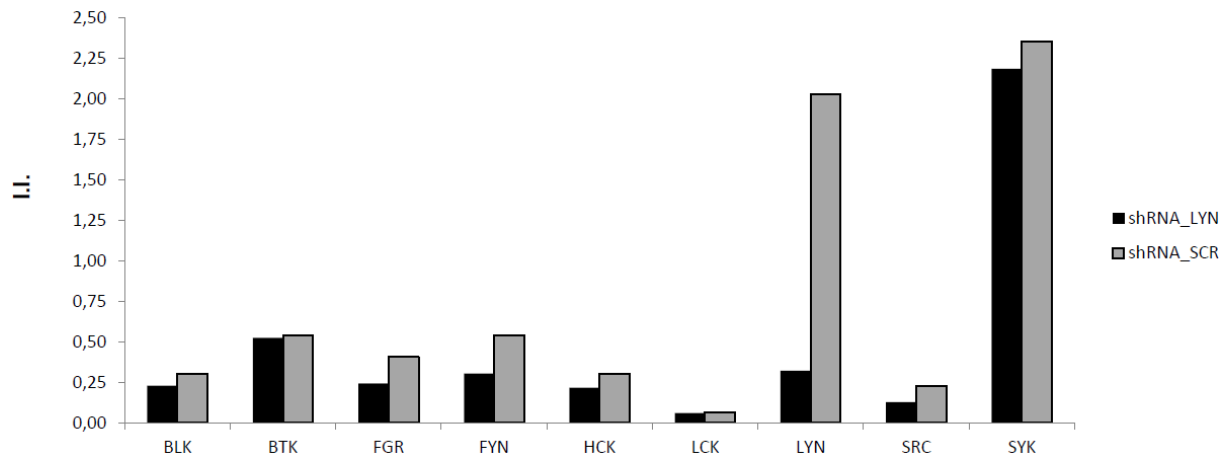


**Figure 19** SFK expression in lentivirally-transduced Nalm6 cells.

Nalm6 cells were transduced either with shRNA\_Lyn or shRNA\_SRC and cultivated for three days in Nalm6 media. Following cell lysis, 20 µg of whole protein lysate were used for immunoblot analysis. Specific antibodies for the eight SFK members and arbitraries I.I. values are depicted. The expression of SYK was determined and is also shown.

The analysis of the lentivirally-transduced Nalm6 cells revealed that the shRNA\_Lyn construct was highly effective in knocking down Lyn expression in these cells at the protein level, in agreement with the results observed in HEK 293T cells (Figure 17B). Despite the high homology exhibited among SFK members, the shRNA\_Lyn construct showed a high specificity for Lyn. It is important to mention that no off-target effects were observed in any of the remaining seven SFK members. The PTK, SYK and BTK, that do not belong to the SFK, were used to evaluate other possible off-target effects of shRNA\_Lyn beyond SFK members. No off-target effects were detected either on SYK or BTK expression. Thus, shRNA\_Lyn induced a highly efficient and specific Lyn repression.

### 4.7. Repression of Lyn in ALL cell lines

Owing to the high Lyn expression observed in ALL patient samples, two cell lines (Nalm6 and CALL3, which show high and low Lyn expression, respectively) were chosen as a model to further investigate Lyn's potential oncogenic driver properties. The selected cell lines subjected to a long-term growth assay. The efficacy of the shRNA\_Lyn construct was confirmed by RT-PCR and the percentage of GFP positive cells was monitored by flow cytometry (FACS) (Figure 20).

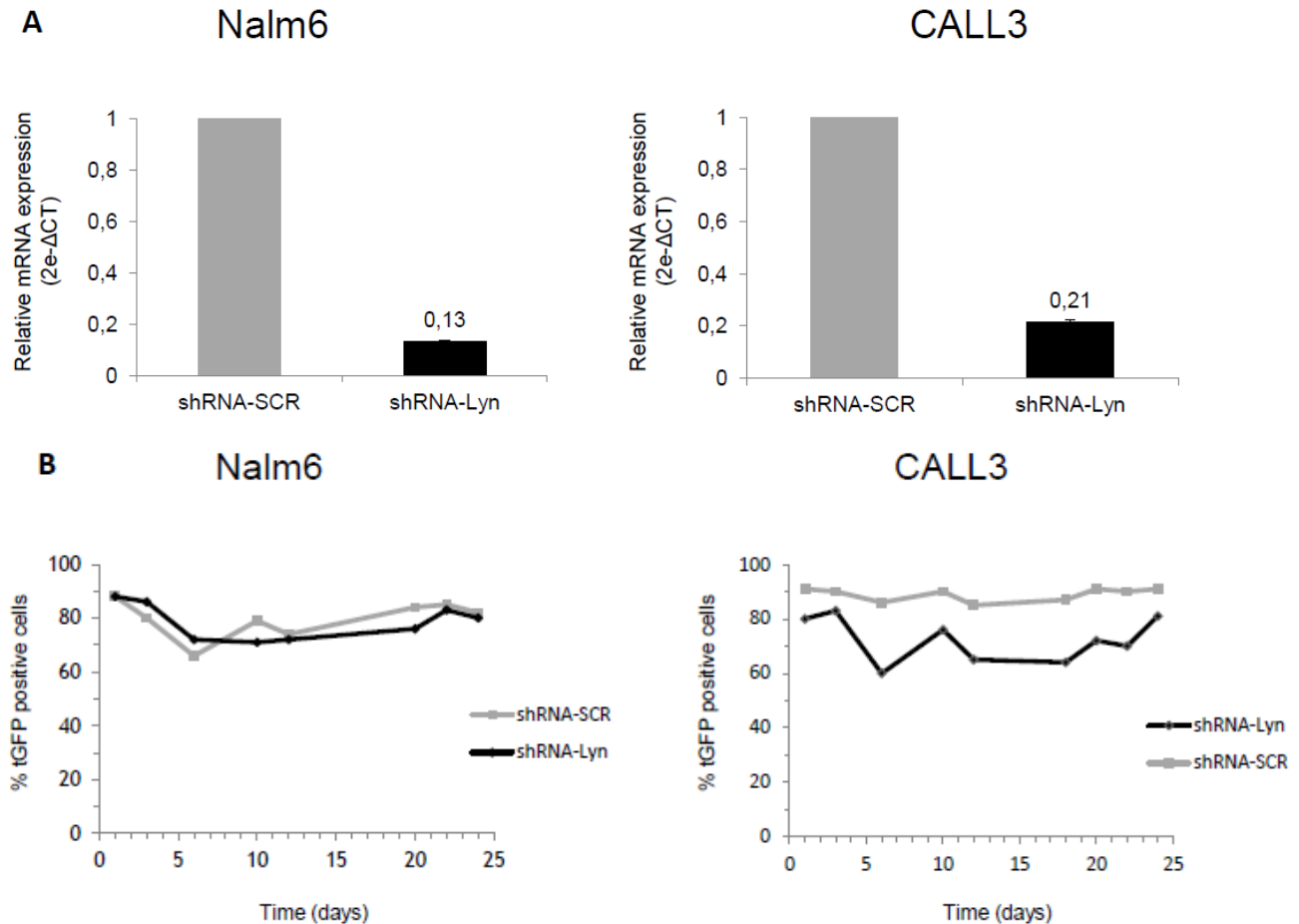


**Figure 20** Monitoring of Lyn repression in Nalm6 and CALL3 cell lines

Nalm6 and CALL3 cells were transduced either with shRNA\_Lyn or shRNA\_SCR and cultivated for three days in Nalm6 and CALL3 media, respectively. Four days after transduction, Nalm6 and CALL3 cells were FACS sorted for GFP expression. A) Quantification of the Lyn gene expression was performed by RT-PCR. Lyn gene expression relative to  $\beta$ 2M was normalized to 1 for shRNA\_SCR. B) The Nalm6 and CALL3 FACS sorted cells were monitored for GFP expression over the indicated period of time. The data are representative of two independent experiments.

In accordance with previous results, Lyn expression was successfully repressed in both Nalm6 and CALL3 cell lines (Figure 20A). Although Lyn repression in Nalm6 cells (>85%) was higher than in CALL3 cells (roughly 80%), the repression of the Lyn expression was prominent in both cases. The monitoring of GFP expression in the sorted Nalm6 or CALL3 cells over a period of 25 days revealed that the survival and/or proliferation of these leukemic cells was not affected by Lyn repression (Figure 20B). In summary, despite the strong reduction of the Lyn expression no impact on the survival or proliferation of Nalm6 or CALL3 GFP sorted cells was observed.

## 4.8. Pre-BCR cross-linking in Lyn-knockdown leukemic cells

Lyn was found to associate with the B-cell receptor (BCR) or the pre-BCR after receptor cross-linking<sup>98</sup>. BCR engagement results in a quick augmentation of Lyn phosphorylation and activation<sup>78</sup>. No effect on survival and proliferation was observed in Lyn-knockdown leukemic cells (Nalm6 and CALL3), the importance of Lyn upon pre-BCR cross-linking was evaluated (because BCR activity is intimately linked to proliferation and/or survival in B-cell development). For this purpose, Nalm6 and CALL3 Lyn-knockdown cells were stimulated with a F(ab')<sub>2</sub> anti-human IgM purified antibody. Activation of downstream proteins in the pre-BCR pathway and cellular proliferation was assessed by immunoblot and proliferation assay, respectively.

### 4.8.1. Specificity of the F(ab')<sub>2</sub> anti-human IgM

The F(ab')<sub>2</sub> anti-human IgM purified antibody is intended to specifically recognize the  $\mu$  chain of the pre-BCR. However, binding specificity was first confirmed by using different cell lines that either expressed the pre-BCR or did not. For this purpose, four different cell lines (REH, 697, CALL3 and Nalm6) were stimulated with the F(ab')<sub>2</sub> anti-human IgM purified antibody at different time points (see section 3.5.8), and immunoblot analyses of whole cellular extracts were performed using the pan-specific anti-phosphotyrosine antibody 4G10. The expression of the pre-BCR on the cellular surface of the selected cell lines was confirmed by FACS analyses (Figure 21A and B).

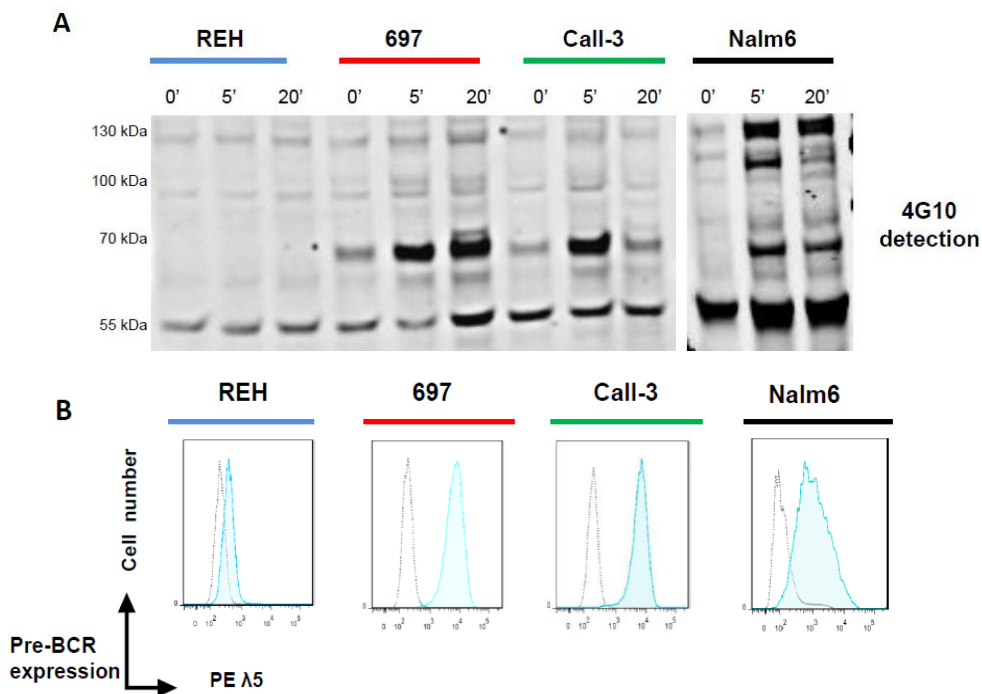


**Figure 21** Specific cross-linking of the pre-BCR by the F(ab')<sub>2</sub> anti-human IgM.

The leukemic cells were stimulated with 20 ng/ml of F(ab')<sub>2</sub> anti-human IgM purified antibody for the indicated time (in minutes). 20  $\mu$ g of whole cellular extracts were used immunoblot analysis. A) 4G10 phosphotyrosine specific antibody

(1:500) was used to detect tyrosine phosphorylated PTK. B) The expression of the pre-BCR was detected by FACS analysis through the use of the PE-conjugated anti-CD179b and PE-conjugated anti-human IgM (blue-shade curves) as a negative control. PE-IgG2a,  $\kappa$  Isotype control was used (gray curve). PE= R-phycoerythrin,  $\lambda$ = lambda. The data are representative of 2 independent experiments.

The pre-B ALL cell lines 697, CALL3 and Nalm6 (which express the pre-BCR, Figure 21B), and the pro-B ALL cell line REH (which does not express pre-BCR, Figure 21B) were selected as positive and negative controls, respectively, to evaluate whether the pre-BCR pathway can be activated by the F(ab')<sub>2</sub> anti-human IgM purified antibody. Additionally, it was assessed whether the activation of tyrosine phosphorylation is specifically restricted to the pre-BCR expressing leukemic cells. Strikingly, after the stimulation with the indicated antibody, an increase in global tyrosine phosphorylation was observed in the pre-BCR positive cells (697, CALL3 and Nalm6) near to the 70 kDa molecular weight marker (Figure 21A). In contrast, no tyrosine phosphorylation was detected in the pre-BCR negative REH cells at the same molecular weight. This 70 kDa protein may correspond to SYK, which is known as the immediate target of Lyn. Further experiments demonstrated that SYK comigrates with this 70 kDa protein upon stripping and retesting of the immunoblot with an anti-SYK antibody (see Figure 22B).

Tyrosine phosphorylation, detected by the phosphotyrosine (pTyr)-specific antibody 4G10, was markedly increased in 697, CALL3 and Nalm6 after 5 min of stimulation in comparison with the unstimulated control. After 20 min of stimulation the degree of phosphorylation drastically decreased in CALL3 cells, while exhibiting only a slight decrease in Nalm6 cells. However, 697 cells presented a notable increase in tyrosine phosphorylation at the same time point (20 min). At high molecular weight, tyrosine phosphorylation was only observed in Nalm6 cells (between 100 and 130 kDa), which reached an activation peak at 5 min and declined slowly thereafter. In general, the differences observed in tyrosine phosphorylation of cellular proteins indicate the activation of distinct signaling pathways in those cell lines. Taken together, the anti-human IgM purified antibody specifically recognizes the pre-BCR, and pre-BCR crosslinking leads to augment tyrosine phosphorylation of downstream signaling proteins.

#### **4.8.2. Tyrosine protein phosphorylation in Lyn-knockdown cells**

To characterize the importance of Lyn for downstream activation of tyrosine phosphorylated proteins, Nalm6 cells were transduced either with shRNA\_Lyn or shRNA\_SCR constructs and pre-BCR crosslinking (Figure 22).

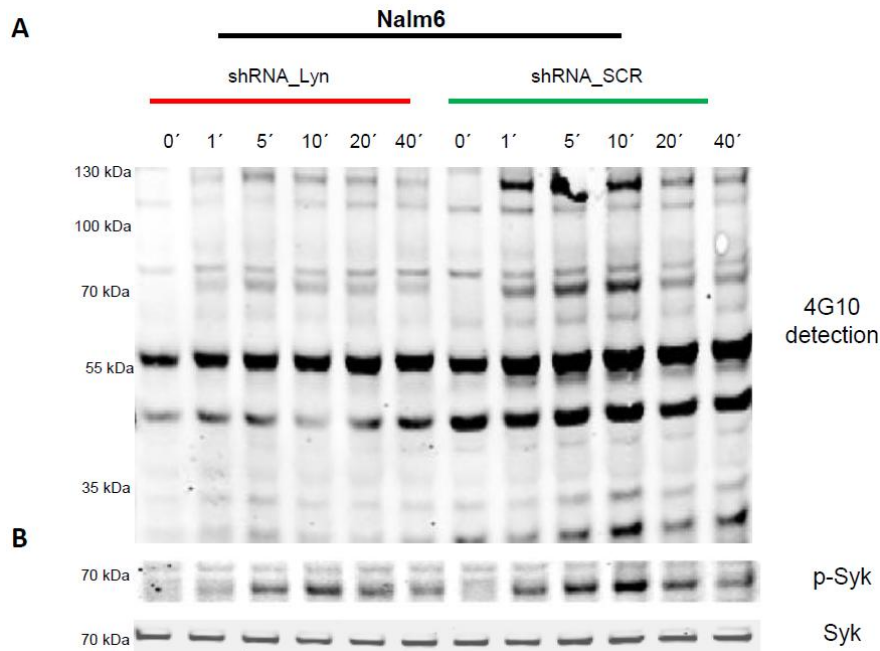


**Figure 22 Tyrosine phosphorylation in Lyn-knockdown Nalm6 cells upon pre-BCR crosslinking.**

The Nalm6 cell line was transduced either with shRNA\_Lyn or shRNA\_SCR, and FACS-sorting of GFP-positive cells was performed. The lentivirally transduced cells were stimulated with 20 ng/ml of F(ab')<sub>2</sub> anti-human IgM purified antibody or media alone for the indicated length of time (in minutes). Cell lysates from each time point were generated. 20 µg of those lysates were separated by SDS-PAGE and transferred to nitrocellulose membranes for immunoblot analysis. A) 4G10 phosphotyrosine specific antibody was used to detect phosphotyrosine. B) After 4G10 detection, the membrane was stripped and re-probed with Syk (1:1,000) and p-Syk (1:1,000) antibodies. The Syk antibody was used as a loading control as well as for indicating the molecular weight of Syk. The data are representative of 3 independent experiments.

Stimulation with the F(ab')<sub>2</sub> anti-human IgM purified antibody in both Nalm6-SCR and Nalm6 Lyn-knockdown cells led to an increase in tyrosine phosphorylation, at 70 and 130 kDa, in Nalm6 control cells. However, corresponding tyrosine phosphorylated proteins were strongly diminished in Nalm6 Lyn-knockdown cells. Additionally, whereas an increase in the tyrosine phosphorylation was detected in the molecular range between 55 and 33 kDa in Nalm6 control cells, this phosphorylation was distinctly reduced in Nalm6 Lyn-knockdown cells. It is noteworthy that a time dependent tyrosine phosphorylation pattern can be distinguished at 70 kDa in Nalm6 control cells. This phosphokinetic pattern attains a maximum level of phosphorylation at 10 min after stimulation. A decrease of the tyrosine phosphorylation was detected at 20 and 40 minutes and a plateau, slightly higher than the unstimulated time point (0 min), was observed. Conversely, a clearly induced phosphokinetic pattern could not be detected in Nalm6 Lyn-knockdown cells at the same molecular weight (70 kDa).

As previously mentioned, Syk (molecular weight 70 kDa) is known to be one of the immediate downstream targets of Lyn. Since the induced phospho bands coincide with the molecular weight of Syk, it was hypothesized that these bands represent Syk. For this purpose the membrane was stripped and

reprobed with an antibody directed against Syk and phospho-Syk (p-Syk), respectively (Figure 22A, B). The phosphokinetic bands were found to comigrate with Syk and a marked increase in the p-Syk detection was found in Nalm6 control cells as compared with Nalm6 Lyn-knockdown cells. As expected, the same phosphokinetic pattern detected at 70 kDa was also observed with the p-Syk specific antibody.

### 4.8.3. Downstream signaling in Lyn-knockdown cells

The pre-BCR ligation induces proliferative expansion of pre-B-cells<sup>99</sup> through the activation of different downstream proteins that together establish the pre-BCR signaling pathways. Previous results highlighted a reduction in the global tyrosine phosphorylation in Lyn-knockdown leukemic cells. The phosphorylation of downstream proteins, involved in proliferative responses (e.g. AKT and ERK 1/2), in the pre-BCR pathways was analyzed. Since previous data unveiled that Lyn was differentially expressed in ALL patient samples as well as ALL cell lines (Figure 18), Nalm6 and CALL3 Lyn-knockdown cells were used to investigate the impact of Lyn in the activation of critical downstream signaling components (Figure 23).

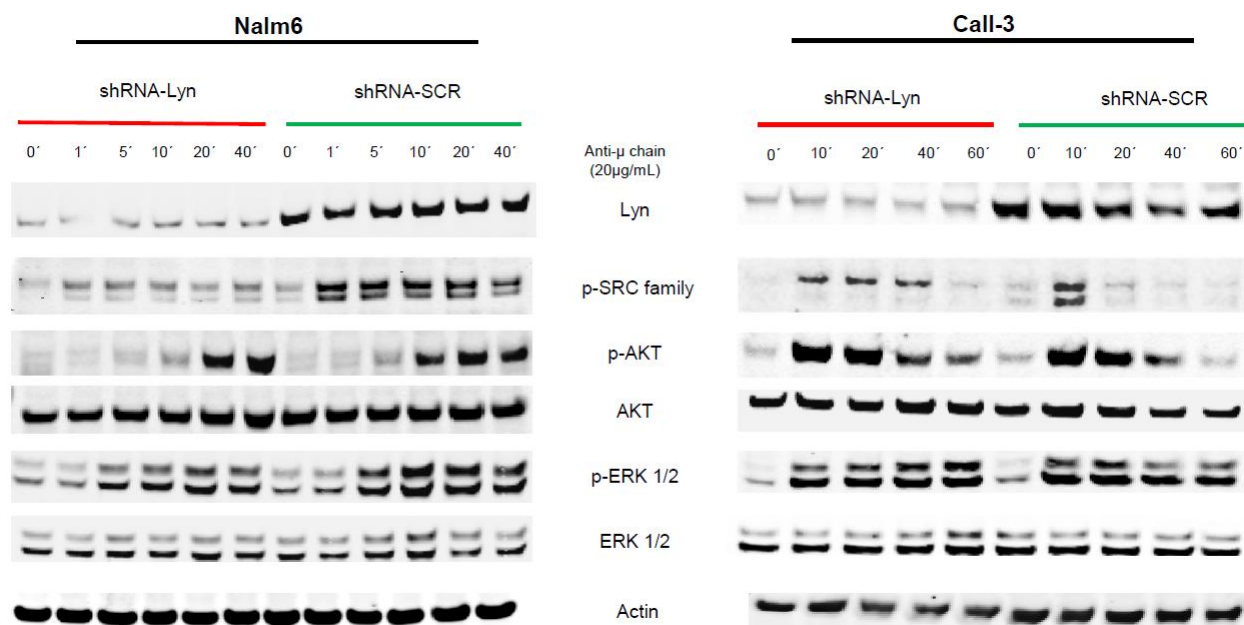


**Figure 23** Activation of AKT and ERK 1/2 in Lyn-knockdown leukemic cells.

The Nalm6 and CALL3 cell lines were transduced either with shRNA\_Lyn or shRNA\_SCR, and FAC-sorting of GFP-positive cells was performed. The lentivirally transduced cells were stimulated with 20 ng/ml of F(ab')<sub>2</sub> anti-human IgM and immunoblot analyses were performed as described above. The nitrocellulose membranes were probed with the following antibodies: anti-Lyn (1:1,000), anti-phospho-Src family (p-Src family)(1:1,000), anti-AKT (1:750), anti-phospho AKT (1:1000), anti-ERK 1/2 (1:500), anti-phospho ERK 1/2 (1:500). AKT= Protein kinase B (also known as PKB), ERK 1/2= mitogen-activated protein kinases (also known as p44/42 MAPK). Total AKT, ERK 1/2 and β-actin were used as a loading control. The data are representative of two independent experiments.

Activation of downstream proteins with or without Lyn repression was performed in Nalm6 and CALL3 cell lines, which recapitulated the high and low Lyn expression profile observed in ALL patient samples and cell lines, respectively. First, the efficiency of Lyn repression in these cells was tested by using a monoclonal antibody directed against Lyn (Figure 23). As expected, a strong reduction of the Lyn expression was observed in both Nalm6 and CALL3 cells, in which Lyn was knocked down via shRNA, in comparison to Nalm6 and CALL3 control cells. The activation status of all SFK following Lyn repression was analyzed using the p-Src family antibody. Similar to the shRNA-mediated Lyn repression, a decrease of SFK phosphorylation was observed in Nalm6 Lyn-knockdown cells as compared with Nalm6 control cells (Figure 23). However, it was not anticipated that phosphorylation of SFK appeared to persist for a longer period of time (up to 40 min after cross-linking) in CALL3 Lyn-knockdown cells as compared with CALL3 control cells upon pre-BCR ligation.

Furthermore, whereas phosphorylation of AKT was detected at 5 min after pre-BCR cross-linking in Nalm6 control cells, the AKT phosphorylation was not detected until 10 minutes after stimulation in Nalm6 Lyn-knockdown cells (Figure 23). In CALL3 Lyn-knockdown cells, AKT phosphorylation was still observed at 60 min after stimulation, whereas AKT phosphorylation was not detected in CALL3 control cells at the same time point. Phosphorylation of AKT at 60 min after stimulation in CALL3 control cells was similar or even less in comparison with the unstimulated sample (0 min) (Figure 23).

An increase in the phosphorylation of ERK 1/2 after pre-BCR cross-linking was observed in Nalm6 control cells, reaching an activation peak at 10 min after stimulation. In contrast, in Nalm6 Lyn-knockdown cells ERK 1/2 exhibited a drastic reduction in phosphorylation and reached an activation peak at 20 min after stimulation (Figure 23). In CALL3 Lyn-knockdown cells, an increase of ERK 1/2 phosphorylation was observed overtime, attaining the maximum activation peak at 60 min after pre-BCR ligation. However, reduction of ERK 1/2 activation was exhibited in CALL3 control cells. In CALL3 control cells ERK 1/2 displayed a marked increase of phosphorylation after 10 min of stimulation, and it decreased overtime. Taken together, Lyn repression in two ALL cell lines that show a differential Lyn expression (high and low Lyn expression in Nalm6 and CALL3, respectively), resulted in a distinctive phosphorylation/activation pattern as compared with corresponding control cells. In high Lyn-expressing cells (Nalm6), repression of Lyn led to reduction in the phosphorylation of SFK and downstream targets. In contrast, in low Lyn-expressing cells (CALL3), Lyn repression enhanced protein phosphorylation, and activation of SFK appeared to persist for a longer period of time.

#### **4.9. Subcellular localization of Lyn**

Lyn has been shown to be mainly restricted to membrane cholesterol-enriched microdomains called lipid rafts<sup>63</sup>. Different levels of Lyn were observed in ALL patient samples and ALL cell lines at the protein level. The subcellular localization of Lyn was assessed to investigate whether the high amounts of this kinase affect its cellular distribution. For this purpose, two different approaches were employed. First, the Lyn distribution within lipid rafts was assessed by using a linear sucrose gradient. Second, Lyn localization was visualized by confocal microscopy.

#### 4.9.1. Distribution of Lyn in isolated lipid rafts

Lipid rafts are sphingolipid- and cholesterol-rich membrane-microdomains. When a detergent (as Triton X-100) is applied, these microdomains are insoluble and "float on the solution. Owing to this detergent insolubility, lipid rafts are also known as "detergent-resistant membranes" (DRM). Due to the low density and large size of this DRM, they can be separated from soluble fractions (non-DRM) by density gradient centrifugation or "flotation"<sup>100</sup>. Based on these characteristics DRMs and non-DRMs were separated by linear sucrose gradient in Nalm6 and CALL3 leukemic cell lines (see section 3.5.11). Distribution of Lyn in the membrane compartments was determined by immunoblot analyses (Figure 24).

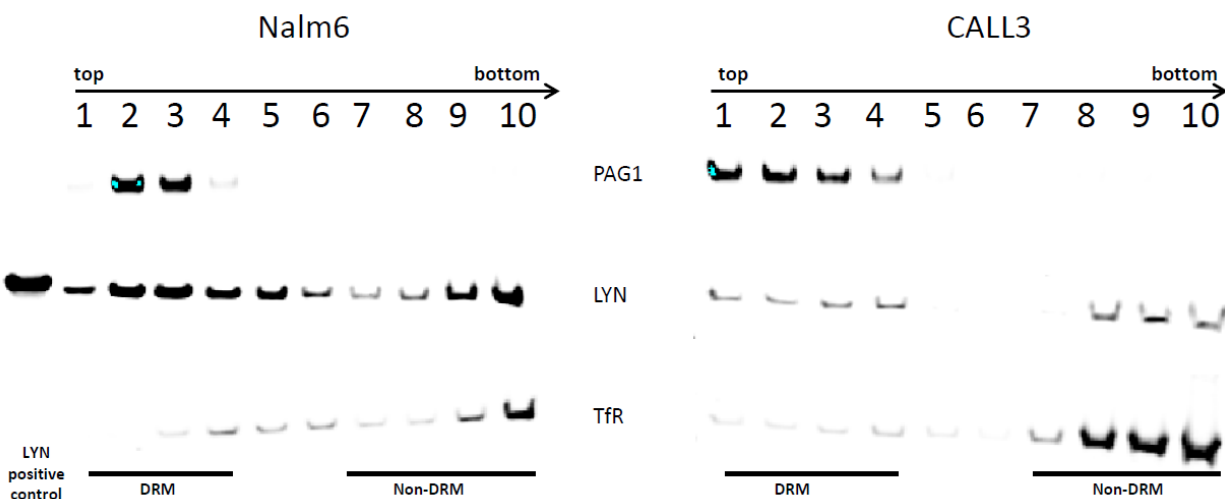


**Figure 24 Isolation of lipid rafts by linear sucrose gradient ultracentrifugation.**

$3 \times 10^7$  Nalm6 and CALL3 cells were lysed using homogenation buffer, and subjected to fractionation on a discontinuous sucrose gradient. 50  $\mu$ l of each fraction was used for immunoblot analysis. Fractionation of detergent-resistant membrane fractions (DRMs) and non-DRMs was evaluated by using anti-PAG1 (1:1000) and anti-TfR (1:500), respectively. Lyn expression was detected by immunoblotting with anti-Lyn (1:1,000, Cell Signaling). Lyn recombinant protein was used as positive control of Lyn detection. PAG1= phosphoprotein associated with glycosphingolipid-enriched microdomains 1, TfR= transferrin receptor.

The investigation of Lyn distribution by fractionation of the membrane compartments using linear sucrose gradient revealed that in Nalm6 cells Lyn was found to be present in all the fractions with a clear predominance in the DRM fractions (fractions 1-4), and in the last non-DRM fractions (fractions 9-10) (Figure 24). Similarly, in CALL3 cells Lyn was distributed either in DRM fractions (fractions 1-4) or non-DRM fractions (fractions 7-10). However, it is worth mentioning that Lyn was also found in Nalm6 cell fractions 5 and 6, whereas in CALL3 cells no expression of Lyn was observed. Successful fractionation of the membrane compartments was confirmed by anti-PAG1 immunoblots, a lipid raft protein marker which was only detected in DRM fractions either in Nalm6 or CALL3 cells. In clear contrast, the transferrin receptor (TfR) was preferentially located in non-DRM fractions in both leukemic cell lines.

Together, these results suggest that in Nalm6 cells Lyn is expressed beyond the buoyant fractions (fractions 1-4), which might indicate that Lyn is also localized outside the DRMs.

#### 4.9.2. Subcellular localization of Lyn by confocal microscopy

To further confirm whether Lyn was also present outside lipid raft structures, the microscopic subcellular localization of Lyn at the plasma membrane was analyzed. For this purpose, immunofluorescence confocal microscopy was used in xeno-ALL 109, as well as in Nalm6 and CALL3 leukemic cells (see section 3.5.10) (Figure 25).

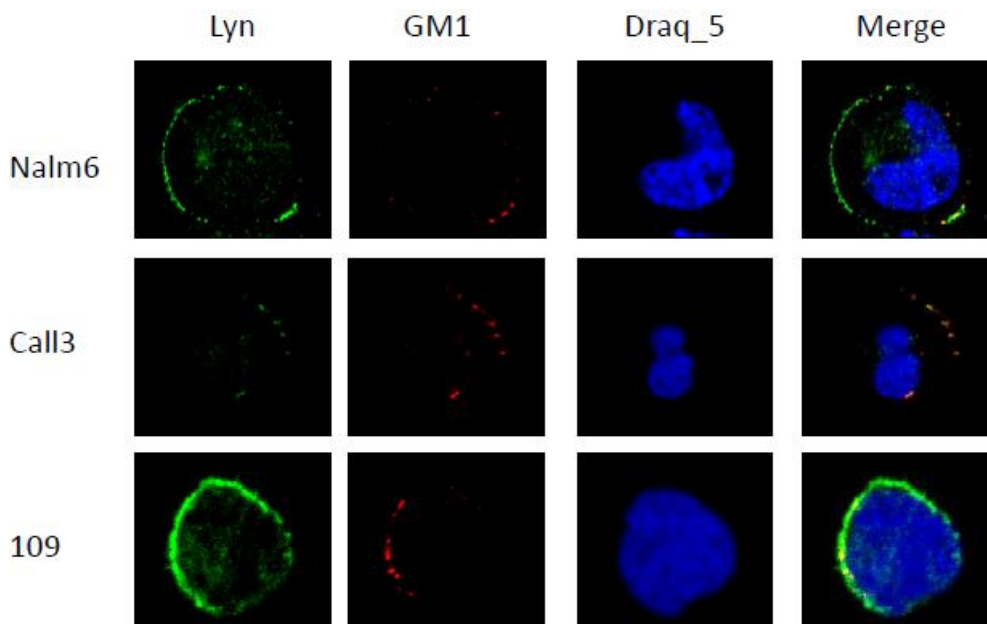


**Figure 25** Subcellular distribution of Lyn.

Subcellular localization of Lyn at the plasma membrane was determined by confocal microscopy of primary ALL 109, Nalm6 and CALL3 cells. Patching of the membrane lipid rafts was performed by using unlabeled cholera  $\beta$ -toxin (Sigma-Aldrich), which binds the GM1-ganglioside. Subsequently, the cholera toxin was detected by anti-cholera  $\beta$ -toxin (1:250, Abcam) and a secondary antibody conjugated to Alexa Fluor<sup>®</sup>488-red (1:750, Invitrogen). Lyn was detected using an anti-Lyn mAb (1:1,000, Cell Signaling), and an Alexa Fluor<sup>®</sup>555-green conjugated secondary antibody (1:750, Invitrogen). Draq\_5 (1:1,000, Cell Signaling) was used for nuclear staining. Fluorescence was detected using a Zeiss confocal microscope at 63x magnification. The pictures were processed through the use of ImageJ 1.45S (National Institutes of Health, USA).

The investigation of Lyn distribution in the plasma membrane of leukemic cell lines revealed that, whereas in CALL3 cells Lyn was exclusively present within defined lipid raft structures, the protein was aberrantly localized all over the membrane in the primary ALL 109 and Nalm6 cells (Figure 25). Notably, the high Lyn expression observed in Nalm6 and primary ALL 109 is associated with the Lyn expression detected by immunoblot analysis (Figure 18).

#### 4.10. Quantification of Lyn expression at transcript levels

In order to examine whether the high Lyn protein expression observed in the primary ALL 109 and Nalm6 cells is also observed at the transcriptional level, cDNA from the xeno ALL 109, Nalm6 and CALL3 cells was used for RT-PCR analysis (Figure 26).

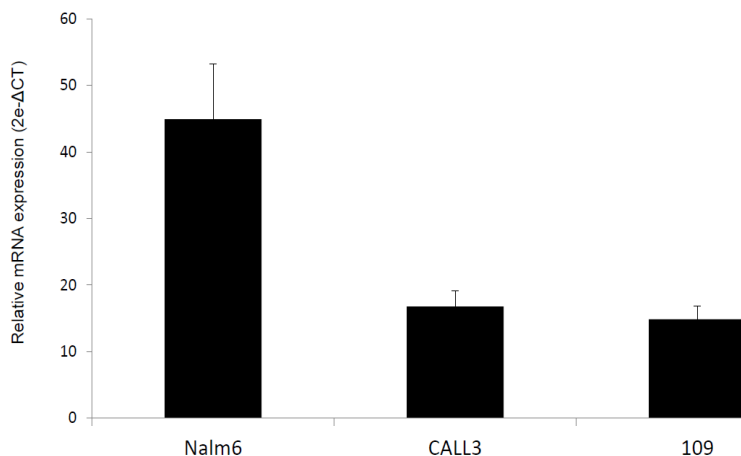


**Figure 26** Transcriptional expression of Lyn in ALL cells.

Relative quantification of the Lyn gene expression in 109 xeno-transplanted primary ALL, Nalm6 and CALL3 leukemic cells was performed by RT-PCR. Lyn gene expression was normalized by  $\beta$ 2M expression. The bars show the mean of relative Lyn mRNA expression ( $2^{-\Delta Ct}$ )  $\pm$  the standard deviation (SD).

As expected, the expression of Lyn at the transcript level in Nalm6 cells was almost three fold higher than in CALL3 cells. These data are in line with previous results of western blot analyses showing high and low Lyn expression at the protein level in Nalm6 and CALL3 cells, respectively. Surprisingly, the primary-ALL 109 showed low Lyn expression, although this leukemia had the highest level of Lyn expression at the protein level (Figure 18 and 25). The transcriptional expression of Lyn in ALL 109 was very similar to the Lyn expression observed in CALL3 cells, in which the expression of Lyn was barely detected at the protein level.

#### 4.11. Analysis of Lyn-dependent proliferation and survival

To examine whether the repression of Lyn has an effect on vital cellular functions (such as proliferation), Nalm6 and CALL3 cells were lentiviral-transduced either with shRNA<sub>Lyn</sub> or shRNA<sub>SCR</sub> constructs, and subsequently, subjected to an MTT assay for assessment of cell proliferation (see section 3.5.9). Cell proliferation was evaluated after 3 days (Figure 27).

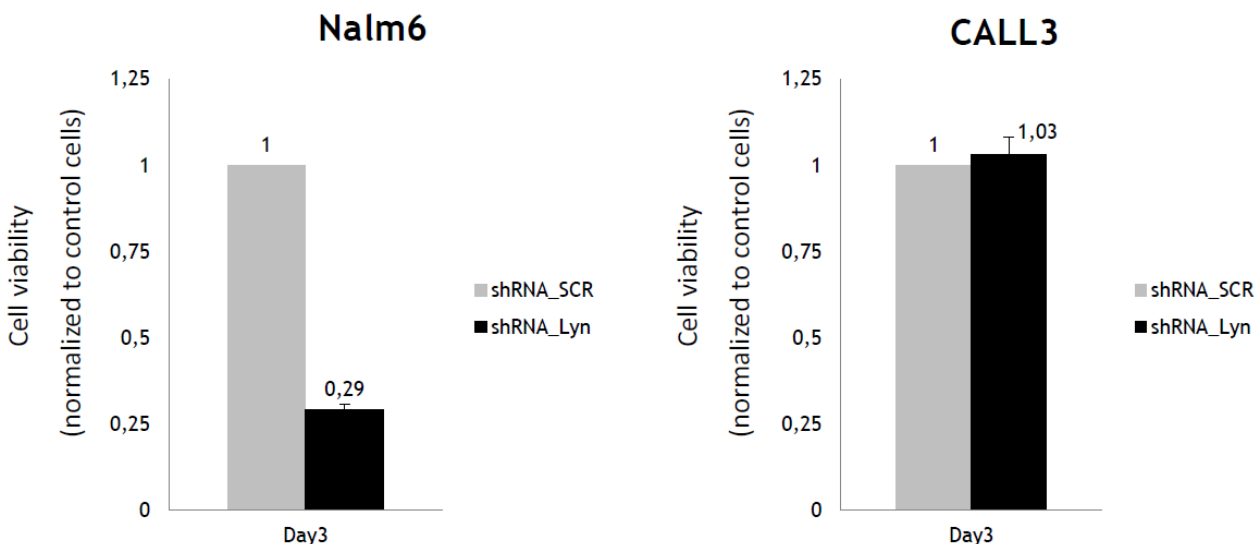


**Figure 27 Cell proliferation in Nalm6 and CALL3 Lyn-knockdown leukemic cells**

Nalm6 and CALL3 cells were lentivirally-transduced either with shRNA\_Lyn or shRNA\_SCR and cultivated for 3 days. 100  $\mu$ l of the infected leukemic cells were seeded out with  $1 \times 10^6$  cells per well on a 96 well plate. Stimulation was carried out every 24 hours by using 20 ng/ml of F(ab')<sub>2</sub> anti-human IgM for 3 days. After 3 days, the cells were subjected to a MTT assay to determine cell proliferation. The optical density of triplicate wells ( $\pm$  SD) normalized to 1 for shRNA\_SCR (control cells) is depicted. The assay is representative of three independent experiments. SD= standard deviation.

Analysis of cell proliferation in Nalm6 and CALL3 cells revealed that in Nalm6 the number of viable cells was strongly reduced to almost 70% compared with Nalm6 Lyn control cells (shRNA\_SCR cells) (upon stimulation with F(ab')<sub>2</sub> anti-human IgM) (Figure 27), whereas in CALL3 cells no difference in cell proliferation between Lyn-knockdown and control cells was observed (upon stimulation). Consequently, the induction of apoptosis after Lyn repression was analyzed. Repression of Lyn in either Nalm6 or CALL3 cells did not induce apoptosis in these cells (data not shown). Cell proliferation assays and apoptosis assays were reproduced three times with similar results (data not shown). Taken together, repression of Lyn only affected cell proliferation in cells that express higher amounts of Lyn (Nalm6). In contrast, cell proliferation was not affected in low Lyn-expressing cells (CALL3).

#### 4.12. SFK inhibition by tyrosine kinase inhibitor (TKI) in ALL cell lines

Pharmacological small-molecule inhibitors are powerful tools to study the biological consequences of disrupting signaling mediated by protein kinases. The compound SU6656 (Calbiochem®) has been described as a specific and potent ATP-competitive inhibitor of Src family kinases<sup>101</sup>. To investigate whether the results previously obtained from the cell proliferation assays in lentivirally-transduced Lyn-knockdown leukemic cells could be recapitulated by using a tyrosine kinase inhibitor (TKI). The cells were stimulated daily with F(ab')<sub>2</sub> anti-human IgM and treated with 5  $\mu$ M of SU6656. Cell proliferation was evaluated after 3 days (Figure 28).

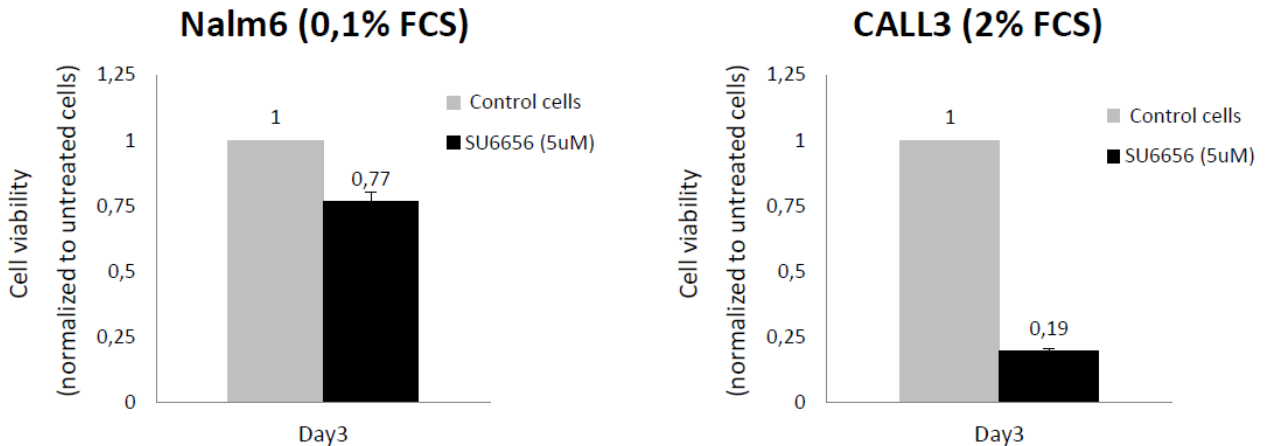


**Figure 28** Cell proliferation of Nalm6 and CALL3 upon SU6656 treatment.

Nalm6 and CALL3 cells were cultivated for 3 days at two FCS concentrations (0.1% and 2% for Nalm6 and CALL3, respectively), treated with 5 $\mu$ M of SU6656 and stimulated daily for 3 days with 20 ng/ml of F(ab')<sub>2</sub> anti-human IgM. After 3 days, cells were subjected to a MTT assay to determine cell proliferation. The bar charts show the optical density of triplicate wells ( $\pm$  SD) normalized to 1 for untreated cells (control cells). The assay is representative of three independent experiments. The optical density was measured at 570 nm with a reference wavelength of 650 nm using an ELISA reader. SD= standard deviation.

Figure 28 displays the analysis of cell proliferation in Nalm6 and CALL3 cell lines under starving conditions after three days of SU6656 treatment. Reduction of cell proliferation was detected in both Nalm6 and CALL3 cells. However, whereas in Nalm6 cells a cell growth reduction of roughly 30% was observed, in CALL3 cells a drastic decrease of cell proliferation (more than 80%) was detected. A reduction in cell growth proliferation was observed when the cells were cultivated under non-starving conditions (10% and 20% for Nalm6 and CALL3 cells, respectively) (data not shown).

Inhibition of SFK by the SU6656 TKI in the low Lyn-expressing CALL3 cells resulted in a more pronounced reduction of cell proliferation (4-fold) than in high Lyn-expressing Nalm6 cells. This result is in clear contrast to previous results regarding cell proliferation of Lyn-knockdown Nalm6 cells, which showed strikingly impaired cell proliferation upon Lyn repression compared to CALL3 Lyn-knockdown cells (Figure 27).

## 5. Discussion

Based on the results of *in silico* transcriptome/proteome analyses of a cohort of childhood ALL patients, 18 non-RTKs were selected as candidates for the assessment of protein expression (Figure 9), and their potential functional role in ALL. Selected candidate genes were cloned and recombinant proteins were used to establish specific and robust immunological detection by quantitative Western Blot.

### 5.1. PTK expression in ALL

The protein expression of 18 selected PTK was assessed in a cohort of 81 ALL patient samples with different ALL immunophenotypes. Additionally, the expression of the selected PTK was analyzed in seven ALL cell lines and six xeno-transplanted primary ALL sample. Finally, mature B- and T-cells, extracted from buffy coats, were used to evaluate the expression status of PTK in non-leukemic cells.

In the analyzed ALL patient material, the expression of 13 out of 18 PTK (72%) was detected at the protein level (Figure 16B). Similar percentages of the selected PTK (66%) were expressed either in ALL cell lines or primary ALL blasts (Figure 15). In mature lymphocytes 13 out of 18 PTK (72%) were detected at the protein level (Figures 15 and 16B). Interestingly, in non-leukemic lymphocytes (CD3<sup>+</sup> and CD19<sup>+</sup>) the expression of Fyn and ZAP70 was relatively high, whereas in ALL patient samples these PTK were barely expressed and completely absent in primary ALL blasts and ALL cell lines. The high expression of Fyn and ZAP70 in mature lymphocytes supports previous findings claiming that these proteins play an important role in B- and T-cell development,<sup>98, 102</sup>. It remains to be determined whether the reduction in the expression of these PTK is critical for leukemogenesis.

Overall, the percentage of PTK expression observed in ALL cells was very similar to the percentage of PTK expression in mature lymphocytes. In both, leukemic and non-leukemic cells, the PTK expression was characterized by a high degree of heterogeneity. Although a specific immunophenotype-related expression profile could not be detected, a similar expression pattern was observed within leukemic T-cells (Figure 14). Although the small size of patients analyzed excluded a proper statistical correlation, PTK expression and their relationship with different patient clinical parameters (e.g. age, percentage of blast at diagnosis and leukemic risk assessment) of the ALL patient samples was assessed. No significant relationship between high expression of Lyn and any clinical parameters could be detected (data not shown).

Furthermore, in order to exclude a differentiation phenomenon one needs to analyze the PTK expression in the course of hematopoiesis, an analysis of cell population at different stages of normal B- and T- cell development would be needed. Such analysis was not feasible due to the quantities of immature lymphoid precursors in bone marrow and peripheral blood. Although CD34-positive stem/progenitor cells were isolated from several healthy cord-blood donors, the amount of protein extracted from the isolated stem cells was insufficient for the evaluation of PTK protein expression (data not shown). This observation highlights an important disadvantage of WB analyses in which high amounts of proteins are

needed although patient material is usually limited. One possible solution to overcome this problem could be by using techniques (e.g. FACS analysis), which require less amount of material than immunoblots; however the availability of specific antibodies for these methods is limited. In sum, the PTK expression was solely evaluated in mature B- and T-lymphocytes isolated from buffy coats of healthy blood donors.

## 5.2. High Lyn expression in a subgroup of ALL patient samples

In Figure 16B, it was shown that the PTK expression profile in ALL patient samples was independent of the immunological phenotype. However, unsupervised cluster analysis using Pearson correlation was employed, which yielded five subgroups based on their PTK expression (Figure 16C). Interestingly, the majority of the analyzed ALL patient samples clustered into two subgroups. These two subgroups were determined by a relatively high expression of Lyn and Blk, respectively. In the remaining three subgroups a relatively high expression of SYK, CSK and Fyn was observed, respectively.

Lyn and Blk, which belong to the Src-family kinases (SFK), were highly expressed in the majority of patient samples five subgroups. There is mounting evidence that SFK are indispensable for B-cell development and signaling. In fact, these kinases are rapidly activated upon aggregation of either the pre-B-cell receptor (pre-BCR) or the BCR<sup>37</sup>, and activation of these SFK trigger a wide range of downstream signaling events, which in turn, regulate critical biological responses such as cell differentiation, proliferation, migration, and apoptosis<sup>37, 98</sup>. Besides the significant and important role of these protein kinases in normal lymphopoiesis, the SFK have also been strongly implicated in many human cancers<sup>61</sup>. It has been observed that either overexpression and/or augmentation in the kinase activity of SFK promote development, progression and metastasis of numerous human malignancies such as colorectal<sup>61</sup>, ovarian<sup>65</sup>, breast<sup>103</sup>, and lung cancers<sup>94, 104</sup>.

Lyn has been implied in myeloid<sup>105</sup> or chronic lymphoid leukemia<sup>86</sup>. Therefore, we decided to investigate whether this relatively high expression of Lyn might be critical for sustaining the leukemic phenotype in acute lymphoblastic leukemia.

Furthermore, the expression of Lyn exhibited a broad spectrum of expression in ALL patient samples (Figure 16). Remarkably, in those ALL patients where Lyn was expressed at lower levels, a predominant expression of the B-cell-specific SFK (Blk) was observed instead. It may suggest a mutual exclusive expression of Lyn and BLK. It has been described that at least five SFK (Lyn, Blk, Fgr, Fyn and Yes) are expressed in normal B-cells<sup>106</sup>. However, there is a clear predominant expression of Lyn, Blk, and Fyn with possible overlapping functions<sup>107</sup>. It is described that Lyn appears to be the main SFK used after pre-BCR cross-linking in B-lymphocytes. However, the other SFK present in those cells can assume Lyn's role<sup>79</sup>. High expression of Blk observed in the subgroup of ALL low Lyn-expression may be the result of a compensatory mechanism, in which Blk took over Lyn's functions, indicative of the apparently redundant role of these kinases<sup>108</sup>. Though this notion might explain the results obtained within this subgroup, the molecular mechanism by which Blk is preferentially expressed and whether Blk expression is crucial for the leukemogenic process remains unknown.

### 5.3. Analysis of protein activation in Lyn-knockdown ALL cell lines

One of the common problems of working with patient material is the limited availability of the samples. Therefore, we sought feasible cell line models which could provide unlimited material. Screening of Lyn expression either in ALL cell lines or primary ALL leukemia cells unveiled that the Nalm6 and CALL3 cell lines exhibited high and low protein levels of Lyn, respectively (Figure 18). Similar results were obtained at the transcript levels (Figure 26). Furthermore, analysis of the Lyn expression in ALL primary blasts showed that the 109 primary pre-B ALL cells recapitulated the expression of Lyn observed either in ALL patient samples or ALL cell lines. The high expression of Lyn in 109 primary leukemia cells represents a good opportunity to study the role of Lyn in leukemogenesis overcoming all the limitations of cell line models. However, propagation of 109 ALL cells into our mouse-model remains to be done. Nevertheless, the two cell lines, Nalm6 (high Lyn-levels) and CALL3 (low Lyn-levels), showed a similar Lyn expression profile observed in ALL patient specimens, and were therefore chosen as a cell line model to further investigate the impact of Lyn repression in those ALL cells.

To repress the expression of Lyn by RNA interference different shRNA plasmids directed against Lyn were selected and of the most effective one, was used for transduction of Nalm6 and CALL3 cells (Figure 17). Because of the highly conserved structure among the SFK members, off-target effects were excluded in Nalm6 cells (Figure 19). Surprisingly, after transduction of Nalm6 and CALL3 cells with the shRNA\_Lyn construct, we could not detect any effect on either survival or proliferation upon Lyn repression (Figure 20). Thus, it was concluded that under standard cell culture media conditions, repression of Lyn does not affect survival or proliferation in the analyzed cell line models, possibly due to the activation of many growth factor receptors by the serum-containing media. Thus, the induction of multiple signaling pathways and the presence of other SFK members could compensate for the reduced Lyn expression. Moreover, the efficiency of RNA interference was not 100%, leading to a residual Lyn expression that might still be sufficient to maintain the biological functions of Lyn, which might explain the lack of a clear phenotype under Lyn knockdown conditions.

To analyze the functional role of Lyn and the activation of downstream proteins in the biological context of pre-BCR signaling, the pre-BCR pathway was potentiated by specific pre-BCR crosslinking in the absence of serum. As mentioned above, previous reports showed that the engagement of the pre-BCR leads to activation of the SFK Lyn, Fyn and Btk<sup>37, 66, 98</sup>. Furthermore, activation of these SFK leads to phosphorylation of immunoreceptor tyrosine-based activation motifs (ITAMs), which in turn, promote recruitment and activation of SYK<sup>37, 109</sup>. SYK is a key protein required for the activation of pathways involved in proliferation<sup>37, 88</sup>. Therefore, the phosphorylation of SFK and downstream targets like SYK as well as critical signaling nodes for proliferative responses (e.g. AKT and ERK1/2, see section 5.4) were analyzed in Nalm6 or CALL3 knockdown cells after pre-BCR cross-linking.

After the presence of the pre-BCR on the cell surface of Nalm6 and CALL3 cells was confirmed (Figure 21A). The specificity of the F(ab')<sub>2</sub> anti-human IgM purified antibody to cross-link the pre-BCR was tested (Figure 21B). As expected, tyrosine phosphorylation patterns were only altered in the pre-BCR-positive

cell lines. A reduction of global tyrosine phosphorylation was detected by 4G10 mAb upon pre-BCR cross-linking in ALL Lyn-knockdown cells (Figure 22). In this regard, we analyzed the activation of several downstream proteins upon pre-BCR cross-linking in Lyn-knockdown ALL cells (Figure 23). Unexpectedly, a different activation profile was observed in Nalm6 cells (high Lyn-expressing cells) as compared to CALL3 (low Lyn-expressing cells). On one hand, repression of Lyn in Nalm6 cells noticeably affected the phosphorylation status of the SFK detected by p-Src family antibody. On the other hand, repression of Lyn in CALL3 cells resulted in a sustained activation of the SFK for a longer period (up to 40 minutes after pre-BCR cross-linking) as compared to CALL3 control cells. These striking differences observed in CALL3 cells led to conclusion that the SFK activation detected in CALL3 Lyn-knockdown cells is due to other SFK members present in CALL3 cells. The analysis using the p-SRC family antibody showed only one band in Lyn-knockdown CALL3 cells, whereas two bands in CALL3 control cells were detected. This result strongly suggested the presence of SFK other than Lyn. Furthermore, analyses of the PTK in this cell line revealed that Blk is the most prominent SFK expressed in CALL3 cells (Figure 15), and therefore, BLK might be able to compensate for Lyn functions. A recent study in splenic B-cells, purified from Lyn<sup>-/-</sup> mice, showed an enhancement of SFK activation after BCR ligation in absence of Lyn<sup>110</sup>.

Moreover, the drastic reduction of the SFK activity in CALL3 control cells (activation is suppressed 10 minutes after pre-BCR cross-linking), strongly implies that Lyn is involved in a negative regulatory mechanism of SFK. Consistent with these results, several studies have shown that Lyn can phosphorylate immunoreceptor tyrosine-based inhibitory motifs (ITIMs)<sup>107, 110</sup>. These ITIMs recruit protein tyrosine phosphatases as SHP-1 and 2 (anti-Src homology phosphatase-1 and 2), which in turn, dephosphorylate the SFK turning off their activity.

Remarkably, a prolonged activation of SFK in Nalm6 control cells upon pre-BCR cross-linking (Figure 23). The sustained activity of the SFK without any apparent negative regulation raised to the question, why do these SFK remain active in Nalm6 cells, when Lyn is highly expressed, and if they escape from SFK regulatory mechanisms. To answer this question, the subcellular distribution of Lyn was assessed, and consequently affects on SFK regulatory mechanisms. It has long been known that the SFK members contain N-terminal lipid modification sites for both myristoylation (present in all SFK) and palmitoylation (present in all SFK but Src and Blk), and this N-terminal domain is responsible for localization of the SFK to membranes<sup>62, 86, 107</sup>. Double acetylated SFK are concentrated in cholesterol enrichment membrane micro-domains or "lipid rafts"<sup>111</sup>. Based on these observations, confocal microscopy analysis of the GM1 (a lipid-raft marker) detected with cholera  $\beta$ -toxin and isolation of lipid rafts by sucrose gradient was used to investigate the subcellular distribution of Lyn in Nalm6 and CALL3 cells (Figures 24 and 25). The results of the Lyn immunofluorescence analysis indicated that, whereas Lyn was exclusively present within defined lipid rafts in CALL3 cells, the protein was aberrantly localized all over the membrane in Nalm6 cells, likely independent of lipid rafts. Interestingly, similar distribution of Lyn was observed in ALL 109. Lyn's abnormal distribution could enable this kinase to interact with other proteins and promote its activation as has been demonstrated in chronic lymphoid leukemia cells (CLL)<sup>86</sup>.

One of the most prominent mechanisms that downregulates SFK activity is the phosphorylation of the regulatory tyrosine residue 530 (Tyr-530) by the C-terminal Src kinase (CSK)<sup>63</sup>. However, CSK is an exclusively cytoplasmic protein (due to the lack of a transmembrane domain and lipid modifications)<sup>62</sup>. Therefore, in order to access its substrates, CSK requires the transmembrane adaptor-like protein Cbp/PAG1 (Csk binding protein/phosphoprotein associated with glycosphingolipid-enriched membrane) present exclusively within lipid raft structures<sup>91</sup>. Thus, a model was proposed in which the unique role of Lyn is phosphorylation of Cbp/PAG1 (necessary for CSK recruitment), and the escape of Lyn from this regulatory mechanism due to its membrane mislocalization when overexpressed (discussed in more detail in section 5.5).

#### **5.4. Repression of Lyn affects proliferation of ALL cells**

As mentioned before, the activation of downstream targets involved in proliferative responses (AKT and ERK 1/2) is altered in Nalm6 or CALL3 Lyn-knockdown cells. To further investigate the effect of Lyn repression on cell viability, RNA interference and small molecule kinase inhibitors were applied.

The analyses of AKT and ERK 1/2 revealed a very distinct activation pattern between Nalm6 and CALL3 Lyn-knockdown cells. In Nalm6 Lyn-knockdown cells, the activation of AKT was only detected 20 minutes after pre-BCR cross-linking, whereas in Nalm6 control cells this activation was detected after 10 minutes. Accordingly, the ERK 1/2 proteins displayed a marked decrease in the activation as compared to control cells. The delay in the activation of AKT and reduction in the phosphorylation of ERK 1/2 are dependent on Lyn repression and the reduction of SFK activation. It needs to be mentioned that although Lyn repression induced delays AKT activation and decreased ERK 1/2 phosphorylation, the pathways were nevertheless activated. However, whether this activation is induced by either other SFK members that are present in Nalm6 Lyn-knockdown cells or by residual Lyn upon RNA interference remains open.

On the other hand, in CALL3 Lyn-knockdown cells, AKT activation was detected up to 60 minutes after stimulation, and activation of ERK 1/2 increased overtime in comparison to CALL3 control cells. As expected, the activation of AKT and ERK 1/2 is consistent with the increasing SFK activity. These data suggest that Lyn might not be the only activating kinase, while its role in inhibitory mechanisms which downmodulate AKT and ERK 1/2 responses appears to be unique.

To test whether the differences in the activation of AKT and ERK 1/2 have an impact on cell proliferation in Nalm6 and CALL3 Lyn-knockdown leukemic cells, MTT assays were performed. As anticipated, reduction in the activation of AKT and ERK 1/2 cells decreased cell proliferation in Nalm6 Lyn-knockdown cells by almost 70% (Figure 27). In CALL3 Lyn-knockdown cells this could not be recapitulated. In CALL3 an increase of AKT- and ERK 1/2 activity did not influence cell proliferation. A possible explanation could be that Blk, and not Lyn, is the most prominent SFK cells, therefore repression of Lyn does not represent a critical cellular insult.

Furthermore the effects of SU66566; a selective Src family kinase inhibitor, in Lyn-knockdown leukemic cells was investigated (Figure 28). CALL3 cells were very sensitivity to SU66566 inhibition in comparison to Nalm6 cells. Moreover, while in CALL3 cells a reduction of almost 80% of cell proliferation was detected; in Nalm6 cells a decrease of 23% in cell proliferation was observed. These results were in clear contrast with the previously discussed data from Lyn-knockdown cells. The reason for this discrepancy remains unclear. However, based on the fact that Lyn was found to be highly expressed and aberrantly distributed in Nalm6 and not in CALL3 cells, a possible explanation would be that the amount of Lyn protein and its cellular distribution might contribute to the observed SU66566 treatment resistance. In agreement with this hypothesis, reduction in cell proliferation in Nalm6 and CALL3 cells was found to be similar only when Nalm6 were incubated with higher concentration of SU66566 (data not shown). This observation raises the question about the clinical relevance of Lyn expression level and TKI treatment resistance. In the light of previous studies that have highlighted the correlation of Lyn overexpression and resistance to TKI in chronic myeloid leukemia<sup>112</sup>. In these studies high Lyn expression, both at the protein and RNA level, was correlated with resistance to nilotinib<sup>112</sup> and imatinib<sup>113</sup> treatment, and sensitivity was restored only after Lyn repression<sup>112, 113</sup>.

### 5.5. Proposed models of the dual functions of Lyn

Based on knoww Lyn function within the pre-BCR pathway<sup>37, 49, 110, 114</sup> and the clear contrast in the activation of SFK in Nalm6 and CALL3 Lyn-knockdown cells, two models are proposed in which the role of Lyn is dependent on both Lyn expression levels and Lyn subcellular localization (Figures 29 and 30).

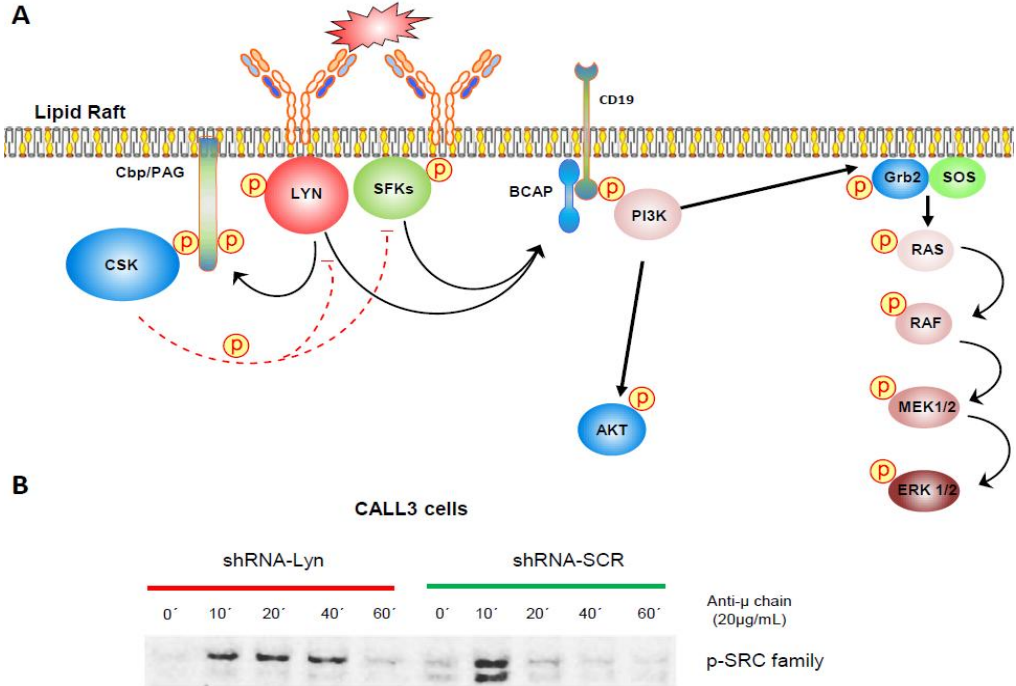


**Figure 29** Proposed model for SFK activation and downregulation by Lyn in CALL3 cells.

Activation of SFK upon pre-BCR cross-linking and regulation of their activity by Lyn. For simplicity the complete pre-BCR pathway is not shown and Lyn functions are emphasized within lipid raft structures. A) After pre-BCR engagement, Lyn as

well as other SFK kinases and SYK (not depicted) are phosphorylated. This phosphorylation results in an increase in their kinase activity and subsequent phosphorylation of several downstream proteins. Both Lyn and SFK activation lead to the activation of PI3K, which in turn, activates AKT and ERK 1/2. Activated AKT and ERK 1/2 regulate several biological responses of cell growth, survival, and proliferation<sup>89</sup>. However, phosphorylation of Cbp/PAG is carried out exclusively by Lyn. The phosphorylated Cbp/PAG protein recruits CSK into lipid rafts, and then CSK downregulates both Lyn and other SFK by phosphorylation of the regulatory tyrosine residue. B) Western blot analyses of the SFK activity in CALL3 Lyn-knockdown and non-depleted cells. Under Lyn repression (shRNA-Lyn) a sustained SFK activation was detected up to 40 minutes after pre-BCR cross-linking, whereas SFK activity is suppressed 10 minutes after cross-linking. Continuous black arrows indicate activation. Dashed arrows indicate repression. BCAP= B-cell adaptor protein. Cbp/PAG= Csk binding protein/phosphoprotein associated with glycosphingolipid-enriched membrane.

Figure 29 depicts the activation and regulation of SFK when Lyn is restricted to lipid raft structures. Since the SFK remain active in CALL3 Lyn-knockdown cells after cross-linking, the induction of negative regulatory effect might be a unique function of Lyn. Thus, under Lyn repression, Cbp/PAG is not phosphorylated and therefore, CSK is not recruited to the lipid rafts. As expected, the absence of the negative regulator, CSK, resulted in prolongation of the SFK activity (Figure 29B). By contrast, in CALL3 control cells Lyn is able to phosphorylate Cbp/PAG, therefore CSK is successfully recruited into lipid rafts, and the activation of SFK is abolished (Figure 29B). In summary, the activating function of Lyn on downstream targets, may be redundant and be compensated by other SFK. Its inhibitory role via CSK recruitment appears to be unique and indispensable.

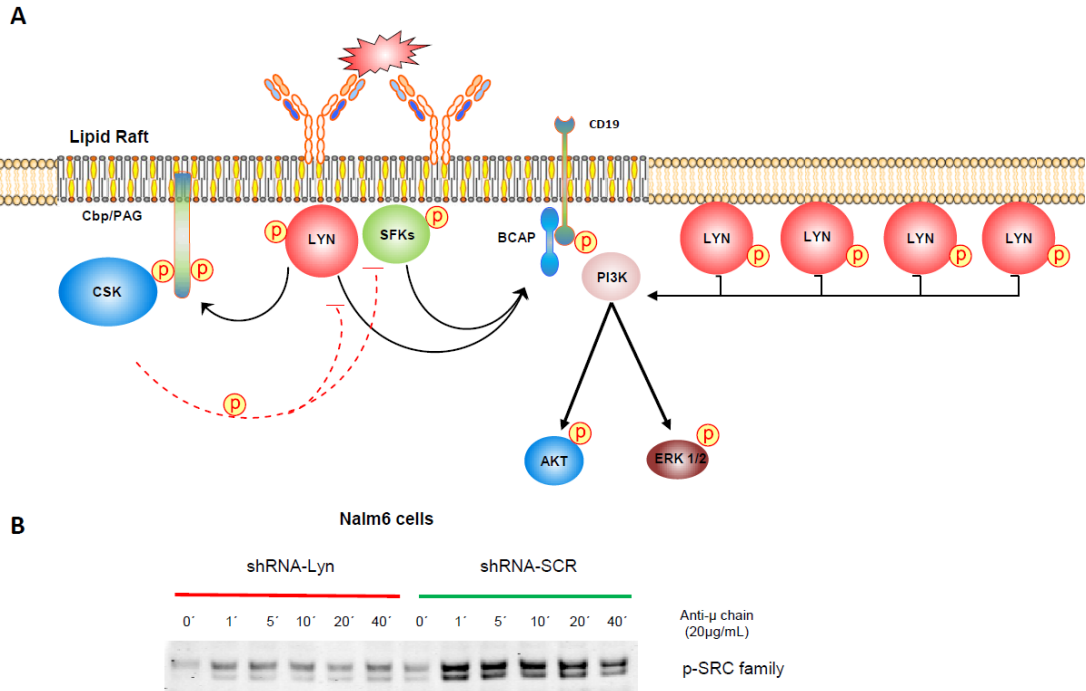


**Figure 30** Proposed model for deregulated activity of SFK in Nalm6 cells.

Based on the model shown in Figure 29, the proposed deregulated SFK activity is depicted. A) Right part of the graphic; Lyn protein abundance exceeds the capacity of lipid raft compartments leading to an abnormal distribution outside lipid rafts. Thus, mislocalized Lyn would escape from the negative feedback of CSK, which is restricted to lipid rafts. B) Western blot analyses of the SFK activity in Nalm6 Lyn-knockdown and non-depleted cells. While in Nalm6 Lyn-

knockdown cells a decrease in SFK activation was observed, in Nalm6 control cells SFK activation remains unaffected after cross-linking. Continuous black arrows indicate activation. Dashed red arrows indicate repression. BCAP= B-cell adaptor protein. Cbp/PAG= Csk binding protein/phosphoprotein associated with glycosphingolipid-enriched membrane.

Figure 30 displays a proposed model in which the high level of Lyn expression and its aberrant distribution, leads to an escape from the inhibitory mechanism mediated by Cbp/PAG-CSK. The loss of this negative regulation is supported by the fact that the SFK remain active after pre-BCR cross-linking (Figure 30B). One could hypothesize that mislocalized Lyn interacts with receptors located outside the lipid rafts through Lyn-SH2 domains, activate PI3K/AKT-ERK 1/2 responses and regulate cell proliferation. Abrogation of Lyn by shRNA led to attenuation of the activation of SFK, AKT and ERK 1/2 (Figure 30B and 23) and impairment of cell proliferation (Figure 27). Consistent with these data, previous studies demonstrated that knocking down Lyn expression decreased cell proliferation of leukemic cells<sup>105, 115</sup>.

## 5.6. Outlook

Futures experiments are needed to recapitulate the functional role of Lyn in proliferation in ALL cells *in vivo*. To this end, primary xenotransplanted ALL (109 primary ALL), which expresses high amounts of Lyn, represent an excellent working model for the *in vivo* analysis of Lyn functions. The mechanistic basis of aberrant Lyn expression should be investigated in the future also comprising the assessment of protein turnover. As such the ubiquitin-proteasome system has been implicated in Lyn degradation<sup>116, 117</sup>.

Although in this work the important function of CSK in downregulating SFK activity has been stressed, there are several protein phosphatases, including SHP1 and SHP2 that might also be implicated in the negative regulation of SFK, and therefore it will be of great interest to determine whether the functional status of these phosphatases is affected upon Lyn overexpression and mislocalization.

Finally, it was shown in this study that CALL3 leukemic cells were highly sensitive to treatment with SFK-specific tyrosine kinase inhibitors (TKI). From a clinical point of view, this underlines the need to investigate the potential of a SFK-specific directed inhibition strategy also in combination with conventional chemotherapy in ALL. Additionally, due to the high resistance of the Nalm6 cells to SFK-specific inhibitors, experiments are already underway to investigate whether repression of Lyn expression in these cells might be accompanied by an increase of sensitivity to TKIs. Together, these experiments might improve our understanding of the molecular mechanism that leads to an aberrantly high Lyn expression, the functional role of Lyn for leukemic proliferation.

## 6. Summary

The aim of this study was to assess the expression of protein tyrosine kinases (PTK) in acute lymphoblastic leukemia (ALL) patient samples at the protein level. Xenotransplanted primary ALL blasts and ALL cell lines were used as model system for the functional analysis of the role of PTK in ALL. The analysis revealed that Lyn, a member of the Src family kinase (SFK), was prominently expressed in a subgroup of ALL patient samples. To further investigate the biological consequence of elevated Lyn expression in ALL cells, Nalm6 and CALL3 cells were used as a model which recapitulated the high and low Lyn expression profile observed in patient specimens, respectively. Lyn is known to be associated with pre-BCR after receptor crosslinking. Analysis of the functional role of Lyn upon shRNA mediated Lyn repression and pre-BCR crosslinking showed that phosphorylation of downstream signaling proteins was strikingly reduced or delayed in Nalm6 cells. In addition, cell proliferation was substantially reduced in Nalm6 Lyn-knockdown cells. Conversely, an increase in the tyrosine phosphorylation was found in CALL3 Lyn-knockdown cells. Membrane microdomain, called lipid rafts, were shown to concentrate and regulate SFK<sup>111</sup>. However, data of the Lyn localization in the plasma membrane indicates that, whereas Lyn was exclusively present within defined lipid rafts in CALL3 cells, the protein was aberrantly localized all over the membrane in Nalm6 cells. The Lyn mislocalization was likely independent of lipid rafts and it could enable Lyn to interact with other proteins located outside rafts structures and promote its activation. Ultimately, preliminary data suggests that overexpression of Lyn is implicated in resistance to tyrosine kinase inhibitor (TKI) treatment.

Altogether these findings suggest that the high expression level and the abnormal subcellular distribution of Lyn allow it to escape from regulatory mechanisms only present in the lipid rafts. Thus, Lyn can cause an increase in the activation of downstream pathways and therefore might contribute to proliferation and possibly confer resistance to TKIs. In contrast, when Lyn was mainly present within the lipid rafts a negative regulation of downstream proteins was observed, pointing at a dual role for Lyn in the pathobiology of ALL.

## 7. Abbreviations

### 7.1. Prefixes

Abbreviation	Prefix	Factor x 10 <sup>x</sup>
n	nano	-9
μ	micro	-6
m	mili	-3
c	centi	-2
k	kilo	3

### 7.2. Units

Abbreviation	Unit
°C	degree Celsius
A	ampere
Da	Dalton
g	gram
h	hour
l	liter
M	molar
m	meter
min	minute
OD	optical density
seg	second

### 7.3. Non-receptor tyrosine kinases

Abbreviation	Name
Blk	B lymphoid tyrosine kinase
Fgr	Gardner-Rasheed feline sarcoma viral oncogene homolog
Fyn	FYN oncogene related to SRC, FGR, YES
Hck	Hematopoietic cell kinase
Lck	lymphocyte-specific protein tyrosine kinase
Lyn	v-yes-1 Yamaguchi sarcoma viral related oncogene homolog
Src	v-src sarcoma (Schmidt-Ruppin A-2 viral oncogene homolog
Yes	v-yes-1 Yamaguchi sarcoma viral oncogene homolog
CSK	c-Src tyrosine kinase
Syk	Spleen tyrosine kinase
Zap70	Zeta-chain (TCR) associated protein kinase 70kDa
Jak	Janus Kinase
FAK	Focal adhesion kinase

<b>FES</b>	Feline sarcoma oncogene
<b>TEC</b>	Tec protein kinase
<b>Abl</b>	Abelson murine leukemia viral oncogen homolog

## 7.4. List of abbreviations

<b>Abbreviation</b>	<b>Name</b>
<b>AKT</b>	V-akt murine thymoma viral oncogen
<b>ALL</b>	acute lymphoblastic leukemia
<b>AML</b>	acute myeloid leukemia
<b>APC</b>	allophycocyanin
<b>BCR</b>	B-cell receptor
<b>Cbp</b>	CSK binding protein
<b>CLP</b>	common lymphoid progenitor
<b>CML</b>	chronic myeloid leukemia
<b>CMP</b>	common myeloid progenitor
<b>ddH2O</b>	double deionized water
<b>DMEM</b>	Dulbecco's modified Eagle's media
<b>DMSO</b>	dimethyl sulfoxide
<b>DRM</b>	detergent resistant microdomains
<b>DSMZ</b>	Deutsche Sammlung von Mikroorganismen und Zellkulturen GmbH
<b>EDTA</b>	ethylenediaminetetraacetic acid
<b>ERK1/2</b>	mitogen-activated Protein kinase kinase kinase 1/2
<b>FACS</b>	fluorescent activated cell sorting
<b>FCS</b>	fetal calf serum
<b>FITC</b>	fluorescein isothiocyanat
<b>FLT3</b>	fms-related tyrosine kinase 3
<b>GFP</b>	green fluorescent protein
<b>GM1</b>	monosialotetrahexosilganglioside
<b>HSC</b>	hematopoietic stem cells
<b>I.I.</b>	integral intensity
<b>Ig</b>	immunoglobulin
<b>ITAM</b>	immunoreceptor tyrosine-based activation motif
<b>MPP</b>	multipotent progenitors
<b>MRD</b>	minimal residual disease
<b>NRTK</b>	non-receptor tyrosine kinase
<b>ON</b>	overnight
<b>PAG</b>	phosphoprotein associated with glycosphingolipid-enriched microdomains
<b>PDVF</b>	polyvinylidene fluoride
<b>PE</b>	R-phycoerythrin
<b>PTK</b>	protein tyrosine kinase
<b>RB</b>	retinoblastoma protein
<b>RPMI</b>	Roswell Park Memorial Institute
<b>RT</b>	room temperature

<b>RTK</b>	receptor tyrosine kinase
<b>SCR</b>	scramble
<b>SFK</b>	Src-family kinase
<b>SH2</b>	Src homology 2 domain
<b>SH3</b>	Src homology 3 domain
<b>shRNA</b>	Short harping ribonucleotide acid
<b>TBST</b>	tris buffered saline tween
<b>TKI</b>	tyrosine kinase inhibitor
<b>WB</b>	Western blot

## 8. Oligonucleotides

Oligonucleotide	Application	Sequence Target	Sequence 5'-3'
ABL1_For	Amplification	NM_005158	gccgccaccatgatgttgagatctgcctgaagctg
ABL1_Rev	Amplification	NM_005158	tcacaggtcctcctcgctgatcagcttctgctccctctgactatgtcactgatttc
ABL1 For-1	Mutagenesis	NM_005158	cccttgccgccaccatgttgagatctg
ABL1 Rev-1	Mutagenesis	NM_005158	cagatctcaacatggtggcggcaagg
ABL1 For-2	Mutagenesis	NM_005158	agtccacgggaagacagtttgactctccac
ABL1 Rev-2	Mutagenesis	NM_005158	gtggacgagtcaaactgtctccctggact
ABL1_ForA	Sequencing	NM_005158	tgc act gta tga tttgtggcc
ABL1_ForB	Sequencing	NM_005158	tct acg tct cct ccg aga g
ABL1_ForC	Sequencing	NM_005158	ccc gtt cta tat cat cac tga g
ABL1_ForD	Sequencing	NM_005158	gga aat tgc tac cta tgg cat g
ABL1_ForE	Sequencing	NM_005158	cctgagatgcctcactccaa
ABL1_ForF	Sequencing	NM_005158	aaagcccagcaatggggct
ABL1_ForG	Sequencing	NM_005158	ccc cca ggc tgg tga aaa a
ABL1_ForH	Sequencing	NM_005158	gggaaattgtccaggctcaaa
ABL1_ForI	Sequencing	NM_005158	gcctcatccctctcatatcaa
ABL1_RevA	Sequencing	NM_005158	aca cag gcc cat ggt acc a
ABL2_For	Amplification	NM_005157	gccgccaccatggtccttgggacagtctcctt
ABL2_Rev	Amplification	NM_005157	tcacaggtcctcctcgctgatcagcttctgctccctctgaccacatcactgatttc
ABL2_ForA	Sequencing	NM_005157	gag tga ccc taa tct ctt cgt t
ABL2_ForB	Sequencing	NM_005157	aat acc act gca gat ggc aag
ABL2_ForC	Sequencing	NM_005157	ggt gtg tgt act ttg gag cc
ABL2_ForD	Sequencing	NM_005157	cgt ctg ggc ttt tgg ggt at
ABL2_ForE	Sequencing	NM_005157	aac agg tgg aga aca agg aga a
ABL2_ForF	Sequencing	NM_005157	tca ctc ctg ccc agc aag a
ABL2_ForG	Sequencing	NM_005157	tca gcc aga aga gaa tgt gga
ABL2_ForH	Sequencing	NM_005157	aac aca ctc cag ctg acg tg
ABL2_ForI	Sequencing	NM_005157	atg gca cag cag gta cta aag t
ABL2_RevA	Sequencing	NM_005157	tgt tca ctg ggg tga tgt agt t
BKL_For	Amplification	NM_001715	gccgccaccatggggctgtaagtagcaaaaag
BKL_Rev	Amplification	NM_001715	tcacaggtcctcctcgctgatcagcttctgctcgggctgcagctctgactgc
BKL_For	Mutagenesis	NM_001715	cccggccccgcagaatccctggg
BKL_Rev	Mutagenesis	NM_001715	gggcccggggcgtcttagggacc
BLK_ForA	Sequencing	NM_001715	cac cgc tat gaa tga tgc gg
BLK_ForB	Sequencing	NM_001715	tac tac atc tcc ccc cgg at
BLK_ForC	Sequencing	NM_001715	aag gag ccc atc tac att gtc a
BLK_ForD	Sequencing	NM_001715	ttg tca ctt atg ggc ggg tg
BLK_RevA	Sequencing	NM_001715	ctt gtt gat tgg agc aag aag c
BMX_For	Amplification	BC016652	gccgccaccatggatacaaaaatctattctagaagaacttc
BMX_Rev	Amplification	BC016652	tcacaggtcctcctcgctgatcagcttctgctcatgctgtcttttcccgaagtgg
BMX_ForA	Sequencing	BC016652	cgctgtagagacagctac
BMX_ForB	Sequencing	BC016652	aaactatggctcccagccac

<b>BMX_ForC</b>	Sequencing	BC016652	ggt tag aaa ttc gag cca agt g
<b>BMX_ForD</b>	Sequencing	BC016652	gat gat caa gga ggg ctc ca
<b>BMX_ForE</b>	Sequencing	BC016652	gaa cag tat gtc agt tca gtc g
<b>BMX_RevA</b>	Sequencing	BC016652	cgt cca cga aga acc cac ta
<b>BTK_For</b>	Amplification	NM_000061	gccgccaccatggccgagtgattctggaga
<b>BTK_Rev</b>	Amplification	NM_000061	tcacaggtcctcctcgctgatcagcttctgctcggattctcatccatgacatctagaata
<b>BTK_ForA</b>	Sequencing	NM_000061	tcctcctccagaaagacagatt
<b>BTK_ForB</b>	Sequencing	NM_000061	gaccagatcttgaagccac
<b>BTK_ForC</b>	Sequencing	NM_000061	tgt gtt tgc taa atc cac agg g
<b>BTK_ForD</b>	Sequencing	NM_000061	ggc tcc atg tct gaa gat gaa t
<b>BTK_ForE</b>	Sequencing	NM_000061	cag tag gct cca aat ttc cag
<b>BTK_RevA</b>	Sequencing	NM_000061	tga atc cac cgc ttc ctt agt t
<b>CSK_For</b>	Amplification	NM_004383	gccgccaccatgctgcaatacaggccgct
<b>CSK_Rev</b>	Amplification	NM_004383	tcacaggtcctcctcgctgatcagcttctgctccaggtgagctcgtgggtttt
<b>CSK_For</b>	Mutagenesis	NM_004383	catgcccctccttctacagctcc
<b>CSK_Rev</b>	Mutagenesis	NM_004383	gtacccgggaggaaggatgtcagg
<b>CSK_ForA</b>	Sequencing	NM_004383	gtgaaggcgggtaccaaact
<b>CSK_ForB</b>	Sequencing	NM_004383	cat gaa gga gct gaa gct gc
<b>CSK_ForC</b>	Sequencing	NM_004383	tgtgctgtgtctgaggaca
<b>CSK_RevA</b>	Sequencing	NM_004383	aca tga tgc ggt agt gct cc
<b>FES_For</b>	Amplification	BC035357	gccgccaccatgggcttcttctgagctgtg
<b>FES_Rev</b>	Amplification	BC035357	tcacaggtcctcctcgctgatcagcttctgctcccgatgccgttctggatgc
<b>FES_ForA</b>	Sequencing	BC035357	agt cag tcc tgg gct gag at
<b>FES_ForB</b>	Sequencing	BC035357	agc tac acc acc agc acc a
<b>FES_ForC</b>	Sequencing	BC035357	gtg aca gat gag ctg gct gt
<b>FES_ForD</b>	Sequencing	BC035357	tca gga atc ttc cgc ccc aa
<b>FES_ForE</b>	Sequencing	BC035357	caa gga caa gtg ggt gct ga
<b>FES_ForF</b>	Sequencing	BC035357	catggagtacctggagagca
<b>FES_RevA</b>	Sequencing	BC035357	ctg tgg gtc ttg gtg agc t
<b>FGR_For</b>	Amplification	BC002836	gccgccaccatgggctgtgttctgcaagaaat
<b>FGR_Rev</b>	Amplification	BC002836	tcacaggtcctcctcgctgatcagcttctgctctgtctgatccccgggctgg
<b>FGR_ForA</b>	Sequencing	BC002836	gattggggtgaccctgttca
<b>FGR_ForB</b>	Sequencing	BC002836	cattacaagatccgaaactgg
<b>FGR_ForC</b>	Sequencing	BC002836	cca tct aca tcg tga ccg ag
<b>FGR_ForD</b>	Sequencing	BC002836	cac tga gct cat cac caa gg
<b>FGR_RevA</b>	Sequencing	BC002836	cac gta gtt gct ggg aat gc
<b>FYN_For</b>	Amplification	NM_002037	gccgccaccatgggctgtgtcaatgtaaggata
<b>FYN_Rev</b>	Amplification	NM_002037	tcacaggtcctcctcgctgatcagcttctgctccaggtttcaccaggtttgtactg
<b>FYN_ForA</b>	Sequencing	NM_002037	ctcttctctacacgggga
<b>FYN_ForB</b>	Sequencing	NM_002037	cacttctatccgtgattggga
<b>FYN_ForC</b>	Sequencing	NM_002037	aat gtc ccc cga atc att cct t
<b>FYN_ForD</b>	Sequencing	NM_002037	agt tcc cca tca agt gga cg
<b>FYN_RerA</b>	Sequencing	NM_002037	gaa tgt aac ctg tct ctc cag t
<b>HCK_For</b>	Amplification	NM_002110	gccgccaccatgggctgatgaagtccaagtt

HCK_Rev	Amplification	NM_002110	tcacaggtcctcctcgctgatcagcttctgctctggctgctgttggtactggct
HCK_ForA	Sequencing	NM_002110	cca ttc acc acg aag acc tc
HCK_ForB	Sequencing	NM_002110	tac ata tcc ccc cga agc ac
HCK_ForC	Sequencing	NM_002110	cat cac gga gtt cat ggc ca
HCK_ForD	Sequencing	NM_002110	ccc tta ccc agg gat gtc aa
HCK_RevA	Sequencing	NM_002110	aac cac tcc tct gtc tcc ag
ITK_For	Amplification	NM_005546	gccgccaccatgaacaactttatcctcctggaagaacagctc
ITK_Rev	Amplification	NM_005546	tcacaggtcctcctcgctgatcagcttctgctcaagctctgattctgcaatttcagcc
ITK_ForA	Sequencing	NM_005546	atc agc atc cca tgc cac tat a
ITK_ForB	Sequencing	NM_005546	tgc tgg aca gtt ctg aga ttc a
ITK_ForC	Sequencing	NM_005546	cat aat gga gga ggc ctg gt
ITK_ForD	Sequencing	NM_005546	attatctacgacccagcgg
ITK_RevA	Sequencing	NM_005546	tct cca gct gag aac agc ac
JAK2_For	Amplification	BC039695	gccgccaccatgggaatggcctgccttacga
JAK2_Rev	Amplification	BC039695	tcacaggtcctcctcgctgatcagcttctgctcagccatgttatcccttatttgatc
JAK2_ForA	Sequencing	BC039695	cta aag ctt gtg gta tca cac c
JAK2_ForB	Sequencing	BC039695	gcc aaa gaa aac gat caa acc c
JAK2_ForC	Sequencing	BC039695	gag aca ctg aca gaa cag gat t
JAK2_ForD	Sequencing	BC039695	ctg tcg agc gag aaa atg tca t
JAK2_ForE	Sequencing	BC039695	ggc gta cga aga gaa gta gg
JAK2_ForF	Sequencing	BC039695	gct tat cag aga aga cag g
JAK2_ForG	Sequencing	BC039695	cagagccatcatacagatctt
JAK2_ForH	Sequencing	BC039695	agtgtggtcggcgtaatct
JAK2_RevA	Sequencing	BC039695	gagcttcagcacctcgagat
JAK2_For	Mutagenesis	BC039695	tggggaggtggtcgtgtaaaaaagcttcagc
JAK2_Rev	Mutagenesis	BC039695	gctgaagctttttacagcgaccacctcccca
JAK3_For	Amplification	NM_000215	gccgccaccatggcaccctccaagtgaagagac
JAK3_Rev	Amplification	NM_000215	tcacaggtcctcctcgctgatcagcttctgctctgaaaaggacaggagtggtgttt
JAK3_For	Mutagenesis	NM_000215	tggcccgcccgccagagcctgc
JAK3_Rev	Mutagenesis	NM_000215	gcaggctctggcggcccgccca
JAK3_ForA	Sequencing	NM_000215	accactccctcttgctctg
JAK3_ForB	Sequencing	NM_000215	tca gct aca agg cct gcc ta
JAK3_ForC	Sequencing	NM_000215	tta cca gga cag aca acc aga t
JAK3_ForD	Sequencing	NM_000215	agt ctt cga gag ctc ctg g
JAK3_ForE	Sequencing	NM_000215	attcctggaagcagcgagct
JAK3_ForF	Sequencing	NM_000215	gag gcg cag aca ctt agc t
JAK3_ForG	Sequencing	NM_000215	acc tca agt aca tct cac agc t
JAK3_ForH	Sequencing	NM_000215	aac atc ctc gtg gag agc ga
JAK3_RevA	Sequencing	NM_000215	aaggatagcactggccaaatc
LCK_For	Amplification	BC013200	gccgccaccatgggctgtggctgcagctc
LCK_Rev	Amplification	BC013200	tcacaggtcctcctcgctgatcagcttctgctcaggtgaggctgtgactggc
LCK_ForA	Sequencing	BC013200	cacagctatgagccctctca
LCK_ForB	Sequencing	BC013200	gct tct aca tct ccc ctc ga
LCK_ForC	Sequencing	BC013200	gaatgacacacttctagactcc

LCK_ForD	Sequencing	BC013200	aga agc cat taa cta cgg gac a
LCK_RevA	Sequencing	BC013200	gat gag gaa gga gcc gtg a
LYN_For	Amplification	NM_002350	gccgccaccatgggatgtataaaatcaaaagggaaagac
LYN_Rev	Amplification	NM_002350	tcacaggtcctctcgtgatcagcttctgctcaggctgctgctgtattgcc
LYN_ForA	Sequencing	NM_002350	gtagccttgaccctatgat
LYN_ForB	Sequencing	NM_002350	tct gga taa tgg ggg cta tta c
LYN_ForC	Sequencing	NM_002350	accaggaggagcccattta
LYN_ForD	Sequencing	NM_002350	tcc ttt gga atc ctc cta tac g
LYN_RevA	Sequencing	NM_002350	gtg ttg agt ttg gcc aca tag t
MATK_For	Amplification	BC003109	gccgccaccatggcggggcaggctctc
MATK_Rev	Amplification	BC003109	tcacaggtcctctcgtgatcagcttctgctcgggctcctggctcgggg
MATK_ForA	Sequencing	BC003109	acg tgg tca cca tcc tgg a
MATK_ForB	Sequencing	BC003109	tgg agc att aca gca agg aca a
MATK_ForC	Sequencing	BC003109	acc tgg tga act ttc tgc gg
MATK_ForD	Sequencing	BC003109	cac tga aag agg tgt cgg ag
MATK_RevA	Sequencing	BC003109	cca aag ctc acg cac agg a
PTK2_For	Amplification	BC035404	gccgccaccatggcagctgcttaccttgacc
PTK2_Rev	Amplification	BC035404	tcacaggtcctctcgtgatcagcttctgctcgtgtgtctcgtctgcccaag
PTK2_ForB	Sequencing	BC035404	ggg gca atg cac tag aaa aga a
PTK2_ForC	Sequencing	BC035404	gtg aag aca agg aca gaa aag g
PTK2_ForD	Sequencing	BC035404	gaa ggc caa ttt gga gat gta c
PTK2_ForE	Sequencing	BC035404	gga atg ttc tgg tgt cct caa a
PTK2_ForF	Sequencing	BC035404	ctgaactaaagctcagctcag
PTK2_ForG	Sequencing	BC035404	tga gac tct ctc gag gca gt
PTK2_ForH	Sequencing	BC035404	gct tgg ccc tga gga cat ta
PTK2_RevA	Sequencing	BC035404	att tcc act cct ctg gtg gg
PTK2B_For	Amplification	NM_004103	gccgccaccatgtctggggtgccgagcc
PTK2B_Rev	Amplification	NM_004103	tcacaggtcctctcgtgatcagcttctgctcctctgcagggtgggtgggc
PTK2B_ForA	Sequencing	NM_004103	gat cat cac ctc cat cct gc
PTK2B_ForB	Sequencing	NM_004103	atatgccccacaatgcacttga
PTK2B_ForC	Sequencing	NM_004103	gcc agg cag tac ttc agc t
PTK2B_ForD	Sequencing	NM_004103	aggtctatgaaggtgtctacac
PTK2B_ForE	Sequencing	NM_004103	aagctgggggactttgttct
PTK2B_ForF	Sequencing	NM_004103	aga tgg aga agg aca ttg cca t
PTK2B_ForG	Sequencing	NM_004103	tggacaaacagcagaagcagat
PTK2B_ForH	Sequencing	NM_004103	ttc acg gac aga gat cga gg
PTK2B_RevA	Sequencing	NM_004103	acg tgc aga cac tca tac ttg t
SYK_For	Amplification	BC002962	gccgccaccatggccagcagcggcatgg
SYK_Rev	Amplification	BC002962	tcacaggtcctctcgtgatcagcttctgctcgttcaccacgtcatagtagtaattgc
SYK_ForA	Sequencing	BC002962	ctgaatggcacctacgccat
SYK_ForB	Sequencing	BC002962	caa atg gaa agt tcc tga tcc g
SYK_ForC	Sequencing	BC002962	gagtactgtgtcattcaatccg
SYK_ForD	Sequencing	BC002962	ccg agt cct gga tgc tag tt
SYK_ForE	Sequencing	BC002962	agtgttgatgtgggaagcattc

SYK_RevA	Sequencing	BC002962	cca tgt ctg ctt cac ata ttc c
TNK1_For	Amplification	BC035782	gccgccaccatgcttctgaggctggctct
TNK1_Rev	Amplification	BC035782	tcacaggtcctctcgctgatcagcttctgctcggcctggccaggacatag
TNK1_ForA	Sequencing	BC035782	cctaagtctaagaactgggtct
TNK1_ForB	Sequencing	BC035782	cag cct ctg cag atg gtg at
TNK1_ForC	Sequencing	BC035782	tgacgtgtggagatgttc
TNK1_ForD	Sequencing	BC035782	aaagtgggcagcttcccag
TNK1_ForE	Sequencing	BC035782	ccc tgg ccc aaa aga aaa cc
TNK1_RevA	Sequencing	BC035782	act tga cag cca ctg gga ca
TXK_For	Amplification	NM_003328	gccgccaccatgatccttctctataacaccatc
TXK_Rev	Amplification	NM_003328	tcacaggtcctctcgctgatcagcttctgctcccaggttccgcaatctctgtg
TXK_ForA	Sequencing	NM_003328	aaacgaaagccactgcctcc
TXK_ForB	Sequencing	NM_003328	tatgggagctagaagaagtacg
TXK_ForC	Sequencing	NM_003328	cattgaagaggccaaagtgatg
TXK_ForD	Sequencing	NM_003328	aat caa gtg gtc ccc tcc tg
TXK_RevA	Sequencing	NM_003328	aac ggt ctc ttg cct tcc ac
TYK2_For	Amplification	BC014243	gccgccaccatgcctctgcgaccactggg
TYK2_Rev	Amplification	BC014243	tcacaggtcctctcgctgatcagcttctgctcgcacacgctgaacactgaagg
TYK2_ForA	Sequencing	BC014243	cctccttgcttcaatctctttg
TYK2_ForB	Sequencing	BC014243	ctt tct gca cct ctg tca cc
TYK2_ForC	Sequencing	BC014243	tga cag gca ctg gtg gca t
TYK2_ForD	Sequencing	BC014243	cac ggc tgg tga tga gca t
TYK2_ForE	Sequencing	BC014243	ccc agg aca ctc aac ctc a
TYK2_ForF	Sequencing	BC014243	aga gta cgt gga gca cgg a
TYK2_ForG	Sequencing	BC014243	gat ctg ctt tga cgg aga gg
TYK2_ForH	Sequencing	BC014243	tga aag ccc tca agg cag ac
TYK2_ForI	Sequencing	BC014243	aag gcc acg agt act acc g
TYK2_RevA	Sequencing	BC014243	ctgtgctgtctgatctgagg
YES1_For	Amplification	NM_005433	gccgccaccatgggctgcattaaaagtaagaaaacaaaa
YES1_Rev	Amplification	NM_005433	tcacaggtcctctcgctgatcagcttctgctctaaattttctcctggctggtactgtg
YES1_ForA	Sequencing	NM_005433	acgccttttgagggtgcatc
YES1_ForB	Sequencing	NM_005433	tcc ctt tct att cgt gat tgg g
YES1_ForC	Sequencing	NM_005433	gcc aga agc ttt cct tca aga a
YES1_ForD	Sequencing	NM_005433	atc aaa tgg aca gct cct gaa g
YES1_RevA	Sequencing	NM_005433	cca ttc ttc tgc ctg aat gga a
ZAP70_For	Amplification	NM_001079	gccgccaccatgccagaccccgcgcg
ZAP70_Rev	Amplification	NM_001079	tcacaggtcctctcgctgatcagcttctgctcggcacaggcagcctcagcc
ZAP70_ForA	Sequencing	NM_001079	aacggcacctacgccattg
ZAP70_ForB	Sequencing	NM_001079	ata cgc cct gtc cct cat ct
ZAP70_ForC	Sequencing	NM_001079	cca gag gag ctc aag gac aa
ZAP70_ForD	Sequencing	NM_001079	cag gtg tcc atg ggg atg aa
ZAP70_RevA	Sequencing	NM_001079	tag tca cgc acc atg gcg t

Table 12 List of Oligonucleotides

The names, application, target sequences and the nucleic acids sequences (5'-3') of the Oligonucleotide are listed.

## 9. Declaration on oath

I hereby declare, on oath, that I have written the present dissertation by my own and have not used other than the acknowledged resources and aids.

Hamburg, October 2013

---

Allan Pernudy Ubau

## 10. Confirmation of linguistic accuracy by a native speaker

Hibernian School of English • Inh. Micheál Ó Muireagáin

Sudetenweg 64 • 21614 Buxtehude

[www.HibernianSchool.de](http://www.HibernianSchool.de) • Email: [info@HibernianSchool.de](mailto:info@HibernianSchool.de) • Phone: 0171-5150612

Discussions • Meetings • Negotiations • Presentations

I hereby declare that I have read the PhD thesis by Mr Allan Pernudy Ubau titled:

**“Functional characterization of non-receptor tyrosine kinase dependent signal transduction in acute lymphoblastic leukemia of childhood”.**

I confirm its accuracy with regard to application of the English language.



Micheál Ó Muireagáin

Buxtehude 2nd September 2013

## 11. Acknowledgement

I would like to express my sincere gratitude to Prof. Dr Martin Horstmann for giving me the opportunity to perform my PhD at the Research Institute Children's Cancer Center Hamburg and for the unconditional support provided.

I thank Prof. Dr. Lüthen for being a part of my dissertation thesis committee.

I acknowledge the "German Academic Exchange Service (DAAD) for the generous financial contribution to support my research project.

I am very much indebted to all the staff of the Research Institute Children's Cancer Center Hamburg. They have been very kind and patient and always willing to help me whenever I approached them. I specially thank Dr. Kevin Dierck for guiding my project with his valuable suggestions. Furthermore I would like to thank Susanne Barkmann and Marcos Seoane for their support and advice.

I would like to thank Micheál Ó Muireagáin for reading this manuscript.

Finally, I express my deep gratitude to my family for their continuous love and their support in my decisions, without their guidance and persistent help this dissertation would not have been possible.

## 12. Literature

1. Pieters, R. & Carroll, W. Biology and treatment of acute lymphoblastic leukemia. *Hematol Onco Clin N Am* **24**, 1-18 (2010).
2. Onciu, M. Acute Lymphoblastic Leukemia. *Hematol Onco Clin N Am* **23**, 655-674 (2009).
3. Pui, C.H., Robison, L.L. & Look, T. Acute Lymphoblastic Leukemia. *Lancet* **371**, 1030-43 (2008).
4. Pui, C.H. & Evans, W.E. Treatment of acute lymphoblastic leukemia. *N Engl J Med* **354**, 166-78 (2006).
5. Zhou, Y. et al. Advances in the molecular pathobiology of B-lymphoblastic leukemia. *Hum Pathol* **43**, 1347-62 (2012).
6. Hilden, J.M. et al. Analysis of prognostic factors of acute lymphoblastic leukemia in infants: report on CCG 1953 from the Children's Oncology Group. *Blood* **108**, 441-51 (2006).
7. Bhojwani, D., Howard, S. & Pui, C.H. High-Risk Childhood Acute Lymphoblastic Leukemia. *Clin Lymphoma Myeloma* **9**, 1-18 (2009).
8. Pui, C.H., Relling, M.V. & Downing, J.R. Acute lymphoblastic leukemia. *N Engl J Med* **350**, 1535-48 (2004).
9. Armstrong, S.A. & Look, A.T. Molecular genetics of acute lymphoblastic leukemia. *J Clin Oncol* **23**, 6306-15 (2005).
10. Pui, C.H. & Evans, W. Acute Lymphoblastic Leukemia. *N Engl J Med* **339**, 605-6015 (1998).
11. Hanahan, D. & Weinberg, R.A. The hallmarks of cancer. *Cell* **100**, 57-70 (2000).
12. Ferrando, A.A., Look, A.T. Gene expression profiling in T-cell acute lymphoblastic leukemia. *Semin Hematol* **40**, 57-70 (2003).
13. Mullighan, C.G. Molecular genetics of B-precursor acute lymphoblastic leukemia. *J Clin Invest* **122**, 3407-3415 (2012).
14. Daley, G.D., Van Etten, R.A., Baltimore, D. Induction of chronic myelogenous leukemia in mice by the P210 BCR-ABL gene of the Philadelphia chromosome. *Science* **247**, 824-830 (1990).
15. Speck, N.A., Gillilan, D.G. Core-binding factors in hematopoiesis and leukemia. *Nat Rev Cancer* **2**, 502-513 (2002).
16. Brasel, K., Escobar, S., Anderberg, R., de Vries, P., Gruss, H.J., Lyman, S.D. Expression of the flt3 receptor and its ligands on hematopoietic cells. *Leukemia* **9**, 1212-1218 (1995).
17. Gilliland, D.G., Griffing, J.D. The roles of FLT3 in hematopoiesis and leukemia. *Blood* **100**, 1532-1542 (2002).
18. Birg, F., Rosnet, O., Carbuccia, N., Bimbaum, D. . The expression of FMS and FLT3 in hematopoietic malignancies. *Leuk Lymphoma* **13**, 223-227 (1994).
19. Armstrong, S.A., et. al. FLT3 mutations in childhood acute lymphoblastic leukemia. *Blood* **103**, 3544-3546 (2004).
20. Favelyukis, S., Till, J.H., Hubbard, S., Miller, W.T. Structure and autoregulation of the insulin-like growth factor 1 receptor kinase. *Nat Struct Biol* **8**, 1058-1063 (2001).
21. Griffin, J.D. Point mutations in the FLT3 gene in ALL. *Blood* **97**, 2193a (2001).
22. Sherr, C.J., McCormick, F. The RB and P53 pathways in cancer. *Cancer Cell* **2**, 103-112 (2002).
23. Rayman, D.H., et. al. E2F mediates cell-cycle dependent transcriptional repression in vivo by recruitment of an HDAC1/mSin3B corepressor complex. *Genes Dev* **16**, 933-947 (2002).
24. Sherr, C.J., Roberts. J.M. CDK inhibitors: positive and negative regulators of G1-phase progression. *Genes Dev* **13**, 1501-1512 (1999).
25. Omura-Minamisawa, M., et.al. Universal inactivation of both p16 and p15 but not downstream components is an essential event in the pathogenesis of T-cell acute lymphoblastic leukemia. *Clin Cancer Res* **6**, 1219-1228 (2000).

26. Ortega, S., Malumbres, M., Barbacid, M. Cyclin D-dependent kinases, INK4 inhibitors and cancer. *biochem Biophys Acta* **1602**, 73-87 (2002).
27. Krug, U., Ganser, A., Koeffler, H.P. Tumor suppressor genes in normal and malignant hematopoiesis. *Oncogene* **21**, 3475-3495 (2002).
28. Vousden, K.H., Lu, X. Live or let die: the cell's response to p53. *Nat Rev Cancer* **2**, 594-604 (2002).
29. Giaccia, A.J., Kastan, M.B. The complexity of p53 modulation: emerging patterns from divergent signals. *Genes Dev* **12**, 2973-2983 (1998).
30. Sherr, C.J. The INK4a/ARF network in tumour suppression. *Nat Rev Mol. Cell Biol.* **2**, 731-737 (2001).
31. Calero Moreno, T.M., Gustafsson, G., Garwicz, S. Deletion of the Ink4-locus (the p16ink4a, p14ARF and p15ink4b genes) predicts relapse in children with ALL treated according to the Nordic protocols NOPHO-86 and NOPHO-92. *Leukemia* **16**, 2037-2045 (2002).
32. Morrison, S.J., Wandycz, A. M., Hemmati, H. D., Wright, D. E. & Weissman, I. L. Identification of a lineage of multipotent hematopoietic progenitors. *Development* **124**, 1929-1939 (1997).
33. Kaushansky, K. Lineage-specific hematopoietic growth factors. *N Engl J Med* **354**, 2034-2045 (2006).
34. Reya, T., Morrison, S.J., Clarke, M.J., Weissman, I.L. Stem cells, cancer cells and cancer stem cells. *Nature* **41**, 105-111 (2001).
35. Dorshkind, K., Rawlings, D. . in Hoffman: Hematology: Basic Principles and Practice (ed. Elsevier) (2005).
36. Lebien, T.W., Tedder, T. F. B lymphocytes: how they develop and function. *Blood* **112**, 1570-1580 (2008).
37. Herzog, S., Reth, M., Jumaa, H. Regulation of B-cell proliferation and differentiation by Pre-B-cell receptor signalling. *Nat Rev Immunol* **9**, 195-205 (2009).
38. Igarashi, H., et. al. Transcription from the RAG1 locus marks the earliest lymphocyte progenitors in bone marrow. *Immunity* **17**, 117-130 (2002).
39. Melchers, F. The pre-B-cell receptor: selector of fitting immunoglobulin heavy chain for the B-cell repertoire. *Nat Rev Immunol* **5**, 578-584 (2005).
40. Fuxa, M., Skok, J.A. Transcriptional regulation in early B-cell development. *Curr Opin Immunol* **19**, 129-136 (2007).
41. Guo, B., Kato, R.M., Garcia-Lloret, M., Wahl, M.I. & Rawlings, D.J. Engagement of the human pre-B-cell receptor generates a lipid raft-dependent calcium signaling complex. *Immunity* **13**, 243-53 (2000).
42. Kitamura, D., Roes, J., Kuhn, R. & Rajewsky, K. A B-cell-deficient mouse by targeted disruption of the membrane exon of the immunoglobulin mu chain gene. *Nature* **350**, 423-6 (1991).
43. Minegishi, Y. et al. Mutations in the human lambda5/14.1 gene result in B-cell deficiency and agammaglobulinemia. *J Exp Med* **187**, 71-7 (1998).
44. Rolink, A.G., Winkler, T., Melchers, F., Andersson, J. Precursor B-cell receptor-dependent B-cell proliferation and differentiation does not require the bone marrow or fetal liver environment. *J Exp Med* **191**, 23-32 (2000).
45. Zhang, M., Srivastava, G., Lu, L. The Pre-B Cell Receptor and Its Function during B Cell Development. *Cellular & Molecular Immunology* **2**, 89-94 (2004).
46. Ohnishi, K. & Melchers, F. The nonimmunoglobulin portion of lambda5 mediates cell-autonomous pre-B-cell receptor signaling. *Nat Immunol* **4**, 849-56 (2003).
47. Gauthier, L., Rossi, B., Roux, F., Termine, E. & Schiff, C. Galectin-1 is a stromal cell ligand of the pre-B-cell receptor (BCR) implicated in synapse formation between pre-B and stromal cells and in pre-BCR triggering. *Proc Natl Acad Sci U S A* **99**, 13014-9 (2002).

48. Bradl, H. & Jack, H.M. Surrogate light chain-mediated interaction of a soluble pre-B-cell receptor with adherent cell lines. *J Immunol* **167**, 6403-11 (2001).
49. Niiro, H., Clark, E. Regulation of B-cell fate by antigen-receptors signals. *Nat Rev Immunol* **2**, 945-956 (2002).
50. Hubbard, S., Miller, W.T. Receptor tyrosine kinase: mechanisms of activation and signaling. *Curr Opin Cell Biol* **19**, 117-123 (2007).
51. Blume-Jensen, P., Hunter, T. Oncogenic kinase signalling. *Nature* **411**, 355-365 (2001).
52. Robinson, D.R., Wu, Y.M., Lin, S. The protein tyrosine kinase family of the human genome. *Oncogene* **19**, 5548-5557 (2000).
53. Hubbard, S., Till, J.H. Protein tyrosine kinase structure and function. *Annu. Rev. Biochem.* **69**, 373-398 (2000).
54. Doepfner, K., Boller, D., Acaro A. Targeting receptor tyrosine kinase signaling in acute myeloid leukemia. *Critical Reviews in Oncology/Hematology* **63**, 215-230 (2007).
55. Kuriyan, J., Cowburn, D. Molecular peptide recognition domain in eukaryotic signaling. *Annu. Rev. Biophys. Biomol. Struct.* **26**, 259-288 (1997).
56. Boggon, T.J. & Eck, M.J. Structure and regulation of Src family kinases. *Oncogene* **23**, 7918-27 (2004).
57. Nollau, P.M., B. Profiling the global tyrosine phosphorylation state by Src homolog 2 domain binding. *PNAS* **98**, 13531-13536 (2001).
58. Pawson, T., Gish, G., Nash, P. SH2 domains, interaction modules and cellular wiring. *TRENDS in Cell Biology* **11**, 504-511 (2001).
59. Machida, K., Mayer, B. The SH2 domain: versatile signaling module and pharmaceutical target. *Biochem Biophys Acta* **1747**, 1-25 (2005).
60. Li, S.S. Specificity and versatility of SH3 and other proline-recognition domains: structural basis and implications for cellular signal transduction. *Biochem J* **390**, 641-653 (2005).
61. Yeatman, T.J. A renaissance for SRC. *Nat Rev Cancer* **4**, 470-80 (2004).
62. Okada, M. Regulation of the SRC family kinases by Csk. *Int J Biol Sci* **8**, 1385-97 (2012).
63. Oneyama, C. et al. Transforming potential of Src family kinases is limited by the cholesterol-enriched membrane microdomain. *Mol Cell Biol* **29**, 6462-72 (2009).
64. Yamaguchi, H. & Hendrickson, W.A. Structural basis for activation of human lymphocyte kinase Lck upon tyrosine phosphorylation. *Nature* **384**, 484-9 (1996).
65. Wiener, J.R.e.a. Activated SRC protein tyrosine kinase is overexpressed in late-stage human ovarian cancers. *Gynecol Oncol* **88**, 73-79 (2003).
66. Geahlen, R.L., Handley, M.D. & Harrison, M.L. Molecular interdiction of Src-family kinase signaling in hematopoietic cells. *Oncogene* **23**, 8024-32 (2004).
67. Schaller, M.D., et al. Autophosphorylation of the focal adhesion kinases, pp125FAK, directs dependent binding of pp60src. *Mol Cell Biol* **14**, 1680-1688 (1994).
68. Wilde, A., et al. EGF receptor signaling stimulates SRC kinase phosphorylation of clathrin, influencing clathrin redistribution and EGF uptake. *Cell* **96**, 677-687 (1999).
69. Songyang, Z., et al. SH2 domains recognize specific phosphopeptide sequences. *Cell* **72**, 767-778 (1993).
70. Nada, S., et al. Identification of the major tyrosine-phosphorylated proteins in Csk-deficient cells. *Oncogene* **9**, 3571-3578 (1994).
71. Masaki, T., et al. Reduced C-terminal Src kinase (Csk) activities in hepatocellular carcinoma. *Hepatology* **29**, 379-384 (1999).
72. Zheng, X., Wang, Y., Pallen, C.J. Cell transformation and activation of pp60c-src by overexpression of a protein tyrosine phosphatase. *Nature* **359**, 336-339 (1992).

73. Kawabuchi, M. et al. Transmembrane phosphoprotein Cbp regulates the activities of Src-family tyrosine kinases. *Nature* **404**, 999-1003 (2000).
74. Kim, M., et al. . Cbl-c suppresses v-Src-induced transformation through ubiquitin-dependent protein degradation. *Oncogene* **23**, 1645-1655 (2004).
75. Kamei, T., et al. . C-Cbl protein in human cancer tissues is frequently tyrosine phosphorylated in a tumor-specific manner. *Int J Oncol* **17**, 335-339 (2000).
76. Filipp, D. et al. Regulation of Fyn through translocation of activated Lck into lipid rafts. *J Exp Med* **197**, 1221-7 (2003).
77. Bromann, P.A., Korkaya, H., Courtneidge, S. A. The interplay between Src family kinases and receptor tyrosine kinases. *Oncogene* **23**, 7957-7968 (2004).
78. Chan, V.W., et al. Characterization of the B lymphocyte populations in Lyn-deficient mice and the role of Lyn in signal initiation and down-regulation. *Immunity* **7**, 69-81 (1997).
79. Xu, Y., et al. Lyn tyrosine kinase: Accentuating the positive and the negative. *Immunity* **22**, 9-18 (2005).
80. Yi, T.L., Bolen, J.B., Ihle, J.N. Hematopoietic cells express two forms of lyn kinase differing by 21 amino acids in the amino terminus. *mol Cell Biol* **102**, 2391-2398 (1991).
81. Ingley, E. Funtion of the Lyn tyrosine kinase in health and disease. *Cell Communication and signaling* **10**, 10-21 (2012).
82. Corey, S., Anderson, S. Src-related protein tyrosine kinases in hematopoiesis. *Blood* **93**, 1-14 (1999).
83. Burkhardt, A.L.e.a. Anti-immunoglobulin stimulation of B lymphocytes activates src-related protein-tyrosine kinase. *Proc Natl Acad Sci U S A* **88**, 7410-7414 (1991).
84. Ikeda, K., et al. Nuclear localization of Lyn tyrosine kinase mediated by inhibition of its kinase activity. *Experimental Cell Research* **314**, 3392-3404 (2008).
85. Luciano, F., et al. The p54 cleaved form of the tyrosine kinase Lyn generated by caspases during BCR- induce cell death in B lymphoma acts as a negative regulator of apoptosis. *The Journal of the Federation of American Societies for Experimental Biology* **17**, 711-713 (2003).
86. Contri, A., Brunati, A.M., Trentin, L., et. al. Chronic lymphocytic leukemia B-cells contain anomalous Lyn tyrosine kinase, a putative contribution to defective apoptosis. *J Clin Invest* **115**, 369–378 (2005).
87. Kurosaki, T. & Hikida, M. Tyrosine kinases and their substrates in B lymphocytes. *Immunol Rev* **228**, 132-48 (2009).
88. Turner, M.e.a. Perinatal lethality and blocked B-cell development in mice lacking the tyrosine kinase Syk. *Nature* **378**, 298-302 (1995).
89. Deane, J.A. & Fruman, D.A. Phosphoinositide 3-kinase: diverse roles in immune cell activation. *Annu Rev Immunol* **22**, 563-98 (2004).
90. Sirvent, A., Benistant, C., Roche, S. Oncogenic signaling by tyrosine kinases of the SRC family in advanced colorectal cancer. *Am J Cancer Res* **4**, 357-371 (2012).
91. Oneyama, C. et al. The lipid raft-anchored adaptor protein Cbp controls the oncogenic potential of c-Src. *Mol Cell* **30**, 426-36 (2008).
92. Holmfeldt, L., et al. The genomic landscape of hypodiploid acute lymphoblastic leukemia. *Nat Genet* **45**, 242-252 (2013).
93. Sirvent, A. et al. Src family tyrosine kinases-driven colon cancer cell invasion is induced by Csk membrane delocalization. *Oncogene* **29**, 1303-15 (2010).
94. Sen, B., Johnson, F. Regulation of Src family kinases in human cancer. *J Signal Transduct* **2011**, 14 pages (2011).

95. Bjorge, J., Pang, A., Fujita, D. Identification of protein-tyrosine phosphatase 1B as the major tyrosine phosphatase activity capable of dephosphorylating and activating c-Src in several human breast cancer cell lines. *J Biol Chem* **275**, 41439-41446 (2000).
96. Zhang, S.Q. et al. Shp2 regulates SRC family kinase activity and Ras/Erk activation by controlling Csk recruitment. *Mol Cell* **13**, 341-55 (2004).
97. Leroy, C., et al. Quantitative phosphoproteomics reveals a cluster of tyrosine kinase that mediates SRC invasive activity in advanced colol carcinoma cells. *Cancer Res* **69**, 2279-2286 (2009).
98. Gauld, S.B., Cambier, J.C. Scr-family kinases in B-cell development and signaling. *Oncogene* **23**, 8001-8006 (2004).
99. Geier, J.K. & Schlissel, M.S. Pre-BCR signals and the control of Ig gene rearrangements. *Semin Immunol* **18**, 31-9 (2006).
100. Lingwood, D. & Simons, K. Detergent resistance as a tool in membrane research. *Nat Protoc* **2**, 2159-65 (2007).
101. Blake, R., . et al. SU6656, a selective Src family kinase inhibitor, used to probe growth factor signaling. *Mol Cell Biol* **20**, 9018-9027 (2000).
102. Palacios, E.H., Weiss, A. Function of the Src-family kinase, Lck, and Fyn, in T-cell development and activation. *Oncogene* **23**, 7990-8000 (2004).
103. Hynes, N.E. Tyrosine kinase signaling in breast cancer. *Breast Cancer Res* **2**, 154-157 (2000).
104. Irby, R.B., Yeatman, T. J. Role of Src expression and activation in human cancer. *Oncogene* **19**, 5636-5642 (2000).
105. Dos Santos, C., Demur, C., Bardet, V., Prade-Houdellier, N., Payrastre, B., Recher, C. A critical role for Lyn in acute myeloid leukemia. *Blood* **111**, 2269-2279 (2008).
106. Stepanek, O., Draber, P., Drobek, A., et.al. Nonredundant roles of Src-family kinases and Syk in the initiation of B-cell antigen receptor signaling. *J Immunol* **190**, 1807-1818 (2013).
107. Lowell, C.A. Src-family kinase: rheostats of immune cell signaling. *Mol Imm* **41**, 631-643 (2004).
108. Hu, Y., et. al. Requirement of Src kinase Lyn, Hck and Fgr for BCR-ABL1-Induced B-lymphoblastic leukemia but not chronic myeloid leukemia. *Nat Genet* **36**, 453-461 (2004).
109. Flaswinkel, H., Reth, M. Dual role of the tyrosine activation motif of the Ig-alpha protein during signal transduction via the B-cell antigen receptor. *EMBO J* **13**, 83-89 (1994).
110. Xu, Y., et al. Phosphatidylinositol-3 kinase activity in B-cells is negatively regulated by Lyn tyrosine kinase. *Immunol Cell Biol* **90**, 903-911 (2012).
111. Pierce, S.K. Lipid rafts and B-cell activation. *nat Rev Immunol* **2**, 96-105 (2002).
112. Mahon, F.X. et al. Evidence that resistance to nilotinib may be due to BCR-ABL, Pgp, or Src kinase overexpression. *Cancer Res* **68**, 9809-16 (2008).
113. Donato, N.J. et al. BCR-ABL independence and LYN kinase overexpression in chronic myelogenous leukemia cells selected for resistance to STI571. *Blood* **101**, 690-8 (2003).
114. Bicocca, V., et al. Crosstalk between ROR1 and the Pre-B receptor promotes survival of t(1;19) acute lymphoblastic leukemia. *Cancer Cell* **22**, 656-667 (2012).
115. Robinson, L.J., Xue, J. & Corey, S.J. Src family tyrosine kinases are activated by Flt3 and are involved in the proliferative effects of leukemia-associated Flt3 mutations. *Exp Hematol* **33**, 469-79 (2005).
116. Bhattacharyya, S.P. Ubiquitination of Lyn-kinase in rat basophilic leukemia RBL-2H3 cells. *Immunol Lett* **75**, 131-6 (2001).
117. Masdehors, P. et al. Deregulation of the ubiquitin system and p53 proteolysis modify the apoptotic response in B-CLL lymphocytes. *Blood* **96**, 269-74 (2000).